SYNTHETIC AND BIOCHEMICAL EXPLORATION OF THE DEGRADATION AND UTILIZATION OF THIAMIN ANALOGS AND PRELIMINARY STUDIES ON METHANOPTERIN METHYLTRANSFERASE

A Dissertation

by

BRATEEN SHOME

Submitted to the Office of Graduate and Professional Studies of
Texas A&M University
in partial fulfillment of the requirements for the degree of

DOCTOR OF PHILOSOPHY

Chair of Committee,	Tadhg P. Begley
Committee Members,	Frank M. Raushel
	Coran M H Watanabe
	Paul Straight
Head of Department	Simon W. North

May 2017

Major Subject: Chemistry

ABSTRACT

Thiaminase I from *Clostridium botulinum* cleaves thiamin to the constituent pyrimidine and thiazole using a wide range of external nucleophiles. The crystal structure of the thiamin bound mutant of thiaminase I from *Clostridium botulinum* revealed the complete active site architecture and all the catalytically important residues were identified. The role of each active site residue was determined by its position and the steady-state kinetic study of the mutant of the corresponding residue. Based on the structural and the kinetic data, the mechanism of thiaminase I is proposed. Thiaminase I accepts a wide variety of cysteine containing nucleophiles, suggesting the possibility of some protein or peptide as its natural nucleophile. A plate assay and an HPLC based assay were developed to identify new thiaminase producing bacteria.

The second part of the thesis is focused on the development of synthetic strategies for thiamin analogs to answer the following biological questions. Firstly, methoxythiamin pyrophosphate synthesized to study the effect of bacimethrin on thiamin-dependent enzymes and ^{13}C and ^{15}N labeled thiamin analog was synthesized to study different intermediate states of thiamin in PDC. Inhibition of thiamin-dependent enzymes was observed and the data indicates that the toxicity arises due to a different binding mode of 2'-methoxythiamin in the active site. Secondly, two fluorine labeled thiamin analogs were designed that can be used as a tracer for PET imaging study in live animals. Thirdly, synthetic methodologies have been developed to utilize thiamin molecule as a delivery vehicle. The impermeable cargo molecules attached to thiamin molecule via ester or

carbamate linkage can be delivered inside the cells through membrane transporters of thiamin. Finally, synthesis of thiochrome was utilized to estimate thiamin content in auxotrophic phytoplankton and preferential utilization of pyrimidine precursors were observed to fulfill the thiamin requirement.

Preliminary studies were done to explore a putative methanopterin methyltransferase MJ0619. This enzyme is air sensitive and copurifies with bound 4Fe-4S clusters. MJ0619 contains at least three 4Fe-4S clusters and can cleave SAM homolytically in reducing conditions, which classifies it as a radical SAM enzyme. It also possesses GTP cyclohydrolase activity to produce 7,8-dihydroneopterin cyclic phosphate from GTP and can cleave N-glycosidic bond of several nucleosides. Methylation of 7,8-dihydro-6-hydroxymethyl pterin is also observed with this enzyme, however the sources of the methyl groups are still unknown.

DEDICATION

This thesis is dedicated to my beloved parents (Ma and Baba) and my dear fiancée Ankita. I thank my parents for their vision, love, encouragement and constant support throughout my life. They taught me to believe in hard work and that so much could be done with so little. I am indebted to my fiancée Ankita for her love, inspiration and selfless support during all the ups and downs I faced.

ACKNOWLEDGEMENTS

I would like to thank my research advisor, Dr. Tadhg P. Begley, for his support, patience and guidance during my graduate career. He has been a continuous source of encouragement and support both at the times of ups and downs. He is a wonderful mentor and his commitment to education inspires me.

I would like to acknowledge my committee chair, Dr. Tadhg P. Begley, and my committee members, Dr. Frank Raushel, Dr. Coran Watanabe and Dr. Paul Straight, for their guidance and advice throughout the course of this research.

I would like to thank my collaborators for their contribution to my projects. Work on the crystal structure of the thiaminase I was done by Dr. Megan Sikowich from Ealick research group at Cornell University, NY. Dr. Natalia Nemeria from Frank Jordan research group at Rutgers University performed all the *in vitro* experiments on thiamin dependent enzymes with methoxythiamin pyrophosphate. Dr. Magdalena Gutowoska from Worden research group at Monterey Bay Aquarium Research Institute, CA, participated in the growth studies of the phytoplanktons and provided me with the cells for thiamin detection and quantification. I would like to thank Dr. Kai Tittmann from Gottingen, Germany, for his interest and inputs in the thiamin analog synthesis projects.

I would like to thank former members of Begley lab Dr. Lisa Cooper and Dr. Benjamin Philmus, for training me in my early days of graduate studies, current lab member Dr. Sameh Abdelwahed for his valuable inputs and discussions on organic

synthetic strategies and Dr. Xiaohong Jian for preparing the mutants of the MJ0619 enzyme.

I am thankful to my master's research mentor, Dr. Dipakranjan Mal, who encouraged me to pursue Ph.D and continued to inspire me.

I thank all my friends, without whom life in College Station would have been dull and boring. Thanks also go to my colleagues and the department faculty and staff who helped me in countless ways and made my time at Texas A&M University a great experience.

Finally, I am grateful to my mother and father for everything they did for me and to my fiancée Ankita for her patience and love.

CONTRIBUTORS AND FUNDING SOURCES

Contributors

This work was supervised by a dissertation committee consisting of Professors Tadhg P. Begley [advisor], Frank M. Raushel and Coran Watanabe of the Department of Chemistry and Professor Paul Straight of the Department of Biochemistry and Biophysics.

The crystal structure data presented in Chapter 1 was provided by Professor Steven E. Ealick from Cornell University and was published in 2013. The biological studies depicted in Chapter 4 and Chapter 6 were conducted in collaboration with Dr. Natalia Nemeria and Dr. Magdalena Gutowoska respectively.

Funding Sources

Graduate study was supported by graduate assistantship from Department of Chemistry, Texas A&M University. The research work is supported by the NIH Grant DK44083 and Robert A. Welch Foundation Grant A-0034 to Tadhg P. Begley.

NOMENCLATURE

Bt	*Bacillus thiaminolyticus*
Cb	*Clostridium botulinum*
Bcm	Bacimethrin
ThF	Free thiamin
ThP	Thiamin monophosphate
ThDP	Thiamin pyrophosphate
MeoThDP	2'-Methoxythiamin pyrophosphate
HMP	Hydroxymethyl pyrimidine
HET	Hydroxyethyl thiazole
PDC	Pyruvate Dehydrogenase Complex

TABLE OF CONTENTS

Page

ABSTRACT ii

DEDICATION iv

ACKNOWLEDGEMENTS v

CONTRIBUTORS AND FUNDING SOURCES vii

NOMENCLATURE viii

TABLE OF CONTENTS ix

LIST OF FIGURES xiv

LIST OF REACTION SCHEMES xx

LIST OF TABLES xxiii

CHAPTER I INTRODUCTION TO THIAMINASE I AND ITS MECHANISTIC INVESTIGATION BY STRUCTURAL AND KINETIC STUDIES 1

1.1 Introduction to thiamin 1
1.1.1 Degradation of thiamin and reaction catalyzed by thiaminase 1
1.1.2 Thiaminase I and its proposed mechanism 3
1.1.3 Structural aspects of thiaminase I 4
1.2 Results 7
1.2.1 Active site architecture of the Cb-Thiaminase 7
1.2.2 Reconstitution of wild-type Cb-thiaminase 9
1.2.3 Choice of active site mutants for kinetic characterization 10
1.2.4 Steady-state kinetics of the wild-type enzyme 11
1.2.5 C143S mutant of Cb-Thiaminase I 12
1.2.6 Y80F mutant of Cb-Thiaminase I 13
1.2.7 D302N mutant of Cb-Thiaminase I 15
1.2.8 E271Q mutant of Cb-Thiaminase I 16
1.2.9 Y46F mutant of Cb-Thiaminase I 18
1.2.10 D94N mutant of Cb-Thiaminase I 19
1.2.11 Search for the natural nucleophile of thiaminase I 21
1.2.12 Development of a methodology to identify thiaminase secreting bacteria 23
1.3 Discussion 27
1.4 Experimental Methods and Materials 28

1.4.1 Cloning, overexpression and purification of Cb-Thiaminase I 28
1.4.2 Determination of the kinetic parameters 29
1.4.3 Assay condition to explore cysteine containing nucleophiles 30
1.4.4 Plate assays for the detection of thiaminase secreting bacteria 31
1.4.5 HPLC assay for the detection of thiaminase secreting bacteria 31

CHAPTER II MODIFIED SYNTHESIS OF 2'-METHOXYTHIAMIN PYROPHOSPHATE AND ITS COMPETENCE IN THIAMIN-DEPENDENT ENZYMES 33

2.1 Introduction to Bacimethrin 33
2.1.1 Biosynthesis of bacimethrin 33
2.1.2 First reported synthesis of bacimethrin 35
2.1.3 First reported synthesis of 2'-methoxythiamin 36
2.1.4 Enzymatic synthesis of methoxythiamin 36
2.2 Results 37
2.2.1 Modification of the methoxythiamin synthetic route 37
2.2.2 Attempt to synthesize 2'-Methoxythiamin via direct coupling of the pyridine and thiazole moieties 38
2.2.3 Modification of aminomethyl-pyridine synthesis 39
2.2.4 Complete synthesis of 2'-Methoxythiamin pyrophosphate 40
2.2.5 Study on thiamin-dependent enzymes with Methoxythiamin pyrophosphate 42
2.3 Discussion 43
2.4 Experimental 44
2.4.1 Overexpression and Purification of Thiamin Pyrophosphokinase 44
2.4.2 Synthetic procedure 44
2.4.3 High Performance Liquid Chromatography (HPLC) conditions for the isolation of 11 48

CHAPTER III SYNTHESIS AND BIOCHEMICAL STUDIES ON $^{13}C2,^{15}N3$-THIAMIN PYROPHOSPHATE 49

3.1 Introduction 49
3.2 Results and Discussion 51
3.2.1 Synthesis of the thiazole moiety 51
3.2.2 Synthesis of the pyrimidine moiety 52
3.2.3 Coupling of the pyrimidine and thiazole: Formation of the thiamin 53
3.2.4 Enzymatic pyrophosphorylation of labeled thiamin 54
3.3 Conclusion 56
3.4 Experimental 56
3.4.1 Synthetic procedure 56
3.4.2 Overexpression and purification of thiamin pyrophosphokinase 59
3.4.3 High Performance Liquid Chromatography (HPLC) conditions for the isolation of 11 59

CHAPTER IV SYNTHETIC STRATEGY OF ^{18}F-LABELED THIAMIN ANALOGS FOR PET IMAGING TO STUDY DISTRIBUTION OF THIAMIN IN LIVE ANIMALS 60

4.1 Introduction to PET imaging 60
4.2 Results and discussion 62
4.2.1 Initial synthetic strategy 62
4.2.2 Second strategy for the synthesis of deoxyfluorothiamin 65
4.2.3 Development of synthetic strategy for the second fluoro-thiamin analog 66
4.2.4 Bacterial growth study with fluorothiazole 69
4.2.5 Synthesis of fluorothiazole using fluoride ion as the source of fluorine 70
4.3 Challenges and future direction 71
4.4 Experimental 72
4.4.1 Synthetic procedure 72
4.4.2 High Performance Liquid Chromatography (HPLC) conditions for the isolation of 1 78

CHAPTER V EXPLOITING THIAMIN AS A DELIVERY VEHICLE FOR CARGO INSIDE LIVING CELL 79

5.1 Introduction 79
5.2 Results 81
5.2.1 Development of synthetic methodology for ester linkage 81
5.2.2 Formation of carbamate linkage 83
5.2.3 Synthesis of (1-aminoethyl)phosphonic acid (Ala-P) and thiamin-Ala-P conjugate 85
5.3 Conclusion and future directions 87
5.4 Experimental 88
5.4.1 Synthetic methods 88

CHAPTER VI ESTIMATION OF THIAMIN QUOTA IN THE HAPTOPHYTES THAT PREFERENTIALLY USE PYRIMIDINE COMPOUNDS TO FULFILL THIAMIN REQUIREMENT 92

6.1 Introduction 92
6.1.1 Thiamin biosynthesis and phytoplankton 92
6.1.2 Thiamin quota: why it is important 94
6.2 Results and discussion 95
6.2.1 Optimization of the thiochrome assay 95
6.2.2 Growth conditions of the haptophyte cells in the laboratory 96
6.2.3 Estimation of the thiamin content in the haptophyte cells by thiochrome assay 97
6.3 Experimental 101
6.3.1 Growth of E. huxleyi in laboratory 101

6.2.2 Sample preparation for thiamin estimation 102
6.3.3 Thiochrome assay and determination of thiamin content in the cell pellets . 103
6.3.4 HPLC condition 104

CHAPTER VII SUMMARY OF RESULTS OF PRELEMINARY STUDIES ON MJ0619, A PUTATIVE METHANOPTERIN METHYLTRANSFERASE 105

7.1 Introduction 105
7.1.1 Methanopterin and its role in methane biogenesis 105
7.1.2 Biosynthesis of methanopterin: Origin of the methyl groups 106
7.1.3 Introduction to radical-SAM enzymes 108
7.1.4 Discovery of MJ0619, putative methanopterin methyltransferase 109
7.2 Results 111
7.2.1 Sequence analysis of MJ0619 111
7.2.2 Overexpression and purification of MJ0619 112
7.2.3 Reconstitution of the 4Fe-4S cluster in the purified MJ0619 114
7.2.4 Measurement of iron and sulfur content in MJ0619 114
7.2.5 Construction of the mutants 115
7.2.6 Spectroscopic analysis of the wild-type protein and the mutants 115
7.2.7 EPR analysis of the wild-type MJ0619 and mutants 117
7.2.8 Homolytic cleavage of SAM by MJ0619: Proof of radical generation 119
7.2.9 Optimization of reaction condition at 37 ^{o}C 120
7.2.10 Generation of 5'deoxyadenosine with Flavodoxin (FldA) / Flavodoxin reductase (FldR) system 121
7.2.11 Assay with GTP, discovery of GTP cyclohydrolase activity 123
7.2.12 The linear triphosphate is the precursor of the cyclic phosphodiester of dihydro neopterin 125
7.2.13 4Fe-4S clusters are necessary for cyclohydrolase activity 127
7.2.14 Phosphatase and nucleosidase activity by MJ0619 128
7.2.15 MJ0619 shows nucleosidase activity on variety of nucleosides 130
7.2.16 Assay with 7,8-dihydro-6-hydroxymethylpterin 131
7.3 Discussion 133
7.4 Experimental 136
7.4.1 Overexpression and purification of MJ0619 136
7.4.2 Estimation of the iron content 138
7.4.3 Estimation of the sulfur content 139
7.4.4 Assay for radical SAM activity 140
7.4.5 Radical SAM activity with FldA / FldR system 140
7.4.6 Assay for GTP cyclohydrolase activity 140
7.4.7 Assay with 7,8-dihydro-6-hydroxymethyl pterin 141
7.4.8 HPLC method 141
7.4.9 LCMS method 142

REFERENCES 143

LIST OF FIGURES

Page

Figure 1.1: Structure of thiamin and its phosphates. 1

Figure 1.2: Structure of ring open thiamin and thiamin disulfide. 2

Figure 1.3: Proposed mechanism for Bt-Thiaminase I. Structure did not identify all the catalytic residues. 4

Figure 1.4: Crystal structure of Bt-Thiaminase I active site. 5

Figure 1.5: X-ray crystal structure of the C143S mutant of the Cb-Thiaminase active site with thiamin bound. All six catalytically active residues are shown. The structure gives a good indication of the positions of the residues around the substrate and their possible roles in the catalysis. 7

Figure 1.6: 2-dimensional representation of the Cb-Thiaminase active site. All distances are given in Å. 8

Figure 1.7: Plot of observed k_{cat} vs. pH of the reaction buffer. pH 8.0 shows a maximum value of k_{cat} reflecting highest activity. 9

Figure 1.8: HPLC chromatogram of the Cb-Thiaminase reaction mixture with all controls. 10

Figure 1.9: Steady-state kinetics of the cleavage of thiamin catalyzed by wild type enzyme. Assays were carried out in 0.1 M potassium phosphate buffer, pH 8.0, 0.1 M KCl, in the presence of 713 mM 2-mercapto ethanol and 0.1 μM enzyme. The k_{cat} value was recorded as $230 \pm 11\ s^{-1}$ and the K_M for thiamin was 452 ± 50 uM 11

Figure 1.10: Position of the Cysteine-143 in the active site. C143 is mutated to serine to get a substrate bound crystal structure in C143S mutant 12

Figure 1.11: Position of Y80 in the active site. The stacking alignment right in parallel to the thiazole ring of the thiamin showing a possibility of potential electrostatic interaction of its hydroxyl group with the positively charged nitrogen. Hydrogen bonding interaction with D94 and Y46 is also evident. 13

Figure 1.12: Steady-state kinetics of thiamin cleavage by 2-mercapto ethanol catalyzed by Y80F mutant. 0.1 M potassium phosphate buffer, pH 8.0, 0.1 M KCl, in the presence of 713 mM 2-mercapto ethanol and 3.1 μM enzyme.

The k_{cat} value was recorded as 1.1 ± 0.1 s^{-1} and the K_M for thiamin was 2 ± 0.1 mM. 14

Figure 1.13: Position of D302 in the active site. Hydrogen bonding type interaction observed between the aspartate and the pyrimidine N-3 of thiamin..... 15

Figure 1.14: Steady-state kinetics of thiamin cleavage by 2-mercapto ethanol catalyzed by D302N mutant. 0.1 M potassium phosphate buffer, pH 8.0, 0.1 M KCl, in the presence of 713 mM 2-mercapto ethanol and 0.3 μM enzyme. The k_{cat} value was recorded as 8.1±0.7 s^{-1} and the K_M for thiamin were 0.3 ± 0.1 mM..... 16

Figure 1.15: Position of E271 in the thiamin bound structure. The cysteine has been mutated to serine. It is in hydrogen bonding distance from both the substrate and the catalytic cysteine..... 16

17

Figure 1.16: Steady-state kinetics of thiamin cleavage by 2-mercapto ethanol catalyzed by E271Q mutant. 0.1 M potassium phosphate buffer, pH 8.0, 0.1 M KCl, in the presence of 713 mM 2-mercapto ethanol and 23.6 μM enzyme. The k_{cat} value was recorded as (11 ± 0.3) x 10^{-3} s^{-1} and the K_M for thiamin was 75 ± 12 μM. 17

Figure 1.17: Position of Tyr 46 in the active site. The distance between Y46 and Y80 is suitable for hydrogen bonding. 18

Figure 1.18: Steady-state kinetics of thiamin cleavage by 2-mercapto ethanol catalyzed by Y46F mutant in 0.1 M potassium phosphate buffer, pH 8.0, 0.1 M KCl, in the presence of 713 mM 2-mercapto ethanol and 0.07 μM enzyme. The k_{cat} value was recorded as 61 ± 4 s^{-1} and the K_M for thiamin was 240 ± 50 μM. 19

Figure 1.19: Position of the D94 residue in the structure. Possible hydrogen bonding distance with Y80 phenol and the pyrimidine C4' amino group is shown. 19

Figure 1.20: Steady-state kinetics of thiamin cleavage by 2-mercapto ethanol catalyzed by D94N mutant. 0.1 M potassium phosphate buffer, pH 8.0, 0.1 M KCl, in the presence of 713 mM 2-mercapto ethanol and 13 μM enzyme. The k_{cat} value was recorded as 0.23 ± 0.02 s^{-1} and the K_M for thiamin was 3.5 ± 0.8 mM. 20

Figure 1.21: HPLC Chromatogram of the reaction of thiamin with Cysteine and cysteine ester as a nucleophile for Cb-Thiaminase..... 22

Figure 1.22: HPLC Chromatogram of the reaction of thiamin with Cysteine-containing peptides B) Gly-Cys-Gly-Gly as a nucleophile for Cb-Thiaminase I. 22

Figure 1.23: A) Plate assay with *Bacillus thiaminolyticus.* B) Comparison of thiaminase-producing *B. thailandensis* colonies vs. *E. coli* colonies in the plate assay. Degradation of thiamin (yellow halo around the colonies) is observed for thiaminase producing strains. 23

Figure 1.24: Normalized peak area of the produced thiazole in the HPLC assays 25

Figure 1.25: Proposed mechanism based on the structural and the kinetic data. 26

34

Figure 2.1: Organization of genes in bacimethrin biosynthetic operon in *C. botulinum* A ATCC 19397. The genes were annotated based on homology – (3) glycosyltransferase (bcmB), (4) thymidylate synthase (bcmA), (5) methyltransferase (bcmC), (6) thiaminase-I (bcmE), (7) pyrimidine kinase (bcmD) 34

Figure 2.2: Steps involved in the bacimethrin biosynthetic pathway. The role of each enzyme is shown. 34

Figure 3.1: Mechanism of the reaction catalyzed by PDC enzyme 50

Figure 3.2: Proton NMR spectrum of the labeled thiazole. 54

Figure 3.2: HPLC chromatogram of the enzymatic phosphorylation of isotopically labeled thiamin. Formation of TPP was only observed in full reaction. 55

Figure 4.1: Structure of the targeted deoxy-fluorothiamin. 62

66

Figure 4.2: Structure of the fluorine- thiamin capable of enzymatic phosphorylation 66

Figure 4.3: Mass spec analysis of the coupling reaction detects the presence of the fluorothiazole as the major product (283.1028). Hydrolysed product hydroxythiamin was also detected at mass of 281.11 (Scheme 4.8) 68

Figure 4.4: Structure of the newly designed thiamin analog 72

Figure 5.1: Reaction condition for converting thiamin thiazolone to thiamin. 81

Figure 5.2: Reduction of the disulfide bond of thiamin disulfide to produce thiamin 81

Figure 5.3: Mass spectra (+ve mode) of the thiamin alanine methyl ester adduct and thiamin-ampicillin adduct 84

Figure 5.4: Structure of the Ala-P molecule..... 84

Figure 6.1: Biosynthetic pathway of thiamin pyrophosphate in bacteria 93

Figure 6.2: Comparison of blank experiments before and after treatment of the water with active charcoal. The thiochrome peak disappears after the treatment. 96

Figure 6.3: Typical chromatogram of the thiochrome assay mixture performed on an *E. huxleyi* cell lysate. 98

Figure 7.1: Chemical structure of A) Methanopterin and B) Folic Acid 106

Figure 7.2: Schematic diagram of steps involved in methanogenesis. 106

Figure 7.3: Biochemical steps involved in Methanopterin biosynthesis. 107

Figure 7.4: Schematic diagram of 4Fe-4S cluster in a radical SAM enzyme. Three iron atoms are ligated by three cysteine residues and the fourth free iron atom binds the SAM molecule during the catalytic cycle..... 108

Figure 7.5: Proposed reactions catalyzed by MJ0619 by Allen et al. A) Reaction proposed for wild-type enzyme, B) proposed reaction catalyzed by C77A mutant and C) no methylation observed with C102A mutant of MJ0619. 110

Figure 7.6: Initial proposal for methylation of the pterin moiety. 'X' group denotes the methyl carrier. 111

Figure 7.7: SDS-PAGE gel of MJ0619 protein after purification. 113

Figure 7.8: UV-Vis spectra of MJ0619 and its mutants. Spectra of A) the wild-type protein, B) M1 mutant, C) M2 mutant and D) M3 mutant. All of them have an absorption band at 418 nm characteristic of 4Fe-4S cluster. The band at ~ 615 nm may be due to a 2Fe-2S cluster or non-specifically bound iron in the protein. 116

Figure 7.9: UV-Vis spectra of reduced and oxidized cluster. Loss of 418 nm band observed upon reduction. 117

Figure 7.10: EPR spectra of A) Wild-type MJ0619, B) M1 mutant, C) M2 Mutant and D) M3 mutant. Two EPR bands are visible in the wild type, M1 and M2, however, in M3, only one EPR signal was observed. 118

Figure 7.11: HPLC chromatogram of substrate uncoupled 5'-deoxyadenosine formation. No product formation in the absence of SAM or MJ0619 enzyme. Little amount of the product formation is observed in the absence of dithionite due to the presence of some reduced clusters. 120

Figure 7.12: SDS-PAGE gel analysis of the purified FldA and FldR. Molecular weights match with the reported values. 121

Figure 7.13: A) Formation of 5'-deoxyadenosine in the presence of FldA / FldR as catalysts and NADPH as reducing agent.. B) The exact mass of 5'-deoxyadenosine confirms the identity of the compound..... 123

124

Figure 7.14: A) Reaction product of MJ0619 with GTP before and after CIP treatment. (I) Neopterin triphosphate, (II) Dihydroneopterin phosphodiester and (III) dihydroneopterin. B) UV-Vis spectra of neopterin cyclic phosphate..... 124

Figure 7.15: A) Coelution experiment (gray trace) of neopterin cyclic phosphate generated by MJ0619 (blue trace) with an authentic sample of the dihydroneopterin cyclic phosphate prepared from GTP and MptA (orange trace). B) Coelution of 7 shown by the extracted ion chromatogram of in LCMS analysis, C) MS-MS spectrum of 7 in negative mode (exact mass 316.0452)..... 125

Figure 7.16: Time course of GTP cyclohydrolase activity of MJ0619 ortholog. 7,8-dihydroneopterin triphosphate (15) (retention time 1.7 min) was the first product to be formed which later converted to 7 (retention time 2.8 min). ... 127

Figure 7.17: Assay for GTP cyclohydrolase activity with the MJ0619 protein in the presence and the absence of bound 4Fe-4S clusters. In the absence of the cluster, the protein was found to be inactive. 128

Figure 7.18: Comparison of GTP cyclohydrolase, phosphatase and nucleoside hydrolase activity of MJ0619. In absence of the 4Fe-4S cluster, the enzyme retains its phosphatase activity, however, the nucleosidase activity was lost. 129

Figure 7.19: HPLC chromatogram of the assay of MJ0619 with a variety of purine and pyrimidine-based nucleosides. HPLC traces: No enzyme control (blue), Reaction with aerobic protein (maroon) and reaction with anaerobic protein (green). The nucleoside hydrolase activity was only observed with the anaerobically purified protein..... 131

Figure 7.20: LCMS analysis of the reaction of MJ0619 with 7,8-dihydro-6-hydroxymethyl pterin as substrate. Formation of a peak at the same retention time and exact molecular weight of the dimethylated product molecule (4) was found. Little formation of the product in no dithionite control is probably due to the presence of pre-reduced clusters in the enzyme 132

Figure 7.21: Product formation is observed in the reaction conducted with CD_3 – SAM. No deuterium incorporation was observed. 133

LIST OF REACTION SCHEMES

Page

Scheme 1.1: Reaction catalyzed by thiaminase. For thiaminase II, X = Water and for thiaminase I, X can be a variety of nucleophiles. Thiaminase II only uses water as a nucleophile, however, thiaminase I can use a variety of nucleophiles to cleave thiamin. 2

Scheme 1.2: Reaction used for the kinetic study of Cb-Thiaminase I..... 9

Scheme 2.1: Synthetic steps of Bacimethrin followed by Drautz et al..... 35

Scheme 2.2: Steps involved in the synthesis of 5-(aminomethyl)-2-methoxypyrimidin-4-amine..... 36

Scheme 2.3: Steps involved in the enzymatic semi-synthesis of 2'-methoxythiamin pyrophosphate..... 37

Scheme 2.4: Proposed synthetic scheme for the synthesis of methoxythiamin by coupling the corresponding pyrimidine bromide with thiazole..... 38

Scheme 2.5: Dimerization of pyrimidine during hydrogenation..... 39

Scheme 2.6: Proposed steps involved in the formation of dimerized pyrimidine during the reduction of nitrile to an amino group by Raney Nickel-catalyzed hydrogenation. 40

Scheme 2.7: A convergent synthetic route for methoxythiamin pyrophosphate. A) Synthesis of the pyrimidine part, B) synthesis of the thiazole precursor and C) coupling of 4 and 7 to give methoxythiamin (16) followed by enzymatic phosphorylation. 41

Scheme 3.1: Synthetic scheme for the labeled thiazole part of the molecule. 52

Scheme 3.2: Synthesis of the pyrimidine part for the coupling reaction. 52

Scheme 3.4: Enzymatic pyrophosphorylation of thiamin using ATP and Mg^{2+} ion 54

Scheme 4.1: Coupling of pyrimidine bromide and thiazole fluoride to form deoxy fluorothiamin 62

Scheme 4.2: Synthesis of A) triflate and B) nosylate of the thiazole precursor..... 63

Scheme 4.3: Synthesis of the 4-methyl-5-fluoroethyl thiazole from the corresponding nosylate with available ^{18}F precursor potassium fluoride. 64

Scheme 4.4: Steps involved in the synthesis of Bromo-pyrimidine (2) 64

Scheme 4.5: Alternative strategy for the synthesis of F-thiamin. 65

Scheme 4.6: Synthetic route for 2-fluoro-2-(4-methylthiazol-5-yl)ethan-1-ol for biological tests 67

Scheme 4.7: Synthesis of Chloro-pyrimidine and its coupling with 20 to form the final thiamin analog (15). 68

Scheme 4.8: Hydrolysis of fluorothiamin to dihydroxythiamin 69

Scheme 4.9: Hydrolysis of the 2-(4-methylthiazol-5-yl)ethan-1-ol to form 2-fluoro-2-(4-methylthiazol-5-yl)ethan-1,2-diol in the aqueous growth media. 69

Scheme 4.10: Planned synthesis of 2-fluoro-2-(4-methylthiazol-5-yl)ethan-1-ol 70

Scheme 4.11: Formation of pyridine-thiazole adduct 70

Scheme 4.11: A) Proposed Synthesis of fluorine labeled thiamin using hydrofluoric acid as the fluorinating agent. B) Strategy proposed for the coupling of the pyrimidine and the thiazole part to give the targeted fluorinated thiamin molecule. 71

Scheme 5.1: Linking cargo molecule with thiamin by an ester linkage. 82

Scheme 5.2: Formation of carbamate linkage with thiamin for amine group containing cargo 83

Scheme 5.3: Attempt to synthesize dimethyl ester of Ala-P 85

Scheme 5.4: Synthesis of (1-aminoethyl) phosphonic acid avoiding the reduction step 85

Scheme 5.5: Strategy for the Synthesis of diethyl (1-aminoethyl)phosphonate. 86

Scheme 5.6: Synthetic scheme for the preparation of diphenyl ester of Alanine phosphonate. 87

Scheme 6.1: Formation of thiochrome from thiamin by potassium ferricyanide in alkaline medium 95

Scheme 7.4: 5'-deoxyadenosyl radical is generated upon transferring one electron from the reduced cluster to SAM molecule. This radical abstracts a hydrogen atom to from 5'-deoxyadenosine. 119

Scheme 7.5: The reaction of GTP cyclohydrolase: conversion of GTP to 7,8-dihydroneropterin-2',3'-cyclic phosphodiester 124

Scheme 7.6: Proposed mechanism of GTP cyclohydrolase activity by MJ0619 126

Scheme 7.7: Dephosphorylation and N-glycosidic bond cleavage of GTP by MJ0619. 129

Scheme 7.8: Reaction catalyzed by MJ0619 in presence of SAM and dithionite 132

LIST OF TABLES

Page

Table 1.1: Kinetic properties of thiaminase activity for Cb-Thiaminase I and six active site mutants. 21

Table 6.1. Measured cellular quotas for thiamin pyrophosphate (TPP), thiamin monophosphate (TMP), and free thiamin (ThF) in *E. huxleyi* CCMP2090. Error represents the s.d. of three independent measurements and are shown in parentheses. 99

Table 7.1: Details of the MJ0619 mutants 115

CHAPTER I

INTRODUCTION TO THIAMINASE I AND ITS MECHANISTIC INVESTIGATION BY STRUCTURAL AND KINETIC STUDIES

1.1 Introduction to thiamin

Thiamin (**1**), commonly known as vitamin B1, is an important cofactor in all forms of life. Bacteria, fungi and plants can biosynthesize thiamin *de novo*, however, the biosynthetic genes of thiamin are absent in animals, and they have to acquire it from their diet. The thiamin molecule is comprised of a pyrimidine ring and a thiazole ring linked by a bridging methylene group. Thiamin is biosynthesized as thiamin monophosphate (**2)**, however, it can be found as diphosphate (**3)** and free thiamin as well (Figure 1.1). The other two forms of thiamin include thiamin triphosphate and adenylated thiamin.[1]

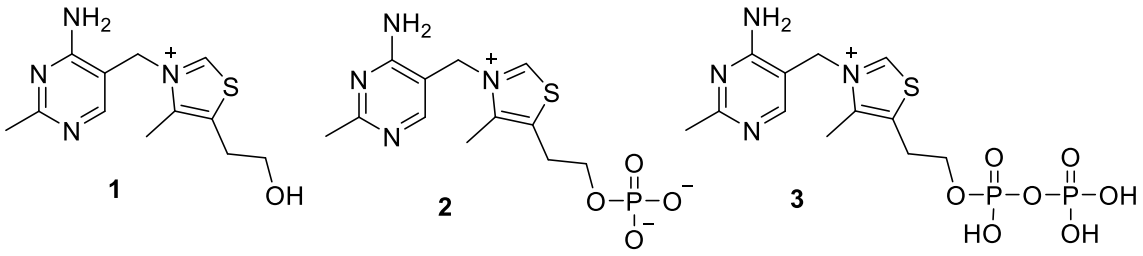

Figure 1.1: Structure of thiamin and its phosphates.

1.1.1 Degradation of thiamin and reaction catalyzed by thiaminase

Thiamin is a stable cofactor in neutral and acidic conditions. In basic medium the thiazole ring of thiamin hydrolyzes to form ring open thiamin (**4**) which might get oxidized to form a dimer known as thiamin disulfide (**5**) (Figure 1.2). Temperature, oxidizing and reducing agents also cause damage to the thiamin molecule.[2] Apart from the chemical and

environmental degradation, thiamin can also be degraded by action of enzymes called thiaminases that are subdivided into two categories. Thiaminase I uses a wide range of nucleophiles for the cleavage reaction whereas thiaminase II uses only water for this purpose (Scheme 1.1).[3-5]

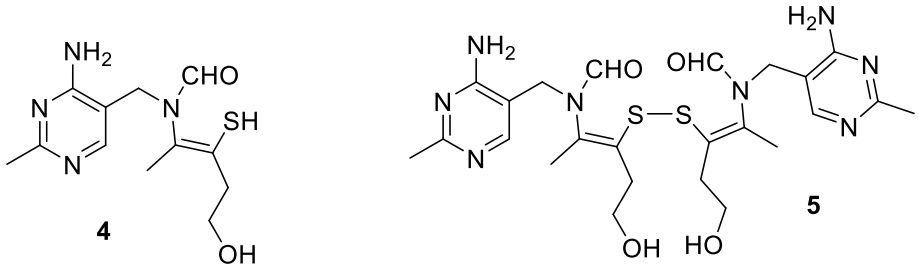

Figure 1.2: Structure of ring open thiamin and thiamin disulfide.

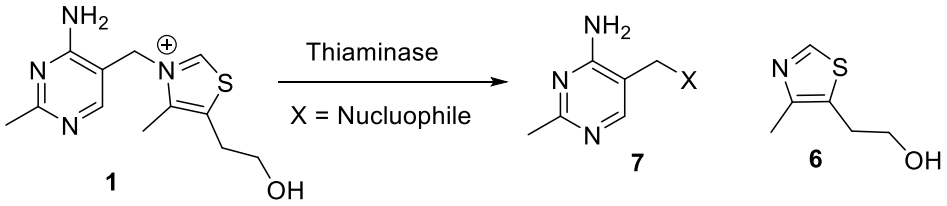

Scheme 1.1: Reaction catalyzed by thiaminase. For thiaminase II, X = Water and for thiaminase I, X can be a variety of nucleophiles. Thiaminase II only uses water as a nucleophile, however, thiaminase I can use a variety of nucleophiles to cleave thiamin.

Thiaminase II is distinct from thiaminase I both in terms of structure and sequence.[6] Intake of thiaminase containing food or infection by thiaminase producing organisms in the body or food material cause lower levels of thiamin and symptoms of thiamin deficiency.[7-10] Effect of thiamin deficiency in humans can result in wet beriberi (affecting cardiovascular system) or dry beriberi (affecting nervous system) with fatal consequenses.[11-12]

1.1.2 Thiaminase I and its proposed mechanism

Thiaminase I was first identified about a decade ago, however, its mechanism was unclear at that time.[13-14] Thiaminase I from *Bacillus thiaminolyticus* (Bt-thiaminase) was first discovered as an extracellular protein and was further characterized by recombinant expression in *E. coli*.[15-16] Leinhard and co-workers first proposed the formation of an enzyme-pyrimidine adduct intermediate during the reaction via kinetic evidence and thereby proposed a mechanism of the reaction.[4] This idea was further supported by inhibition of thiaminase I from *B. thiaminolyticus* by 4-amino-5-(aminomethyl)-6-chloro-2-methyl pyrimidine (**6**).[17] The only cysteine of the enzyme was identified as the active site nucleophile forming the covalent linkage with the substrate and later the inactive enzyme was crystallized and a mechanism is proposed (Figure 1.3).[3, 18] It has also been observed that in the reaction of pyrimidine adduct formation the configuration of the methylene carbon is retained suggesting that the nucleophile attacks from the same direction that the thiazole moiety leaves.[19] In alkaline pH thiaminase I also degrades thiamin very slowly for few turnovers and releases the thiazole moiety, however, no HMP-OH (7, X = OH) was formed, the fate of the pyrimidine part was later discovered as the adduct of the ring open thiamin.[20]

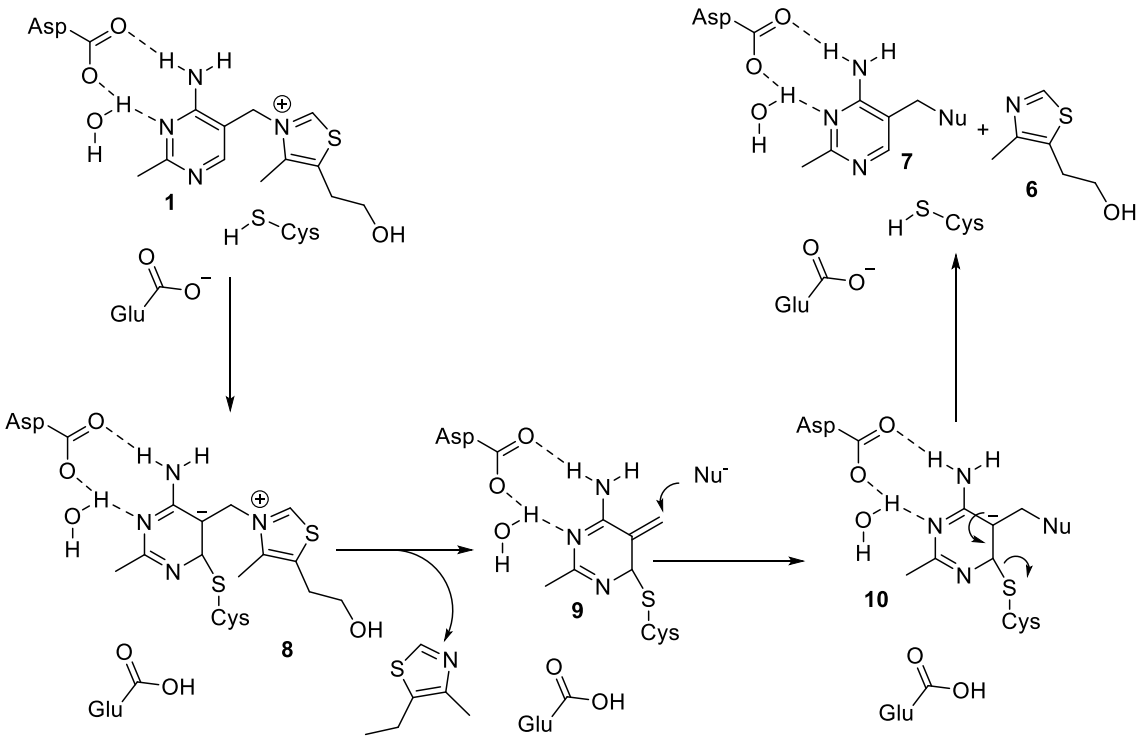

Figure 1.3: Proposed mechanism for Bt-Thiaminase I. Structure did not identify all the catalytic residues.

1.1.3 Structural aspects of thiaminase I

Thiaminase I from *Bacillus thiaminolyticus* is structurally homologous to the group II periplasmic binding proteins (PBPs).[6, 21] PBPs are responsible for binding small molecules and delivering them to the ABC-type transporter for cellular uptake. These proteins have two conformations, open conformation with no ligand bound and a closed conformation with the ligand bound.[21] Bt-thiaminase is structurally similar to the periplasmic thiamin-binding protein (TbpA) which is the carrier of thiamin, thiamin monophosphate and thiamin diphosphate for many prokaryotes.[22] The eukaryotic thiamin pyrimidine synthase, Thi5, is a member of the group II PBP superfamily and also a

structural homolog to ThiY.[23-24] ThiY is a periplasmic protein that is used by some prokaryotes for binding N-formyl HMP, which is a thiamin degradation product.[25]

The reported structure of Bt-thiaminase, crystallized with mechanism-based irreversible inhibitor 4-amino-6-chloro-2,5-dimethylpyrimidine (Figure 1.4), showed that the active site is located in a V-shaped cleft between its two domains.[18] An interesting similarity is observed between its active site location and the ligand binding sites of PBPs. The activator glutamate residue, responsible for the deprotonation of the catalytic cysteine for the nucleophilic attack at C6, is also observed in the structure. Despite the major differences in their size, structure, and sequence, thiaminase-I and most of the thiaminase-II use a cysteine residue for the covalent linkage formation.

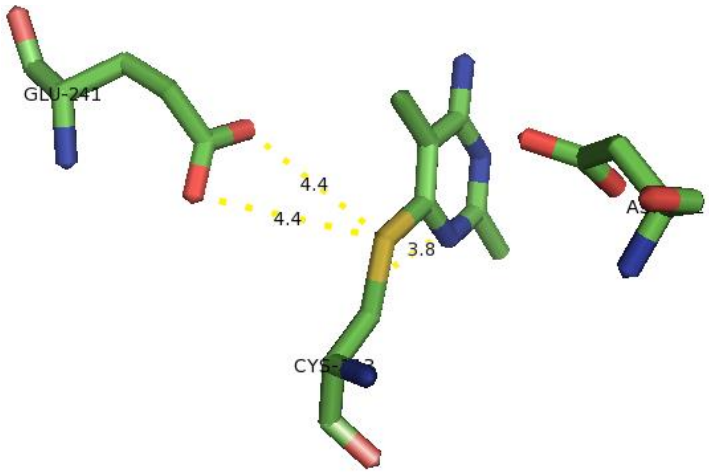

Figure 1.4: Crystal structure of Bt-Thiaminase I active site.

A new thiaminase-I is discovered in *Clostridium botulinum* associated with the biosynthetic gene cluster of Bacimethrin, a thiamin antivitamin.[26] It has 51% sequence identity with Bt-thiaminase. The catalytic cysteine residue was identified by sequence

alignment with other thiaminase-I(s) and it was mutated to design an inactive enzyme. The mutant enzyme was co-crystallized with the substrate thiamin and the first structure of thiaminase I complexed with substrate was reported by our collaborator Ealick research group from Cornell University.[27] This structure reveals the complete active site structure and the residues involved in binding and catalysis are identified. Kinetic studies on appropriately chosen mutants of these residues can confirm their roles in the catalysis assigned by the structural data providing a better understanding of the enzyme's mechanism. A search for the natural nucleophile of Cb-thiaminase I was also conducted. Primarily cysteine containing nucleophiles are screened against Cb-thiaminase to test whether some protein can act as the natural nucleophile for the thiaminase catalyzed reaction.

Thiaminase enzymes are responsible for numerous well-documented thiamin deficiency case studies involving humans, fish, horses, cattle, sheep, chickens, and foxes and appear to be globally distributed. However, the extent of thiaminase distribution on land and water and their physiological significance is still unclear. Considering the impact of thiamin deficiency caused by thiaminases upon the animal kingdom, the distributions and roles of these enzymes in the environment need greater clarification. To that end, unidentified soil bacteria from China, which showed thiamin catabolic properties were screened for thiaminase I activity. The subsequent discovery of new thiaminase I-producing bacteria is discussed herein.

1.2 Results

1.2.1 Active site architecture of the Cb-Thiaminase

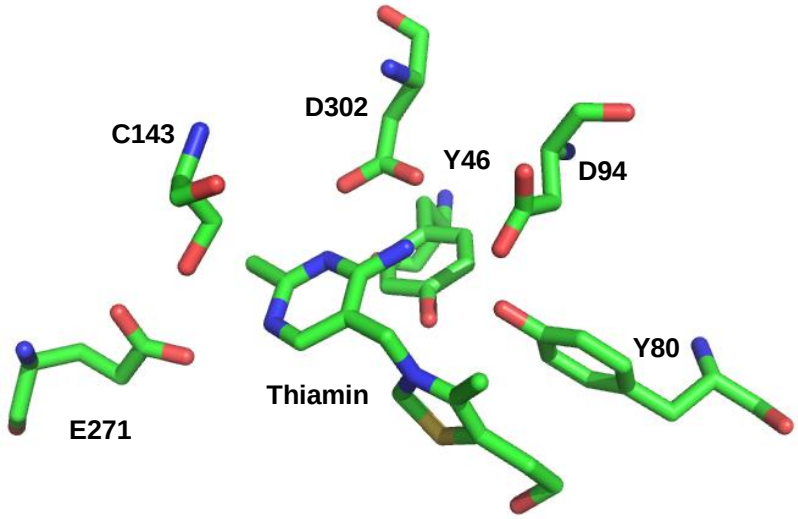

Figure 1.5: X-ray crystal structure of the C143S mutant of the Cb-Thiaminase active site with thiamin bound. All six catalytically active residues are shown. The structure gives a good indication of the positions of the residues around the substrate and their possible roles in the catalysis.

Our collaborator Ealick research group at Cornell University has determined the crystal structure of the Cb-thiaminase C143S with bound thiamin in the active site at 2.2 Å resolution. The structure of the protein appeared to be a dimer containing residues 39-404 for the first monomer and 40-404 for the second one. Size exclusion chromatography showed that Cb-thiaminase is a monomer in solution. This structure also clearly reveals the substrate-binding site (Figure 1.5). Each monomer has a thiamin molecule bound in its V-shaped cleft (dimensions: depth – 17 Å, length – 15 Å and width - 12 Å.). There are six tyrosine residues at the outer collar of the cleft, and most of the active site residues are located at the bottom of it. Thiamin binds to the active site in the F-conformation with

torsion angles of ϕT = −10° (C5′−C7′−N3−C2) and ϕP = −93.6° (N3−C7′−C5′−C4′) and the N3−C7′−C5′angle is 108°.[28] The dihedral angle between the planes of pyrimidine and the thiazolium ring is 85.9° suggesting that they are almost perpendicular to each other. The pyrimidine part is positioned towards the bottom of the binding pocket, and the thiazole part is pointed outward. The pyrimidine is in the hydrogen bonding distance with Asp302, Asp94 and Glu271 (Figure 1.6). However, the thiazolium group does not interact with the enzyme except through van der Waals contacts with the 5-hydroxyethyl group extended out toward the solvent region.

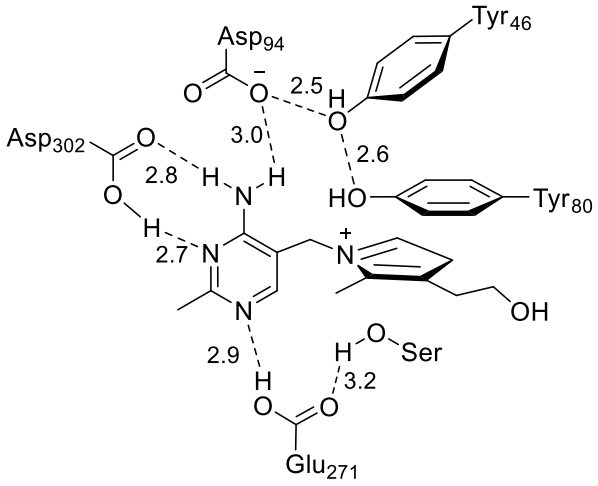

Figure 1.6: 2-dimensional representation of the Cb-Thiaminase active site. All distances are given in Å.

1.2.2 Reconstitution of wild-type Cb-thiaminase

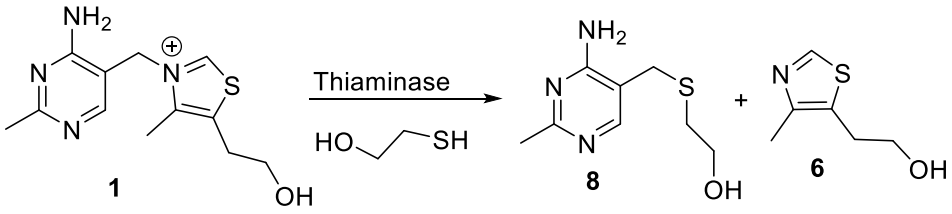

Scheme 1.2: Reaction used for the kinetic study of Cb-Thiaminase I

Mercaptoethanol was used as the nucleopile to study the kinetic proterties of Cb-Thiaminase I. Several reaction conditions were tried to optimize the activity for thiamin cleavage reaction (Scheme 1.2). The enzyme was found to be active at room temperature. The reaction was carried out in buffers of different pH and the highest k_{cat} was observed at pH 8.0 (Figure 1.7).

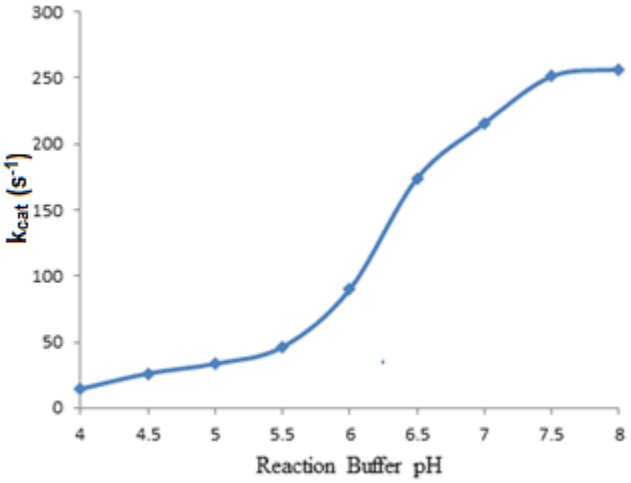

Figure 1.7: Plot of observed k_{cat} vs. pH of the reaction buffer. pH 8.0 shows a maximum value of k_{cat} reflecting highest activity.

The reaction mixture was analyzed by HPLC to observe the formation of the products. No product formation was observed in no enzyme or no thiamin control (Figure

1.8). Some product formation was observed in no thiol control due to the presence of ring-open thiamin in the reaction mixture.[20]

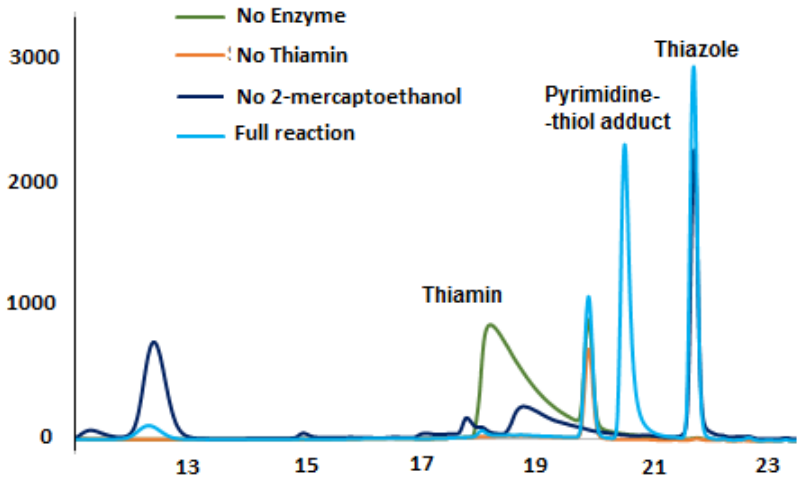

Figure 1.8: HPLC chromatogram of the Cb-Thiaminase reaction mixture with all controls.

1.2.3 Choice of active site mutants for kinetic characterization

All the active site residues were identified from the crystal structure. Six residues were found that are directly interacting with the substrate molecule or the residues involved in the catalysis. Six mutants were prepared, and one of these six amino acids were mutated in each of them. All these mutants were overexpressed, and the kinetic parameters were determined. Role of each mutated amino acid was rationalized from the data.

List of mutants

- **CbThi1(pTHT) Y80F ------- (A)**
- **CbThi1(pTHT) C143S ------ (B)**
- **CbThi1(pTHT) D302N ------ (C)**
- **CbThi1(pTHT) E271Q ------ (D)**
- **CbThi1(pTHT) Y46F ------- (E)**
- **CbThi1(pTHT) D99N ------ (F)**

1.2.4 Steady-state kinetics of the wild-type enzyme

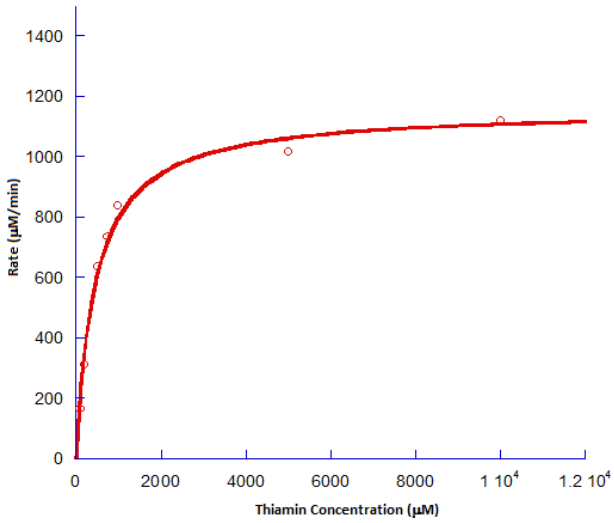

Figure 1.9: Steady-state kinetics of the cleavage of thiamin catalyzed by wild type enzyme. Assays were carried out in 0.1 M potassium phosphate buffer, pH 8.0, 0.1 M KCl, in the presence of 713 mM 2-mercapto ethanol and 0.1 µM enzyme. The k_{cat} value was recorded as 230 ± 11 s^{-1} and the K_M for thiamin was 452 ± 50 uM

The k_{cat} and the K_M of the wild-type enzyme were measured and used as the standard with which kinetic constants of all other mutants were compared. The wild-type

enzyme was the fastest among all the mutants with the highest k_{cat} value of ~ 230 s^{-1}. The role of each active site residue in the catalysis was deduced by comparing the k_{cat} of the corresponding mutant with the wild type.

1.2.5 C143S mutant of Cb-Thiaminase I

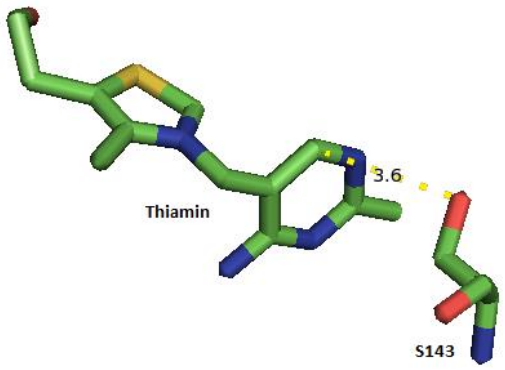

Figure 1.10: Position of the Cysteine-143 in the active site. C143 is mutated to serine to get a substrate bound crystal structure in C143S mutant

C143 is the key catalytic residue in Cb-Thiaminase I (Figure 1.10). It adds to the C6 of the pyrimidine ring by a nucleophilic addition reaction and forms a covalent adduct. This activates the thiamin molecule and displaces the thiazole moiety. Addition of an external nucleophile takes place after that. When C143 is mutated to serine, the enzyme appears to be non-functional and no product formation was detected by HPLC after 4 hours of incubation. As serine is not as nucleophilic as cysteine, the activation of the pyrimidine ring of thiamin molecule cannot happen. However, serine is the closest amino acid to cysteine regarding size and shape, so it does least perturbation to the active site

geometry. Thus the thiamin bound crystal structure of this mutant protein gives the most accurate and reliable structure of the active site.

1.2.6 Y80F mutant of Cb-Thiaminase I

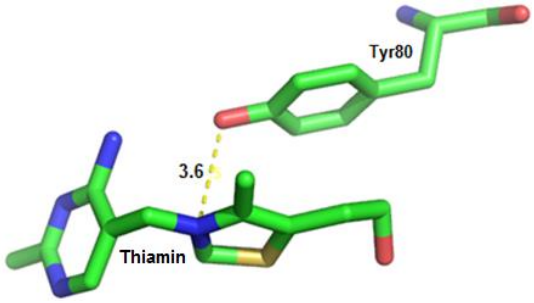

Figure 1.11: Position of Y80 in the active site. The stacking alignment right in parallel to the thiazole ring of the thiamin showing a possibility of potential electrostatic interaction of its hydroxyl group with the positively charged nitrogen. Hydrogen bonding interaction with D94 and Y46 is also evident.

Tyr-80 is the unique residue in the active site whose phenyl ring stays in parallel to the thiazole ring of the thiamin molecule (Figure 1.11). Such critical positioning of this residue initially suggested a pi stacking type interaction between the two aromatic systems. Corresponding phenylalanine mutant should sustain this interaction and not much difference in the kinetic constants was expected. However, the increment of the K_M to 2 ± 0.1 mM in this mutant ruled out that possibility, indicating a different type of interaction between the tyrosine and substrate thiazolium. A closer look on the structure revealed that the oxygen atom of the phenolic hydroxyl group of this tyrosine is directly over the thiazole ring nitrogen, and the distance is 3.6 Å (Figure 11). Both the structural and the kinetic data leads to the proposal that the oxygen atom of Y80 hydroxyl group

electrostatically interacts with the positively charged thiazolium ion. The resulting binding energy is used for substrate binding and catalysis. After the detachment of the thiazole ring from thiamin, the positive charge on it is lost, and Y80 also loses hydrogen bonding with D94 facilitating the departure of thiazole as a product.

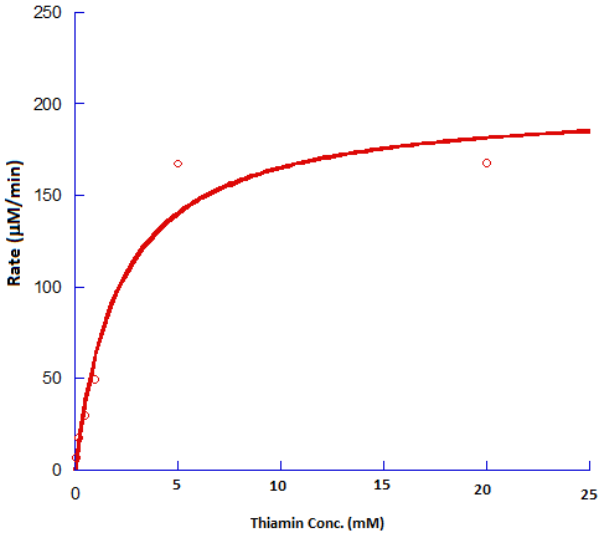

Figure 1.12: Steady-state kinetics of thiamin cleavage by 2-mercapto ethanol catalyzed by Y80F mutant. 0.1 M potassium phosphate buffer, pH 8.0, 0.1 M KCl, in the presence of 713 mM 2-mercapto ethanol and 3.1 µM enzyme. The k_{cat} value was recorded as 1.1 ± 0.1 s^{-1} and the K_M for thiamin was 2 ± 0.1 mM.

1.2.7 D302N mutant of Cb-Thiaminase I

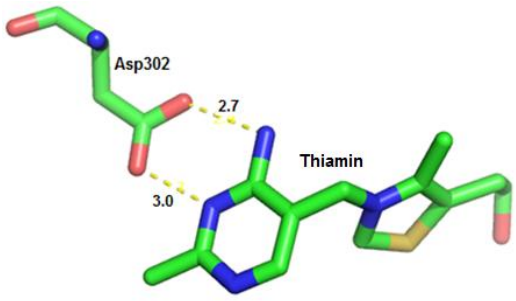

Figure 1.13: Position of D302 in the active site. Hydrogen bonding type interaction observed between the aspartate and the pyrimidine N-3 of thiamin.

Asp-302 is situated in a hydrogen bonding distance from both the N-3 and the C-4 amino group of the pyrimidine ring of bound thiamin (Figure 1.13). The hydrogen bonding capabilities of aspartate and asparagine for the pyrimidine ring nitrogen atoms are similar, which is reflected in the similarity in the K_M value between wild-type enzyme and D302N mutant (Table 1.1). A small decrease in K_M is observed as the substrate spends more time in the active site due to slow reaction rate (Figure 1.14). However, the k_{cat} value is decreased by 28 fold which indicates its involvement in catalysis. It forms hydrogen bond type interaction with pyrimidine ring nitrogen making the ring more electron deficient, and thus activates the ring for the nucleophilic addition of C143 at C6. The activation process takes higher energy for the amide compared to the acid due to the difference in hydrogen bond energy, and that makes the rate slower.

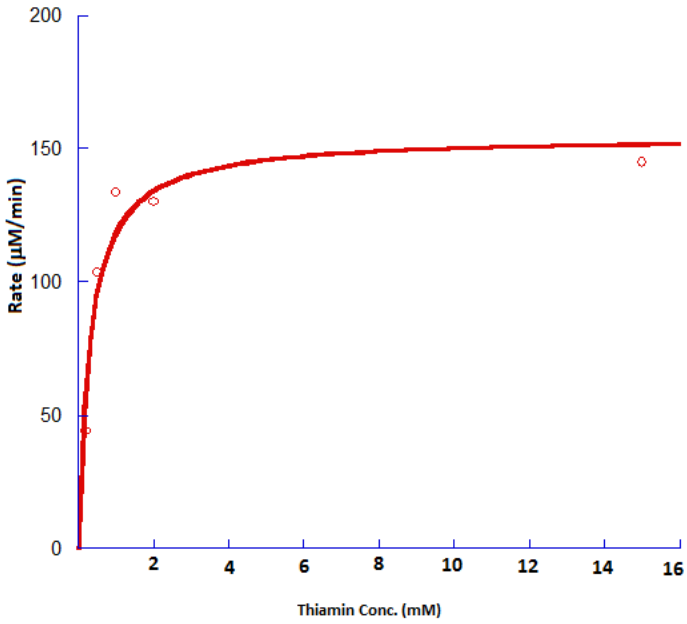

Figure 1.14: Steady-state kinetics of thiamin cleavage by 2-mercapto ethanol catalyzed by D302N mutant. 0.1 M potassium phosphate buffer, pH 8.0, 0.1 M KCl, in the presence of 713 mM 2-mercapto ethanol and 0.3 µM enzyme. The k_{cat} value was recorded as 8.1±0.7 s^{-1} and the K_M for thiamin were 0.3 ± 0.1 mM

1.2.8 E271Q mutant of Cb-Thiaminase I

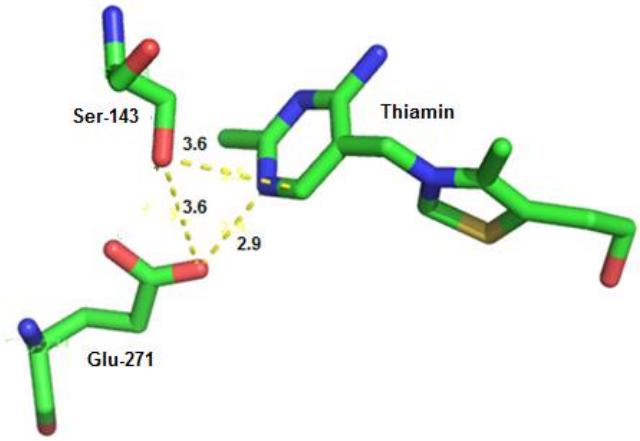

Figure 1.15: Position of E271 in the thiamin bound structure. The cysteine has been mutated to serine. It is in hydrogen bonding distance from both the substrate and the catalytic cysteine.

This mutant has a comparable K_M value with the wild type enzyme however, a large decrease in the k_{cat} value is observed. The structure shows that Glu-271 is within the hydrogen bonding distance from the N-1 of the substrate thiamin and the thiol group of the cysteine (Figure 1.15). However, this dipolar interaction would be present with glutamine as well. Glu-271 has a dual function in the catalysis. It serves as the base to C143 and generates the sulfide nucleophile and acts as an acid to protonate the N1 of the pyrimidine. Decrease in k_{cat} value in the order of four reflects the big difference in the proton abstraction capability between glutamate and glutamine from the thiol group and thus its importance in the catalysis. The decrease in K_M value is consistent with K_M approaching K_d when the chemical steps are retarded.

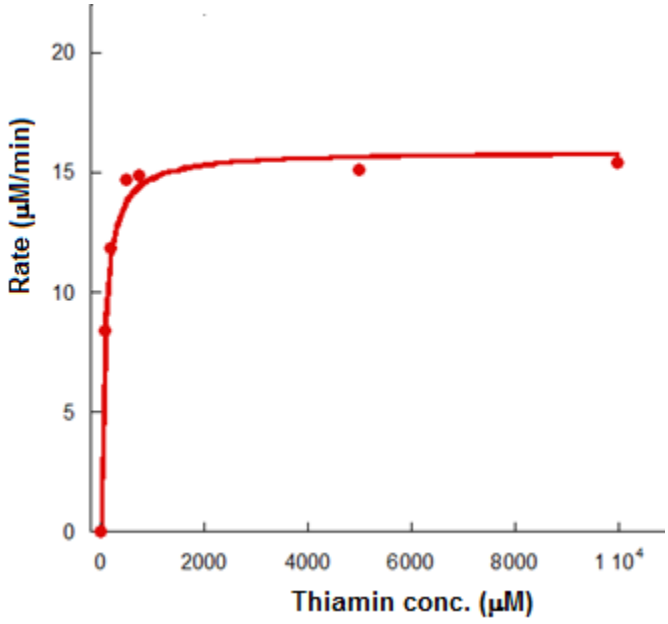

Figure 1.16: Steady-state kinetics of thiamin cleavage by 2-mercapto ethanol catalyzed by E271Q mutant. 0.1 M potassium phosphate buffer, pH 8.0, 0.1 M KCl, in the presence of 713 mM 2-mercapto ethanol and 23.6 µM enzyme. The k_{cat} value was recorded as (11 ± 0.3) x 10^{-3} s^{-1} and the K_M for thiamin was 75 ± 12 µM.

1.2.9 Y46F mutant of Cb-Thiaminase I

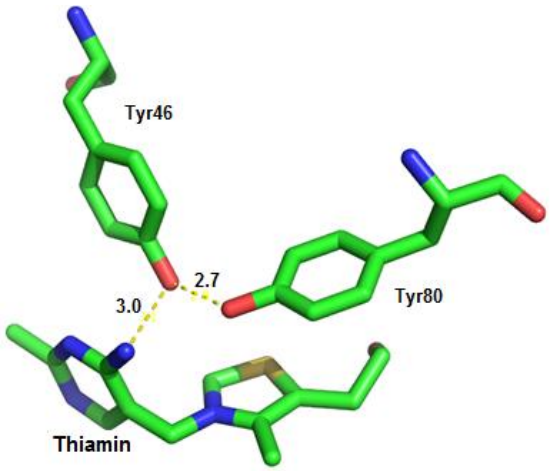

Figure 1.17: Position of Tyr 46 in the active site. The distance between Y46 and Y80 is suitable for hydrogen bonding.

Minimal effect on k_{cat} and K_M was observed upon mutating Tyr-46 to phenylalanine. The structure shows that the Tyr-46 phenolic hydroxyl group is in hydrogen bonding distance with the Tyr-80 phenol (Figure 1.17). The residue is most likely to modulate the pKa of Y80. There is an only four-fold decrease in the k_{cat} value indicating that Tyr80-Tyr46 hydrogen bond is not critical in the catalysis. A ten-fold increase in the K_M value suggests its importance in controlling the electrostatic interaction between Tyr-80 and the substrate. It may have some effect on Asp-302 protonation state as the distance between them is only 4.0 A.

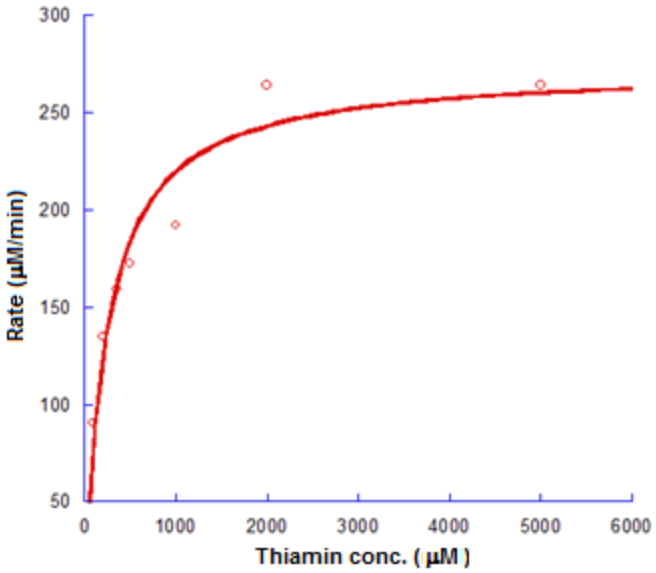

Figure 1.18: Steady-state kinetics of thiamin cleavage by 2-mercapto ethanol catalyzed by Y46F mutant in 0.1 M potassium phosphate buffer, pH 8.0, 0.1 M KCl, in the presence of 713 mM 2-mercapto ethanol and 0.07 µM enzyme. The k_{cat} value was recorded as 61 ± 4 s^{-1} and the K_M for thiamin was 240 ± 50 µM.

1.2.10 D94N mutant of Cb-Thiaminase I

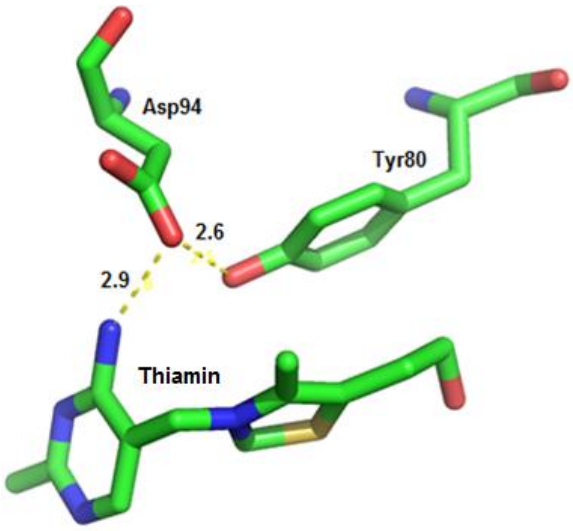

Figure 1.19: Position of the D94 residue in the structure. Possible hydrogen bonding distance with Y80 phenol and the pyrimidine C4' amino group is shown.

D94 deprotonates the C4 amino group of the thiamin pyrimidine and activates it for the expulsion of thiazole (Figure 1.19). It also reprotonates the pyrimidine-imine in concert with the addition of the nucleophile to the methylene group. Since the proton abstraction step is obstructed in this mutant, a big change in k_{cat} is highly expected. It is presumed to play some role in the initial steps of substrate binding by hydrogen bond formation with the hydroxyl group of Tyr80 thereby accumulating partial negative charge on the oxygen and this interaction is lost in the mutant.

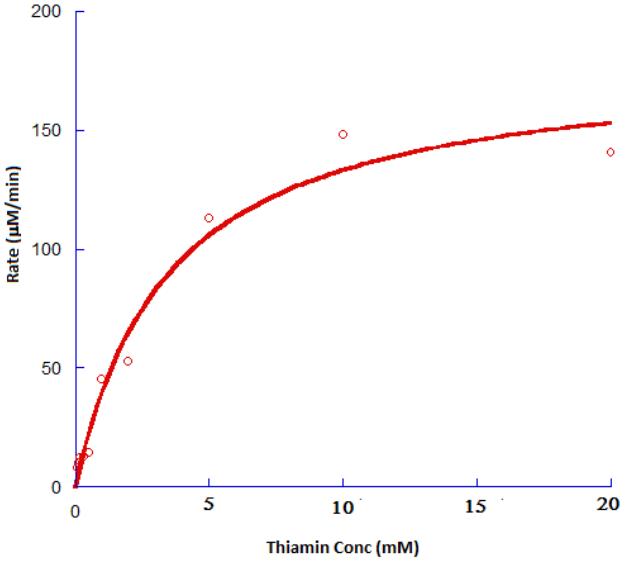

Figure 1.20: Steady-state kinetics of thiamin cleavage by 2-mercapto ethanol catalyzed by D94N mutant. 0.1 M potassium phosphate buffer, pH 8.0, 0.1 M KCl, in the presence of 713 mM 2-mercapto ethanol and 13 µM enzyme. The k_{cat} value was recorded as 0.23 ± 0.02 s^{-1} and the K_M for thiamin was 3.5 ± 0.8 mM.

Table 1.1: Kinetic properties of thiaminase activity for Cb-Thiaminase I and six active site mutants

Mutant	K_{cat} (s^{-1})	K_M (M)	K_{cat} / k_M ($M^{-1}s^{-1}$)
WT	230 ± 11	(452 ± 50) x 10^{-6}	(51 ± 6.2) x 10^{4}
C143S	-	-	-
Y80F	1.1 ± 0.1	(2 ± 0.1) x 10^{-3}	550 ± 57
D302N	8.1 ± 0.7	(0.3 ± 0.1) x 10^{-6}	(27 ± 9.3) x 10^{3}
E271Q	(11 ± 0.3) x 10^{-3}	(75 ± 12) x 10^{-6}	150 ± 24
Y46F	61 ± 4	(240 ± 50) x 10^{-6}	(25 ± 5.6) x 10^{4}
D94N	(23 ± 2) x 10^{-2}	(3.5 ± 0.8) x 10^{-3}	70 ± 16

1.2.11 Search for the natural nucleophile of thiaminase I

All the nucleophiles that thiaminase I was tested with, are primarily synthetically prepared organic compounds. However, in the natural habitat, it must use some nucleophile that is available in the environment. Pyridoxal was reported as a nucleophile for Bt-thiaminase I, which is a naturally occurring cofactor, however, keeping the efficiency of thiol-containing nucleophiles in mind cysteine and cysteine-containing peptides are the obvious guesses as a natural nucleophile. Cysteine, methyl ester of cysteine and N-acetyl cysteine were all accepted as a nucleophile by Cb-thiaminase I while the methyl ester of cysteine showed highest efficiency and N-acetyl cysteine showed the

lowest (Figure 1.21). There was no selectivity between D and L-cysteine by Cb-thiaminase I while choosing them as nucleophiles.

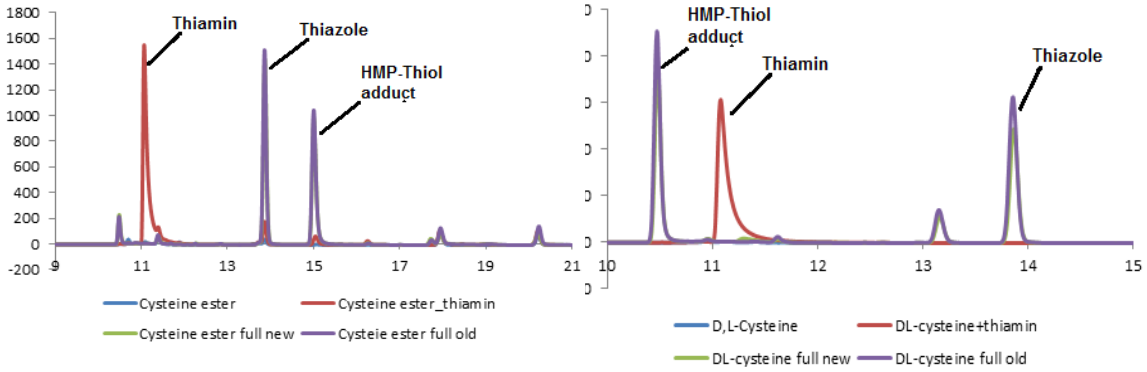

Figure 1.21: HPLC Chromatogram of the reaction of thiamin with Cysteine and cysteine ester as a nucleophile for Cb-Thiaminase.

After observing the acceptance cysteine and its derivatives as nucleophiles, we looked towards cysteine containing peptides. Small peptides with cysteine in the terminal position and non-terminal positions were tested. In both cases, consumption of the substrate and formation of new product confirms their acceptance as nucleophiles (Figure 1.22).

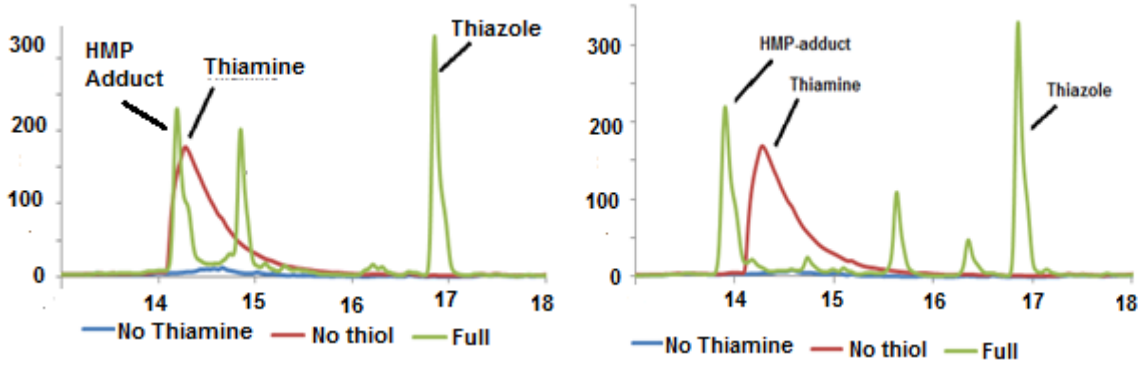

Figure 1.22: HPLC Chromatogram of the reaction of thiamin with Cysteine-containing peptides B) Gly-Cys-Gly-Gly as a nucleophile for Cb-Thiaminase I.

1.2.12 Development of a methodology to identify thiaminase secreting bacteria

Our collaborator Dr. Xiaohong Jian provided soil bacteria from locations in the United States and China with apparent thiamin catabolic properties. They were categorized "EK1 (1.1-1.8)", "EK2 (2.1-2.2)", and "EK3 (3.1-3.5)" depending on their source of origin. The bacteria were further screened for thiamin degrading properties both individually and in groups using a previously reported diazonium reagent with overlaid soft agar technique.[29] The plate assay gave clear and easily interpretable positive results, as reported with known thiaminase I producer *Bacillus thiaminolyticus* (Figure 1.23A) and *Burkholderia thilandensis* (Figure 1.23B) and an appropriately negative result for E. coli as a negative control. However, the results obtained for the experimental strains were at times unreproducible and difficult to interpret. A new methodology based on HPLC analysis was therefore developed to identify thiaminase I activity more directly.

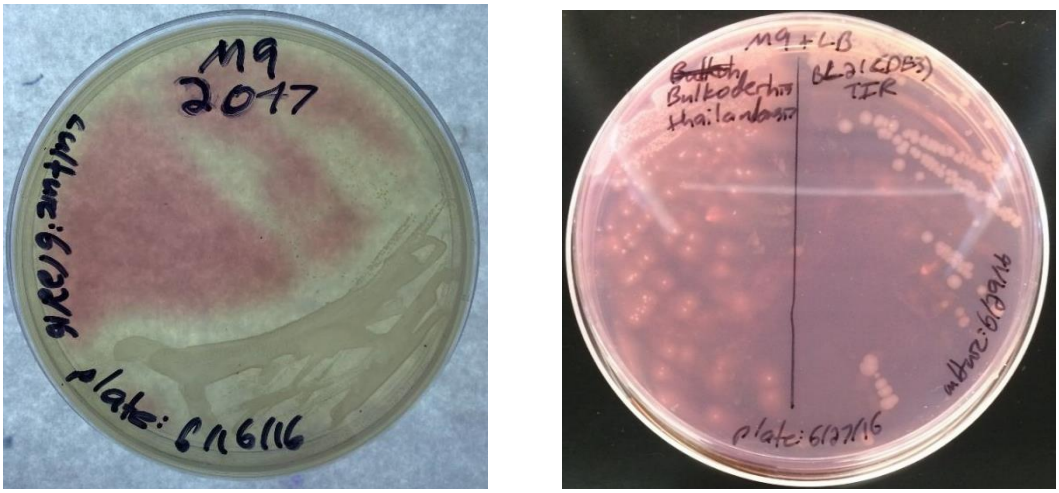

Figure 1.23: A) Plate assay with *Bacillus thiaminolyticus.* B) Comparison of thiaminase-producing *B. thailandensis* colonies vs. *E. coli* colonies in the plate assay. Degradation of thiamin (yellow halo around the colonies) is observed for thiaminase producing strains.

To carry out the HPLC assays, the sets of unknown bacteria were grown individually and in combinations, in minimal media in the presence of thiamin and 2-mercaptoethanol. After the growth, filtered media was analyzed by HPLC to observe any thiaminase activity. As thiaminase enzyme is secreted outside, it will catalyze the reaction between thiamin and the thiol to produce thiazole as a product. *E. coli* culture was used as the control, and the blank media was also tested. The thiamin degradation was normalized by cell density in the culture. Figure 1.24 summarizes the results of the HPLC analysis. It has been observed that EK 1.4, EK-3.3 and EK-3.5 are the only three strains that showed moderate thiaminase activity when grown individually. The combination of several EK strains exhibited degradation of thiamin more efficiently, suggesting some intercellular signaling for thiamin secretion (Figure 1.24). Further investigations are underway to identify the thiaminase gene and downstream catabolic pathway.

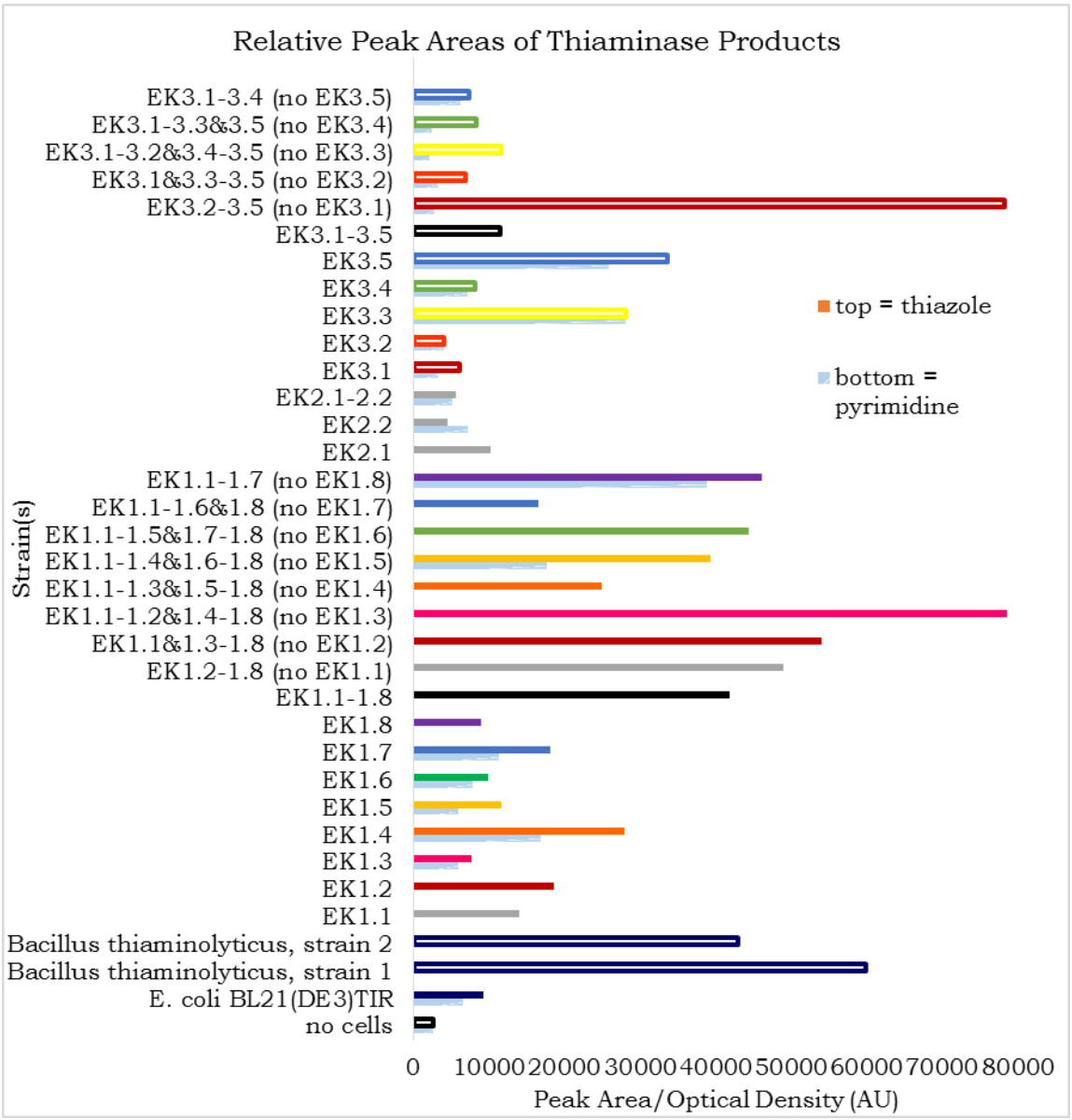

Figure 1.24: Normalized peak area of the produced thiazole in the HPLC assays

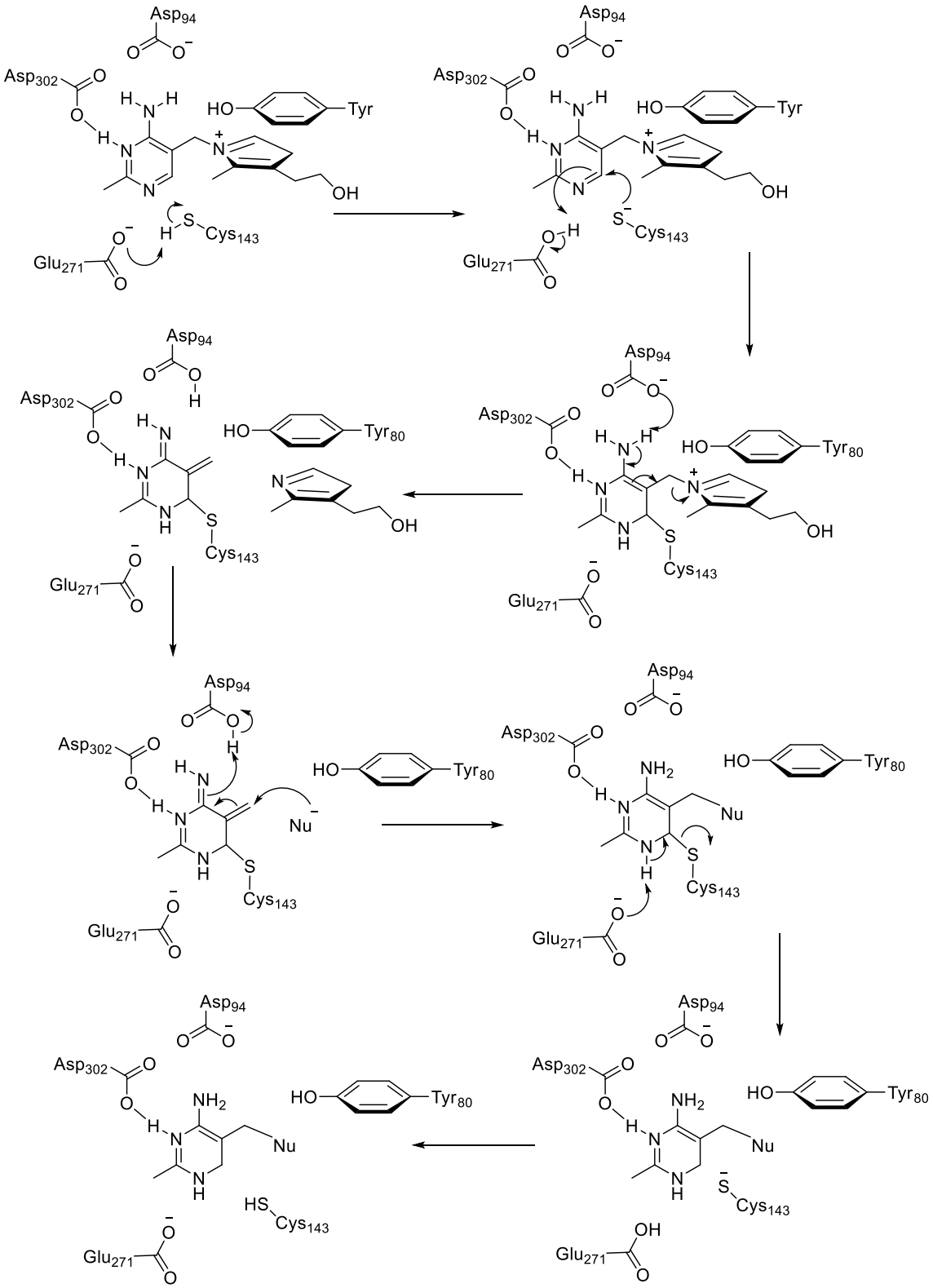

Figure 1.25: Proposed mechanism based on the structural and the kinetic data.

1.3 Discussion

The reaction catalyzed by Cb-thiaminase I follows a ping-pong type mechanism. Firstly, a nucleophilic attack by the active site cysteine takes place on the substrate and the thiazole moiety leaves. It is followed by the addition of an external nucleophile on the pyrimidine moiety to form the pyrimidine-nucleophile adduct. Based on the positions of the active site residues and the kinetic data of the mutants, a detailed mechanism of the reaction is proposed (Figure 1.25). At the beginning of the catalytic cycle, D94 stays in an anionic form, which can form a hydrogen bond with the Tyr80 phenol. Y46 also forms a hydrogen bond with Tyr80 phenolic hydroxyl group. These two interactions make the Tyr80 hydroxyl oxygen partially negative and anchor it in a position where it can bind to the thiazolium of thiamin electrostatically and can hold it in a position perpendicular to the plane of the pyrimidine moiety perfect for its departure as a leaving group. Asp302 binds at the N3 atom of thiamin pyrimidine in the active site by forming hydrogen bond and activates the ring for nucleophilic attack. Glu-271 deprotonates the cysteine creating a free sulfide nucleophile which then attacks the C-6 of the activated thiamin pyrimidine forming a covalent linkage. After D94 abstracts a proton from the amino group of thiamin the hydrogen bonding with Y80 is lost, and the electrostatic interaction between Y80 and thiazolium is disrupted. Loss of the stabilization factor facilitates the departure of thiazole as a leaving group. Finally, an external nucleophile attacks at the electrophilic methylene carbon and all the catalytic steps are reversed. After the release of pyrimidine product, the enzyme becomes ready for its next cycle (Figure 1.25).

Cb-thiaminase I accepts cysteine, its derivatives and oligopeptides with cysteine in both the terminal and non-terminal position as nucleophiles for thiamin cleavage. This observation indicates that some cysteine or thiol containing natural products like glutathione or a peptide with an exposed cysteine residue can act as the natural nucleophile for thiaminase I. Thiaminase producing bacteria secrete the enzyme, which can then cleave thiamin in the surrounding in the presence of an external nucleophile. Degradation of thiamin can be detected by analyzing the growth media with HPLC. Three new putative thiaminase-producing strains were detected using this newly developed HPLC assay. This observation will potentially contribute towards the identification of the thiaminase gene and discovery of the first thiamin catabolic pathway in bacteria.

1.4 Experimental Methods and Materials

1.4.1 Cloning, overexpression and purification of Cb-Thiaminase I

Our collaborator Ealick research group cloned the thiaminase I gene bcmE from C. botulinum str. ATCC 19397.The gene was inserted into pTHT, a modified pET-28 plasmid containing a tobacco etch virus (TEV) protease cleavage site after the N-terminal His_6 tag. Standard PCR-based site-directed mutagenesis protocol was used to construct all the mutants.[30]

The plasmid containing the bcmE or mutant gene was transformed into E. coli BL21(DE3) cells and were grown in kanamycin (40 μg/mL) containing agar. Starter cultures (15 mL) were grown from single colony overnight at 37 ^{o}C. To grow larger cultures, 10 mL of the starter culture was added directly to 1.5 L of sterile LB media and

were shaken at 37 ^{o}C until OD_{600} reaches 0.6. The incubator temperature was reduced to 15 ^{o}C and isopropyl β-D-1-thiogalactopyranoside (IPTG) was added to a final concentration of 0.5 mM to initiate protein overexpression. After 18 hours of shaking at 15 ^{o}C, the cells were harvested by centrifugation at 5000 rpm for 15 minutes. The cell pellet was collected after discarding the spent media and stored at -80 ^{o}C.

The cell pellet was later thawed and resuspended in 45 mL of lysis buffer (100 mM KPi, 150 mM NaCl, ten mM imidazole, pH 7.8) containing 20 mg lysozyme, and lysed by sonication. The lysed cells were then centrifuged at 15000 rpm for 30 min at 4 ^{o}C. After discarding the cell debris, the supernatant was loaded onto a five mL Ni-Nitrilo acetic acid column, freshly charged and preincubated with lysis buffer. The column was washed with 45 mL of the lysis buffer, 4 column volume of the wash buffer (100 mM KPi, 150 mM NaCl, 50 mM imidazole, pH 7.8) and then the protein was eluted with 2 column volumes of the elution buffer (100 mM KPi, 150 mM NaCl, 2000 mM imidazole, pH 7.8). The purity of the protein fractions was checked by SDS-PAGE gel. The pure fractions were pooled and concentrated and buffer exchanged with the storage buffer (100 mM KPi, 150 mM NaCl, 15% glycerol, pH 7.5). The purified protein was stored in 100 μL aliquots at -80 ^{o}C freezer.

1.4.2 Determination of the kinetic parameters

Steady state kinetic analysis was performed for six Cb-thiaminase I mutant proteins that were selected on the basis of the crystal structure of the C143S/thiamin complex. Reactions were carried out in 100 mM potassium chloride and 50 mM phosphate

buffer at pH 8.0 using 713 mM β-mercaptoethanol as the exogenous nucleophile. For the pH profile of the enzymatic reaction, sodium acetate – acetic acid buffer system was used for the pH range 4.0 – 5.5. All reactions were incubated at 25 °C except the E271Q Cb-thiaminase I, which was measured at 37 °C due to low activity levels. The reactions were initialized by the addition of enzyme to the reaction volume containing thiamin, with thiamin concentrations ranging from 100 μM to 20 mM. Aliquots were taken from the reaction mixture after defined time intervals, quenched with 1 M HCl, neutralized, filtered through a 10 000 Da cutoff membrane to remove the enzyme and analyzed by HPLC. In the HPLC method, the ratio of 100 mM phosphate buffer at pH 6.6 (P) to methanol (M)/water mixture was varied over time in minutes (t). The gradient was carried out following the scheme (t, M%, H2O%, P%): (0, 0, 0, 100), (5, 0, 10, 90), (9, 15, 25, 60), (14, 65, 20, 15), (19, 0, 0, 100), (25, 0, 0, 100). Peak areas of the product in the enzyme e assays were measured and the concentrations were calculated based on a calibration curve relating peak area to 4-methyl-5-hydroxyethylthiazole concentration. The initial rates were calculated from plots of product concentration against time. Initial rates were then plotted and fit to the Michaelis−Menten equation for calculation of kinetic parameters.

1.4.3 Assay condition to explore cysteine containing nucleophiles

Reactions were carried out in 100 mM potassium chloride and 50 mM phosphate buffer at pH 8.0 using various cystenyl nucleophiles with the final concentration of 10 mM The reactions were initialized by the addition of enzyme to the reaction mixture containing 1 mM thiamin. All reactions were incubated at 37 °C for 2 hours and then the

reaction was quenched with 1 M HCl, neutralized, filtered through a 10 000 Da cutoff membrane to remove the enzyme and analyzed by HPLC.

1.4.4 Plate assays for the detection of thiaminase secreting bacteria

Cultures were either streaked directly onto agar plates from glycerol stocks or first grown overnight in LB liq-uid medium before streaking. Plates were incubated at 37oC until sufficiently grown (approximately 1-2 days in most cases). Approximately 8 mL soft agar composed of 3 mM thiamin hydrochloride, 6 mM pyridoxine (vitamin B6), 0.5% Difco agar noble, and 25 mM Na2HPO4 at 6.5 pH at roughly 37oC was poured onto each plate and let solidify. Plates were then incubated for either 1 hour or 3 hours at 37oC. The diazonium reagent reported by Abe *et al.* was made, and approximately 8.5 mL of the final rea-gent was poured onto each plate at room temperature immediately after preparation and decanted after 5 minutes.[16] p-Acetylphenyldiazonium in the solution re-acts with deprotonated 1 as shown in Scheme 3 to produce a purple-red color. Yellow regions or haloes of less intense purple-red color around colonies than in regions of no growth therefore indicated potential thiamin degradation according to literature precedent. Absence of any halo indicated no thiamin degradation.

1.4.5 HPLC assay for the detection of thiaminase secreting bacteria

Cultures were grown from glycerol stocks in 5 mL LB liquid medium overnight at 37oC in a shaking incubator. The cultures were then centrifuged at 5,000 rpm and 23oC for 5 minutes, decanted, and resuspended in 1 mL M9. They were again centrifuged,

decanted, resuspended in 1 mL M9, centrifuged, and decanted. The cells were resuspended in the minimal volume of M9 necessary to provide 100 μL aliquots for each subsequent sample. 100 μL aliquots were transferred to 5 mL liquid M9 medium with 1 mM MgSO4, 0.1 mM CaCl2, 0.0625 g/mL glucose, 5 mM 2-mercaptoethanol, and 20 mM thiamin chloride unless otherwise indicated for approximately 48 hours at 37°C in a shaking incubator. For combinations of individual strains, the strains were grown separately in LB and then 100 μL aliquots of each were transferred into the same tube to make the combination samples. After approximately 48 hours incubation, the optical density of each sample at 600 nm was recorded and aliquots were centrifuged at 15,000 rpm and 4°C for 20 minutes. Su-pernatants were stored at 4°C and then centrifuged after thawing at room temperature for an additional 20 minutes at 15,000 rpm and 4°C before analysis via HPLC.

In the HPLC method, the ratio of 100 mM phosphate buffer at pH 6.6 (P) to methanol (M)/water mixture was varied over times in minutes (t). The gradient was car-ried out following the scheme (t, M%, H2O%, P%): (0, 0, 0, 100), (7, 0, 10, 90), (12, 15, 25, 60), (22, 65, 25, 10), (25, 0, 0, 100). The HPLC column was an Agilent Eclipse XDB-C18 (5μm) 4.6 x 150 mm followed by a diode array detec-tor set to 250 nm for the analysis. To normalize cell density, peak areas at 17.8 and 18.8 minutes were obtained from the HPLC and divided by respective optical density.

CHAPTER II

MODIFIED SYNTHESIS OF 2'-METHOXYTHIAMIN PYROPHOSPHATE AND ITS COMPETENCE IN THIAMIN-DEPENDENT ENZYMES

2.1 Introduction to Bacimethrin

Bacimethrin (**4**), a structural analog of the thiamin pyrimidine, is a thiamin antagonist first isolated from *Bacillus megaterium*.[31] It exhibits antibiotic activity against a variety of yeast and bacteria.[32] It acts as a thiamin antagonist due to its conversion to 2'-methoxythiamin a thiamin analog inside the bacterial cell. Another bacterium *Streptomyces albus* also produces bacimethrin. Bacimethrin was harvested and purified from the culture medium of the bacteria suggesting that the compound is secreted outside the cell and released into the surrounding environment.[33] The toxicity of bacimethrin is due to the formation of 2'-methoxythiamin pyrophosphate by the endogenous thiamin biosynthetic genes. Due to the structural similarity with thiamin, 2'-methoxythiamin can inhibit a subset of essential enzymes that utilizes thiamin pyrophosphate as a cofactor. Addition of thiamin into the culture medium completely counteracts the toxicity caused by bacimethrin.[34]

2.1.1 Biosynthesis of bacimethrin

Cooper *et al.* identified the biosynthetic gene cluster, and characterized each of the enzymes involved in the pathway (Figure 2.1).[26]

Figure 2.1: Organization of genes in bacimethrin biosynthetic operon in *C. botulinum* A ATCC 19397. The genes were annotated based on homology – (3) glycosyltransferase (bcmB), (4) thymidylate synthase (bcmA), (5) methyltransferase (bcmC), (6) thiaminase-I (bcmE), (7) pyrimidine kinase (bcmD)

BcmA is a thymidylate synthase that catalyzes the hydroxymethylation of cytidine-5'-monophosphate (CMP, **1**) using methylene tetrahydrofolate as the co-substrate. BcmB is a nucleoside hydrolase that cleaves the N-glycosidic bond of **2** and produces 5-hydroxymethylcytosine (**3**). BcmC is a SAM-dependent nucleophilic methyltransferase that catalyzes the methylation of C-2 hydroxyl group of **3** to form bacimethrin (**4**) (Figure 2.2). BcmD is the bacimethrin pyrophosphokinase that pyrophosphorylates bacimethrin, which will then couple with thiazole phosphate inside the cell and can form 2'-methoxythiamin.

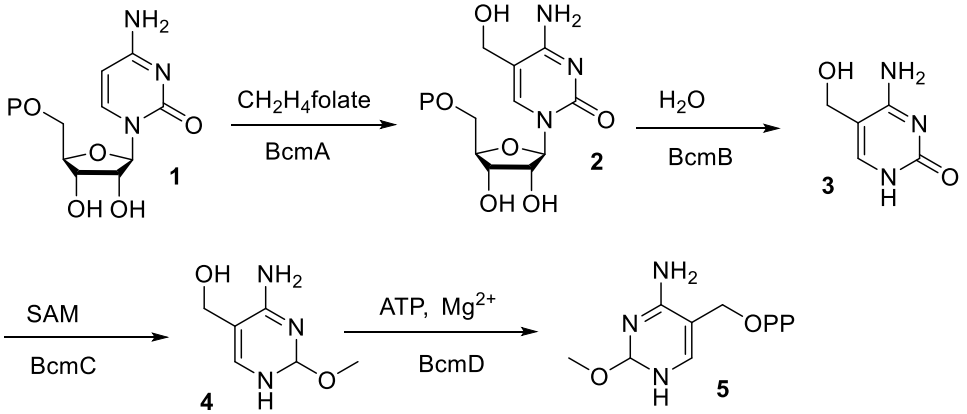

Figure 2.2: Steps involved in the bacimethrin biosynthetic pathway. The role of each enzyme is shown.

2.1.2 First reported synthesis of bacimethrin

Drautz *et al.* first reported the synthesis of bacimethrin.[33] The cyano-HMP (8) was prepared by the condensation of O-methyl isourea with ethoxymethylene malononitrile in the presence of sodium methoxide as a base (Scheme 2).[35] The obtained cyano-HMP was then reduced to formyl-HMP (9) using $LiAlH_4$ as a reducing agent. The final step was carried out using sodium borohydride for a further reduction of **9** to obtain bacimethrin (**4**).

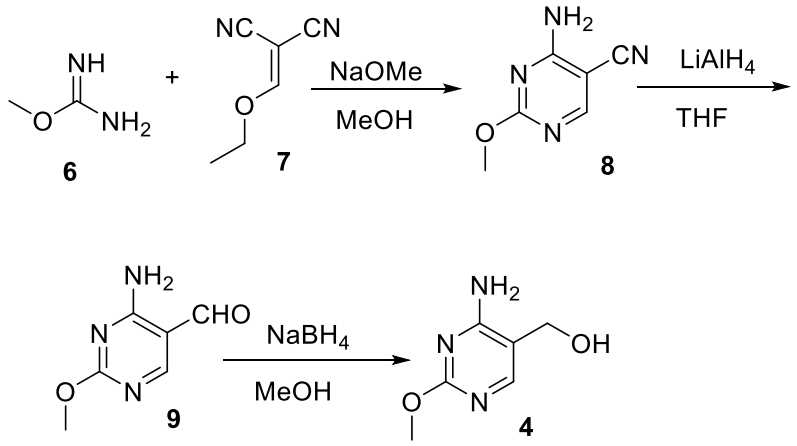

Scheme 2.1: Synthetic steps of Bacimethrin followed by Drautz et al.

Another synthetic method of 4-amino-5-hydroxymethyl-2-methyl pyrimidine was also reported in the literature with little changes in the reduction procedure.[36] This method can also be a good strategy to be employed for the synthesis of bacimethrin.

2.1.3 First reported synthesis of 2'-methoxythiamin

A synthetic scheme for bacimethrin was later reported in the literature, which was further extended to synthesize 2'-methoxythiamin.[37-38] The synthesis of cyano-HMP (**8)** was same as the previous method. In the next step, instead of $LiAlH_4$ reduction, a Palladium-charcoal catalyzed high pressure (45-50 psi) hydrogenation was performed in a Parr apparatus in acidic medium at room temperature for one hour to make the formyl-HMP (**9)**. However, if the same reaction was continued for three hours bacimethrin was formed as the product. A suspension of bacimethrin in THF was treated with diphenyl phosphoryl azide in the presence of DBU as a base to form azido-pyrimidine (**14**). **14** was then reduced to aminomethyl-pyrimidine (**15**) by Palladium-charcoal catalyzed hydrogenation at room temperature and pressure. This compound was used to synthesize methoxythiamin and the thiazole ring was constructed using a method originally developed for thiamin synthesis.[39]

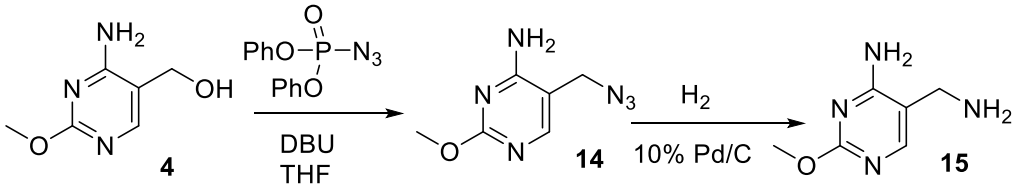

Scheme 2.2: Steps involved in the synthesis of 5-(aminomethyl)-2-methoxypyrimidin-4-amine

2.1.4 Enzymatic synthesis of methoxythiamin

Begley group has also demonstrated the synthesis of methoxythiamin phosphate from bacimethrin (**4**) and 5-hydroxyethyl thiazole (**10**) using thiamin biosynthetic

enzymes ThiD, ThiM, ThiE, and ThiL.[34] Bacimethrin (**4**) was synthesized using the reported method and it was pyrophosphorylated to **5** using the thiamin pyrimidine kinase ThiD. Similarly, thiazole ethanol (**10**) was also phosphorylated by ThiM and ATP to give **11**. These two were linked together using ThiE enzyme to form methoxythiamin phosphate (**12**). The formation of thiamin moiety was determined by highly sensitive thiochrome assay. A reaction catalyzed by ThiL enzyme converted the monophosphate to the methoxythiamin diphosphate (**13**).

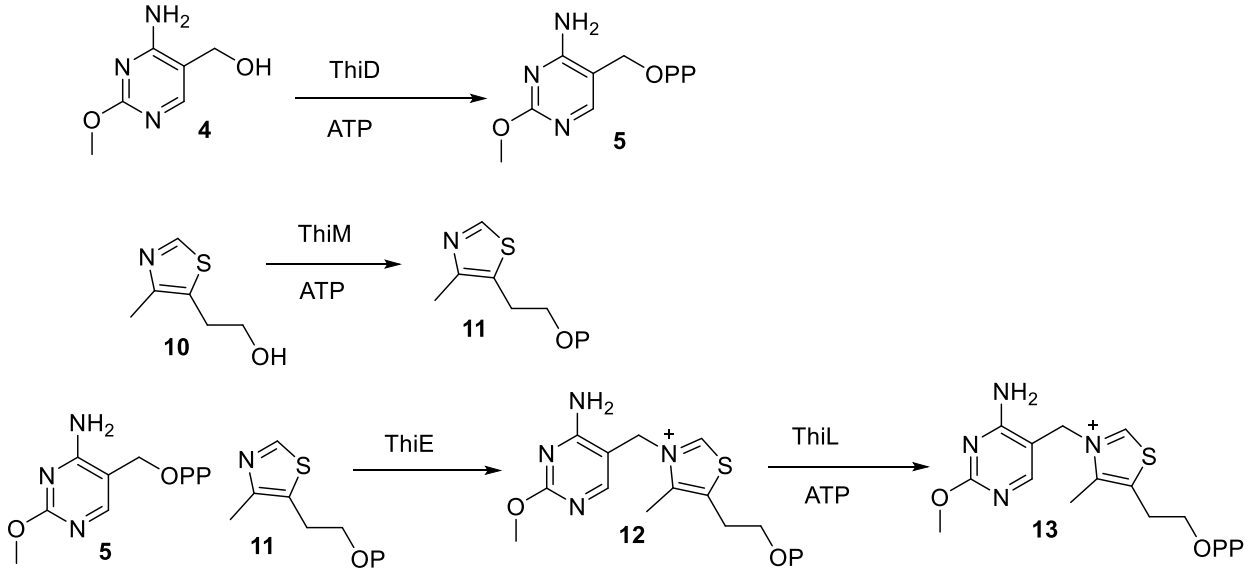

Scheme 2.3: Steps involved in the enzymatic semi-synthesis of 2'-methoxythiamin pyrophosphate**.**

2.2 Results

2.2.1 Modification of the methoxythiamin synthetic route

No *in vitro* experiment has been done yet to study the effect of methoxythiamin pyrophosphate on the thiamin-dependent enzymes. A collaboration was established with

Jordan research group in Rutgers University, NJ to develop a modified method of methoxythiamin synthesis and to study its effect of thiamin dependent enzymes *in vitro*. In this method, mouse thiamin pyrophosphokinase was used for the first time to pyrophosphorylate the synthesized compound.

2.2.2 Attempt to synthesize 2'-Methoxythiamin via direct coupling of the pyridine and thiazole moieties

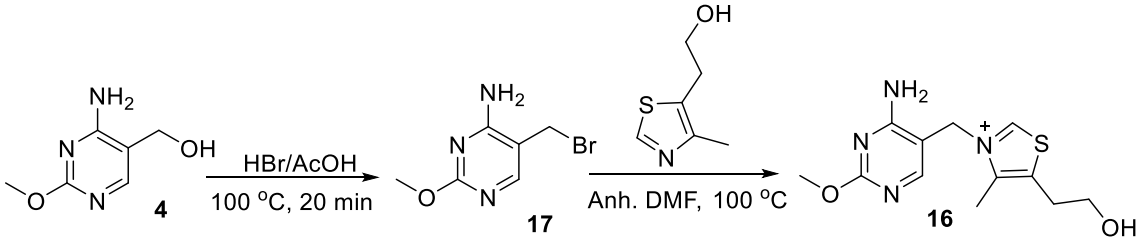

Scheme 2.4: Proposed synthetic scheme for the synthesis of methoxythiamin by coupling the corresponding pyrimidine bromide with thiazole.

The synthesis of methoxythiamin was originally planned using the coupling between the thiazole and the pyrimidine bromide (**17**). First, bacimethrin (**4**) was synthesized using the procedure reported in the literature.[33] of the Several attempts to synthesize the pyrimidine bromide (**17**) was made, however, the methyl aryl ether linkage was observed to be very unstable in acidic conditions at high temperature (Scheme 2.4). Hydrolysis of the methyl ether during the reaction yielded the hydroxyl pyrimidine. This strategy required modification for the successful synthesis of bacimethrin.

2.2.3 Modification of aminomethyl-pyridine synthesis

The synthesis of cyano-HMP (**8**) was performed following the literature procedure.[35] The previous synthesis of aminomethyl pyrimidine (**15**) required four synthetic steps after starting with cyano-HMP. An attempt was made to complete the synthesis only in one step. Reduction of cyano- pyrimidine by Raney nickel and hydrogen in high pressure was previously reported.[40] H-Cube continuous flow catalytic hydrogenator was used to carry out the reaction in our experiment.

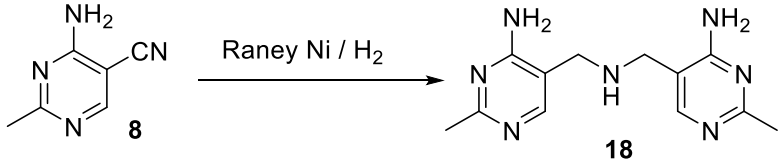

Scheme 2.5: Dimerization of pyrimidine during hydrogenation.

When the reaction was attempted in the absence of liquid ammonia, a new product was formed. It was later identified as the dimerized amino pyrimidine (**18**) (Scheme 2.5). The cyano- pyrimidine (**8**) is first reduced to the corresponding imine which was then further reduced to the amine. Not all the molecules are reduced up to the amine at the same time. The newly formed amines are now available to react with the imine form inside the reactor. As imines are very electrophilic, they undergo nucleophilic addition with the amines, followed by elimination of ammonia and a further reduction to form the dimer.

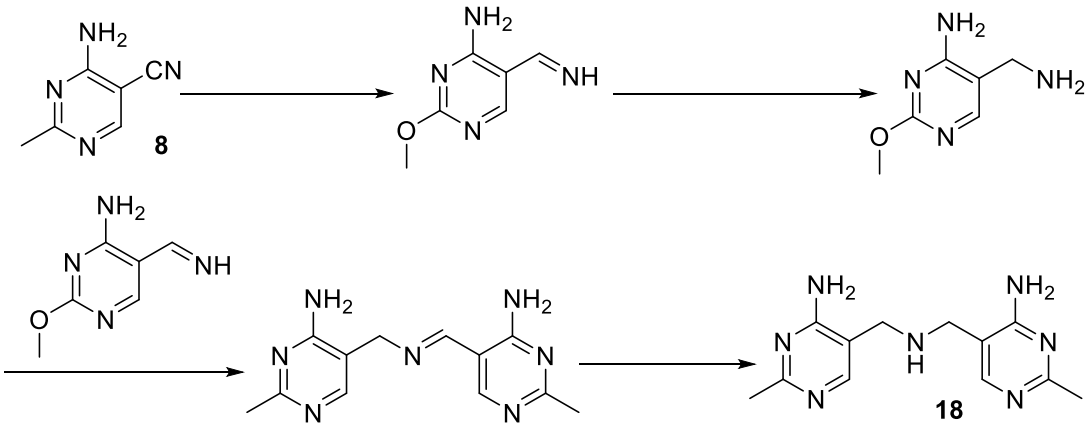

Scheme 2.6: Proposed steps involved in the formation of dimerized pyrimidine during the reduction of nitrile to an amino group by Raney Nickel-catalyzed hydrogenation**.**

This issue was later addressed by adding methanolic ammonia solution (7M) to the reaction mixture, so that the final concentration of ammonia becomes 1.4M. The ammoniacal solution of the **8** was passed through the hydrogenator at 70 ^{o}C and 60 bar using Raney Nickel as a catalyst.

2.2.4 Complete synthesis of 2'-Methoxythiamin pyrophosphate

The other precursor, compound **22**, was synthesized using little modification to the literature described method (Scheme 8B).[4] Acetyl butyrolactone (**20**) was chlorinated at room temperature using sulfuryl chloride followed by acid catalyzed decarboxylation to afford **21** which was further acetylated to produce **22**. The intermediate compound **24** was prepared by reacting **19** and **22** with carbon disulfide followed by acid catalyzed dehydration. The purification of the intermediate **23** was bypassed to avoid potential product loss in column chromatography. Oxidation of **24** with acidic hydrogen peroxide

affords 2'-methoxythiamin (**16**). After neutralization, the pH of the solution was adjusted to 4.0 and barium chloride was added to isolate the sulfate by-product.

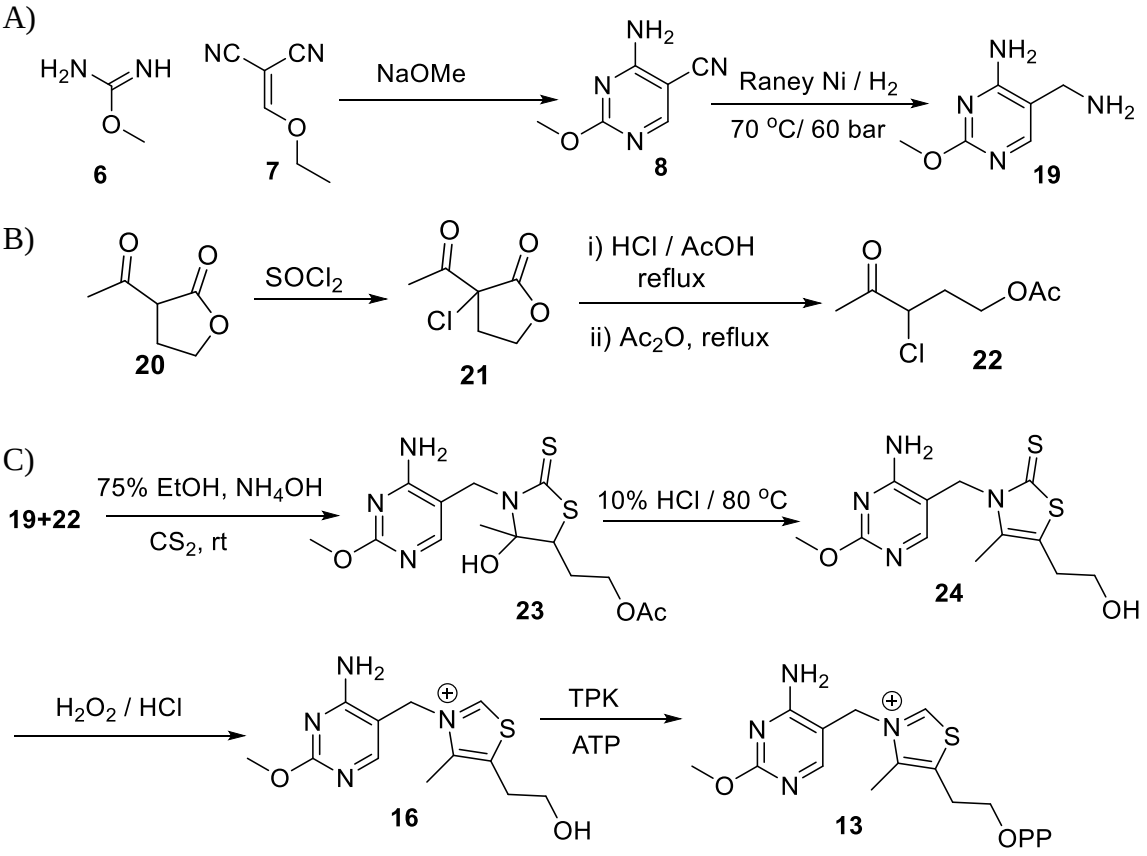

Scheme 2.7: A convergent synthetic route for methoxythiamin pyrophosphate. A) Synthesis of the pyrimidine part, B) synthesis of the thiazole precursor and C) coupling of 4 and 7 to give methoxythiamin (**16**) followed by enzymatic phosphorylation.

Here we also report the first synthesis of methoxythiamin diphosphate from methoxythiamin using mouse thiamin pyrophosphokinase (TPK) and ATP. Use of this enzyme was reported to produce thiamin pyrophosphate from thiamin in preparative scale.[41] The reaction was performed with a little modification where instead of the potassium bicarbonate buffer (pH - 8.0), potassium phosphate buffer (100 mM, pH – 7.5)

was used. High Performance Liquid Chromatography (reverse phase) was used as the tool of purification to harvest the compound (**13**) efficiently (Scheme 8C).

2.2.5 Study on thiamin-dependent enzymes with Methoxythiamin pyrophosphate

Five thiamin-dependent enzymes were studied where thiamin diphosphate (ThDP) was replaced by the synthesized 2'-Methoxythiamin pyrophosphate (MeO-ThDP). These enzymes are pyruvate dehydrogenase complexes from *E. coli* and human (PDHc-ec and PDHc-h), 1-deoxy-D-xylulose-5-phosphate synthase (DXPS) from *E. coli* and 2-oxogluterate dehydrogenase complexes from *E. coli* and human (OGDHc-ec and OGDHc-h). A high percentage of tightly bound thiamin was observed in OGDHc-ec and OGDHc-h enzymes, and that could not be replaced by MeO-ThDP. Hence, the major focus of the study was on the rest of the three enzymes. MeO-ThDP was found to be a functionally competent analog of ThDP. However, it inhibits the activity of thiamin-dependent enzymes by several folds. Approximately 5.9-11% of NADH production was detected with PDHc-ec. This number rises to 48-75% in case of PDHc-h, making it most efficient enzyme using MeO-ThDP. 8.8-14% DXP formation was recorded upon replacement of ThDP with MeO-ThDP in *E. coli* DXPS. Jordan research group observed that MeO-ThDP binds to the active site of the thiamin-dependent enzyme with binding constant similar to that of ThDP. However, the circular dichroism (CD) and fluorescence quenching data indicate that the mode of binding is probably different. Our second collaborator, Tittmann research group, at Gottingen, Germany, has crystallized transketolase with **18** bound at the active site (Unpublished). The structure indicates a

steric interaction between the methoxy group of **18** and an active site glutamate responsible for the activation of the cofactor.

2.3 Discussion

Replacement of thiamin by 2'-methoxythiamin pyrophosphate in thiamin-dependent enzymes could restore a little activity to the enzyme, however, the enzymes are inhibited to different extents.[13] There can be two possible reasons for the inhibition, steric and electronic. Thiamin binds in its signature V-conformation in the active site of all thiamin-dependent enzymes.[14-15] In this conformation both of the pyrimidine and the thiazole ring stays in a way so the pKa of the amino group can modulate the acidity of the proton attached to the C-2 of thiazolium. Replacing the methyl with methoxy group in the pyrimidine ring adds an extra pair of electrons from the oxygen atom that can be delocalized over the ring and can alter the pKa of the amino group. This alteration, in turn, affects the catalytic activity. On the other hand, due to the presence of the bigger methoxy group the binding mode of the thiamin can be different and the proper conformation of the cofactor molecule cannot be retained. This difference will also change the catalytic property of the coenzyme and thus will inhibit the enzyme. Methoxythiamin pyrophosphate was successfully synthesized and tested on different thiamin-dependent enzymes *in vitro.* The data from Jordan group indicated that methoxythiamin pyrophosphate binds to the thiamin-dependent enzymes with a binding affinity similar to thiamin but with a different binding mode. The presence of the bulkier methoxy group makes it a poorer fit in the enzyme active site. This hypothesis was further reinforced by

Tittmann research group who obtained the crystal structure of transketolase, with methoxythiamin bound at the active site. The structure showed that there is a steric interaction between the methoxy group and the key catalytic glutamate residue. Due to this interaction, the glutamate residue cannot be positioned properly with respect to thiamin and hence the enzyme is inhibited. This observation ruled out the possibility of inhibition due to the change in the electronic properties of the cofactor molecule.

2.4 Experimental

2.4.1 Overexpression and Purification of Thiamin Pyrophosphokinase

A plasmid encoding mouse thiamin pyrophosphokinase (TPK) in a pET28a vector was transformed into *E. coli* BL21 (DE3). The gene was overexpressed in LB media at 37 ^{o}C, and the cell lysate was passed through a GE HisTrap HP (5 mL) column. After washing with 30 mL wash buffer (100 mM potassium phosphate, 150 mM NaCl, 25 mM Imidazole, 2 mM TCEP, pH – 7.5) the protein was eluted with 15 mL elution buffer (100 mM potassium phosphate, 150 mM NaCl, 250 mM Imidazole, 2 mM TCEP, pH – 7.5). After concentration and desalting 3 mL of 1.0 mM purified protein was obtained.

2.4.2 Synthetic procedure

*4-amino-2-methoxypyrimidine-5-carbonitrile (**8**):* Sodium (250 mg, 11 mmol) and o-methylisourea bisulfate (1.00 g, 5.8 mmol) were added to 30 mL of ethanol and stirred for 1 hour. The precipitate was filtered, and the filtrate was refluxed for 4 hours with ethoxymethylene malononitrile (800 mg, 6.5 mmol). The reaction mixture was stirred at

room temperature for an additional 2 hours to give the product as a yellow precipitate. This was filtered and purified by column chromatography (10% chloroform-methanol) to yield **3** (475 mg, 55%) as a bright yellow solid.

^{1}H NMR (400 MHz, DMSO d_6): δ 3.84 (3H, s), 8.46 (1H, s)

^{13}C NMR (100 MHz, DMSO-d_6): δ 54.45, 83.74, 115.62, 163.50, 164.29, 165.94.

*5-(aminomethyl)-2-methoxypyrimidin-4-amine (**19**):* Methanolic ammonia (10 mL, 7M) was added to a solution of **8** (300 mg, 2 mmol) in 40 mL of methanol. The mixture was then passed through a Thalesnano H-cube hydrogenator with Raney Nickel catalyst at 70 ^{o}C and 60 bar hydrogen gas pressure at a flow rate of 0.7 mL/min. The solution was then concentrated, and **19** (230 mg, 75%) was purified by column chromatography (25% chloroform-methanol) as a pale yellow solid.

^{1}H NMR (400 MHz, DMSO d_6): δ 3.51 (2H, s), 3.73 (3H, s), 6.79 (2H, s), 7.76 (1H, s)

^{13}C NMR (100 MHz, DMSO-d_6): δ 39.53, 53.45, 112.15, 154.16, 163.99, 164.22.

*3-acetyl-3-chlorodihydrofuran-2(3H)-one (**21**)* Acetyl-γ-butyrolactone **20** (5g. 0.039mol) was cooled to -18 ^{o}C in a salt-ice bath under a nitrogen atmosphere and sulfuryl chloride (5.4g, 0.04 mol) was added dropwise over a period of 1 hr. The reaction mixture was warmed to room temperature, stirred overnight, poured onto ice, extracted with ethyl acetate and dried over anhydrous Na_2SO_4. Upon evaporation of the solvent, the crude product **21** (5g, 80%) was obtained as a colorless liquid, it was used into the next step without further purification.

^{1}H NMR (400 MHz, $CDCl_3$): δ 2.45 (3H, s); 2.61 (1H, m); 3.11 (1H, m); 4.41 (2H, m)

^{13}C NMR (100 MHz, DMSO-d_6) 25.51, 35.20, 66.22, 68.85, 170.48, 198.14

*3-chloro-4-oxopentyl acetate (**22**)* Compound **21** (4 g, 24.6 mmol) was added to a mixture of glacial acetic acid (4.5 mL), water (0.7 mL) and concentrated HCl (0.2 mL) and refluxed overnight. After cooling to room temperature, acetic anhydride (5g) was added. The reaction mixture was then heated at 120 ^{o}C for 36 hours. Finally, the reaction mixture was diluted with diethyl ether and purified by column chromatography (10% ethyl acetate-hexane) to give pure **7** (2.77g, 63%) in the form of a pale yellow oil.

^{1}H NMR (400 MHz, DMSO d_6): δ 1.98 (3H, s), 2.03s (1H, m), 2.26 (1H, m), 2.27 (3H, s), 4.10 (2H, m), 4.70 (1H, dd, J = 13.76, 3.48 Hz);

^{13}C NMR (100 MHz, DMSO-d_6): δ 20.47, 26.45, 31.69, 60.16, 60.79, 171.87, 201.72

*3-((4-amino-2-methoxypyrimidin-5-yl)methyl)-5-(2-hydroxyethyl)-4-methylthiazole-2 (3H)-thione (**24**)* In order to synthesize **9** the following components were added in a small round-bottomed flask (25 mL); 3.3 mL absolute ethanol, 0.3 mL 20% ammonium hydroxide and 0.75 mL water. Compound **4** (300 mg, 1.95 mmol), compound **7** (500 mg, 2.81 mmol) and carbon disulfide (0.15 mL) were added to it. The reaction mixture was stirred at room temperature for 15 hours, and the product **8** was extracted with ethyl acetate This product was used in the next step without further purification or characterization. A crude mixture of **8** was dissolved in 4 mL 10% HCl and stirred at 80 ^{o}C for 20 minutes. Upon neutralization with 25% ammonium hydroxide solution the product separated as a

precipitate. After filtration and drying, **9 (**420 mg, 70%) was isolated as a pale yellow solid.

^{1}H NMR (400 MHz, DMSO d_6): δ 2.08 (3H, s), 2.69 (2H, t, J = 5.94), 3.52 (2H, dd, J = 17.12, 5.48), 3.74 (3H, s), 5.23 (2H, s), 7.02 (2H, s), 7.42 (1H, s).

^{13}C NMR (100 MHz, DMSO-d_6): δ 12.46, 29.26, 44.08, 53.59, 60.22, 104.37, 120.44, 135.84, 154.45, 162.58, 164.55, 185.45

*2'-Methoxythiamin (**16**):* Hydrogen peroxide (250 μL 30%) was added to a solution of **8** (310 mg) in 3 mL of 10% HCl. The reaction mixture was stirred on an ice bath for 30 minutes and then at room temperature for 1 hour. A $BaCl_2$ solution was added to precipitate the sulfate ions generated in the previous step. The mixture was filtered. The filtrate was evaporated to dryness to yield 252 mg (72%) 2-methoxythiamin chloride hydrochloride.

^{1}H NMR (400 MHz, D_2O): δ 2.67 (3H, s), 3.29 (2H, t, J=5.74 Hz), 3.98 (2H, t, J = 5.76 Hz), 4.24 (3H, s), 5.61(2H, s), 8.11 (1H, s), 9.70 (1H, s). ^{13}C NMR (100 MHz, D_2O) 11.24, 29.33, 50.01, 57.08, 60.42, 102.08, 136.60, 143.02, 146.50, 154.11, 158.74, 165.0

*2'-Methoxythiamin pyrophosphate (**13**)* Methoxythiamin hydrochloride **10** (3 mg) and ATP (12 mg) were dissolved in potassium phosphate buffer (5 mL, 100 mM, pH-8.0) containing $MgSO_4$ (20 mM). Purified thiamin pyrophosphokinase enzyme solution (100 μL, 1.0 mM) was added to the mixture and incubated at 37 ^{o}C for 12 hours.

Methoxythiamin pyrophosphate **13** was purified by reverse phase HPLC in quantitative yield.

2.4.3 High Performance Liquid Chromatography (HPLC) conditions for the isolation of 11

Agilent 1200 series instrument; Supelcosil SPLC-18-DB column (25 cm x 10 mm, 5 μm). The following gradient was used with (A) water, (B) 10 mM ammonium acetate and (C) methanol; 0 min, 100% B; 5 min, 10% A/90% B; 9 min, 25% A/60% B/15% C; 14 min, 25% A/10% B/65% C; 19 min to 25 min, 100% B.

^{1}H NMR (400 MHz, D_2O): δ 2.69 (3H, s), 3.98 (2H, t, J = 5.38 Hz), 4.04 (3H, s), 4.28 (2H, dd, J = 17.88 Hz, 6.24 Hz), 5.47 (2H, s), 8.13 (1H, s), 9.42 (1H, s). ^{13}C NMR (100 MHz, D_2O) δ 11.23, 27.58, 50.93, 54.99, 64.70, 101.18, 135.27, 143.19, 159.51, 164.12, 165.68, 180.27

CHAPTER III

SYNTHESIS AND BIOCHEMICAL STUDIES ON ^{13}C2,^{15}N3-THIAMIN PYROPHOSPHATE

3.1 Introduction

Pyruvate dehydrogenase complex (PDC) enzyme that catalyzes pyruvic acid decarboxylation and acyl group transfer to coenzyme-A uses thiamin pyrophosphate as a cofactor. The catalytic mechanism is already known, and it is shown in Figure 3.1.[42] All the intermediates of thiamin diphosphate in this mechanism are not fully characterized. Large size and insolubility of the fully assembled PDC make the study of the mechanism intermediates by solution NMR difficult. Crystal structure of this complex is also unavailable. To overcome these limitations solid state NMR is emerging as an effective technique for structural investigation of these kinds of supramolecular assemblies.[43] Isotopically labeled thiamin diphosphate analogs are reported as probes to study the catalytic mechanism in E1 component of PDC by tracking the states of ionization and tautomerization of specific bonds in the molecule by solid state NMR spectroscopy.[44-45] ^{13}C2 and ^{15}N3 labeled thiamin pyrophosphate (**12**) was chosen as a probe to investigate the intermediate states of thiamin in fully assembled PDC. 2D hetero-correlation NMR experiments on ^{13}C-^{15}N will be used as a tool to get atom specific information.

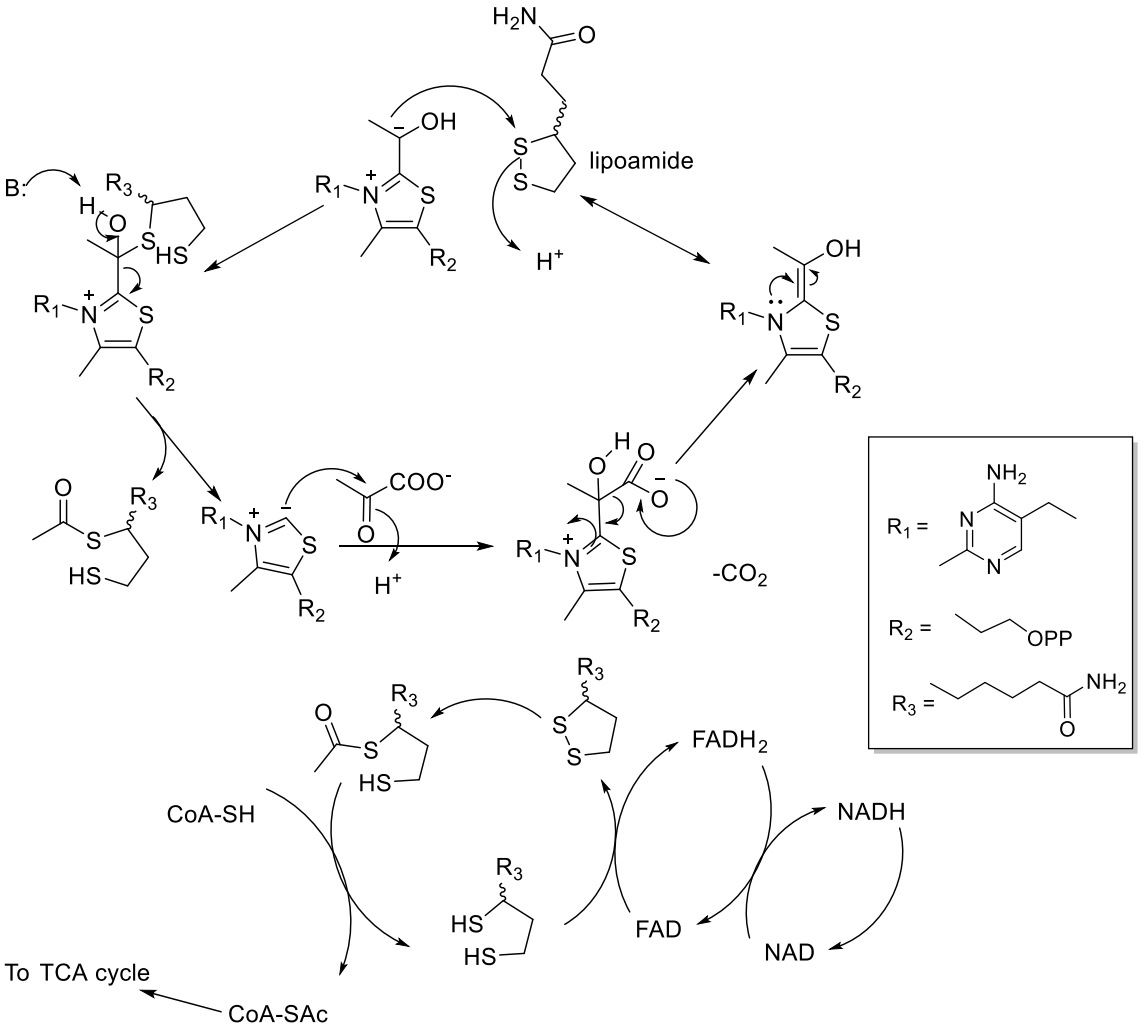

Figure 3.1: Mechanism of the reaction catalyzed by PDC enzyme

Firstly, a strategy has been designed to incorporate labels at the designated positions of the thiamin pyrophosphate, and the labeled analog was successfully synthesized after. The synthesized molecule was then sent to our collaborator Dr. Kai Tittmann in Gottingen, Germany for further biochemical investigations

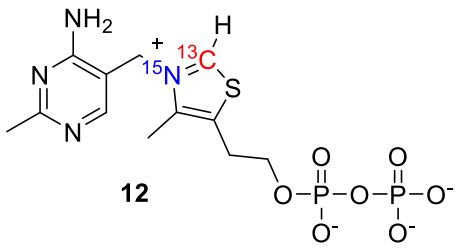

Figure 3.2: Structure of the thiamin molecule with location of isotopic labeling

3.2 Results and Discussion

The target molecule (**12**) (Figure 3.2) has to be synthesized with the labels at the designated positions so a strategy was designed where a proper labeled precursor/ building block can be used. The strategy we followed here is making the pyrimidine and the thiazole part separate followed by coupling them together to form the thiamin molecule. Finally, the synthesized molecule was planned to be phosphorylated enzymatically by ATP and thiamin pyrophosphokinase.

3.2.1 Synthesis of the thiazole moiety

The precursor that was found to be suitable for the synthesis was ^{13}C and ^{15}N labeled thiourea. The synthetic strategy was adopted from an old literature method for synthesizing ^{14}C lableled thiazole at the C2 of the heterocyclic ring (Scheme 3.1).[46] 2-acetyl butyrolactone was reacted with sulfuryl chloride to yield 2-acetyl-2-chloro butyrolactone (**2**). It was then refluxed with acetic acid and hydrochloric acid mixture to give 3-chloro-4-oxopentyl acetate (**3**). After purification, **3** was dissolved in dry ethanol and condensed with ^{13}C and ^{15}N labeled thiourea (**4**). This condensation product 2-amino-4-methyl-5-β-acetoxyethylthaizole (**5**) which was hydrolyzed to give **6** without further

purification. Compound **6** was then purified followed by diazotization and deamination to yield the labeled 4-methyl-5-β-hydroxyethylthaizole (**7**). This diazotization reaction was achieved at -5 ^{o}C, using a salt-ice bath. The entire scheme was first optimized with non-labeled compound and finally the targeted thiamin analog was prepared from ^{13}C and ^{15}N labeled precursor.

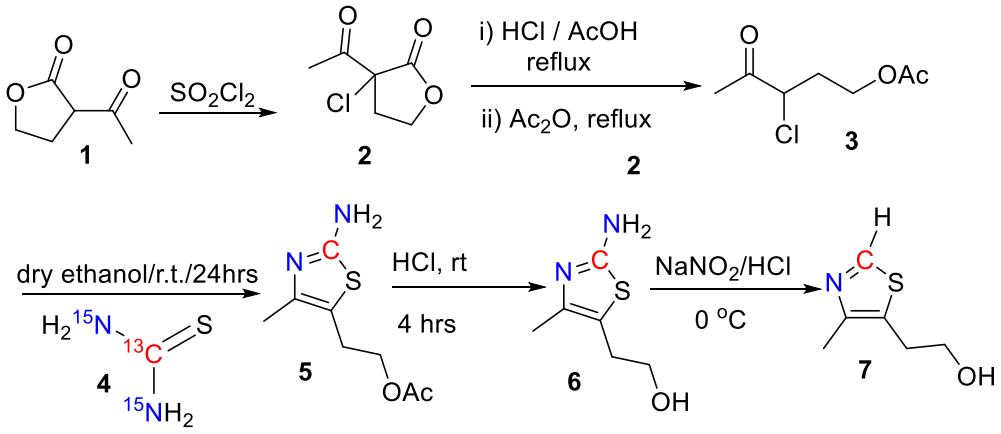

Scheme 3.1: Synthetic scheme for the labeled thiazole part of the molecule.

3.2.2 Synthesis of the pyrimidine moiety

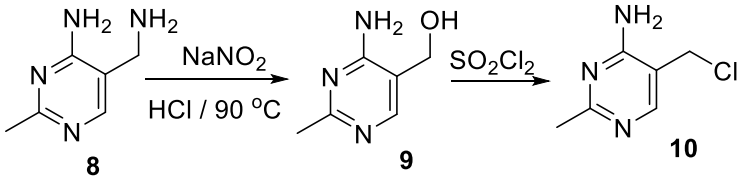

Scheme 3.2: Synthesis of the pyrimidine part for the coupling reaction.

The pyrimidine part of the thiamin was designed to assimilate a nucleophilic attack by the synthesized thiazole moiety. To carry out this strategy, a chloride group was

introduced to the methylene carbon to make it electrophilic (Scheme3.2). Grewe diamine (**8**) was a generous gift from Roche. The amino methyl group of **8** was converted to hydroxymethyl by diazotization and hydrolysis.[38] This molecule (**9**) was then treated with thionyl chloride and 4-amino-5-chloromethyl-2-methyl pyrimidine (**10**) was separated as a yellow solid.[47]

3.2.3 Coupling of the pyrimidine and thiazole: Formation of the thiamin

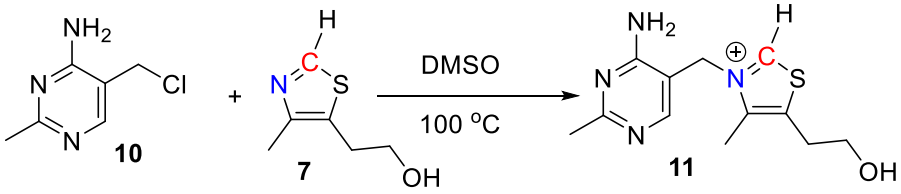

Scheme 3.3: Formation of labeled thiamin by coupling of the electrophilic pyrimidine and nucleophilic thiazole

In the final reaction, these two precursor molecules (**7** and **10**) were mixed with a few drops of anhydrous DMSO and heated at 100 °C for 15 minutes (Scheme 3.3). Dilute hydrochloric acid was added, and the aqueous phase was filtered and evaporated to yield the product. No further purification was required. Splitting of the proton attached to the C-2 of thiazolium confirms the presence of the labeling (Figure 3.2). Rapid exchange of the C-2 proton with deuterium was observed when the NMR was taken in D_2O as the solvent. Due to the presence of attached deuterium and ^{15}N atom splitting of the labeled ^{13}C signal was also observed.

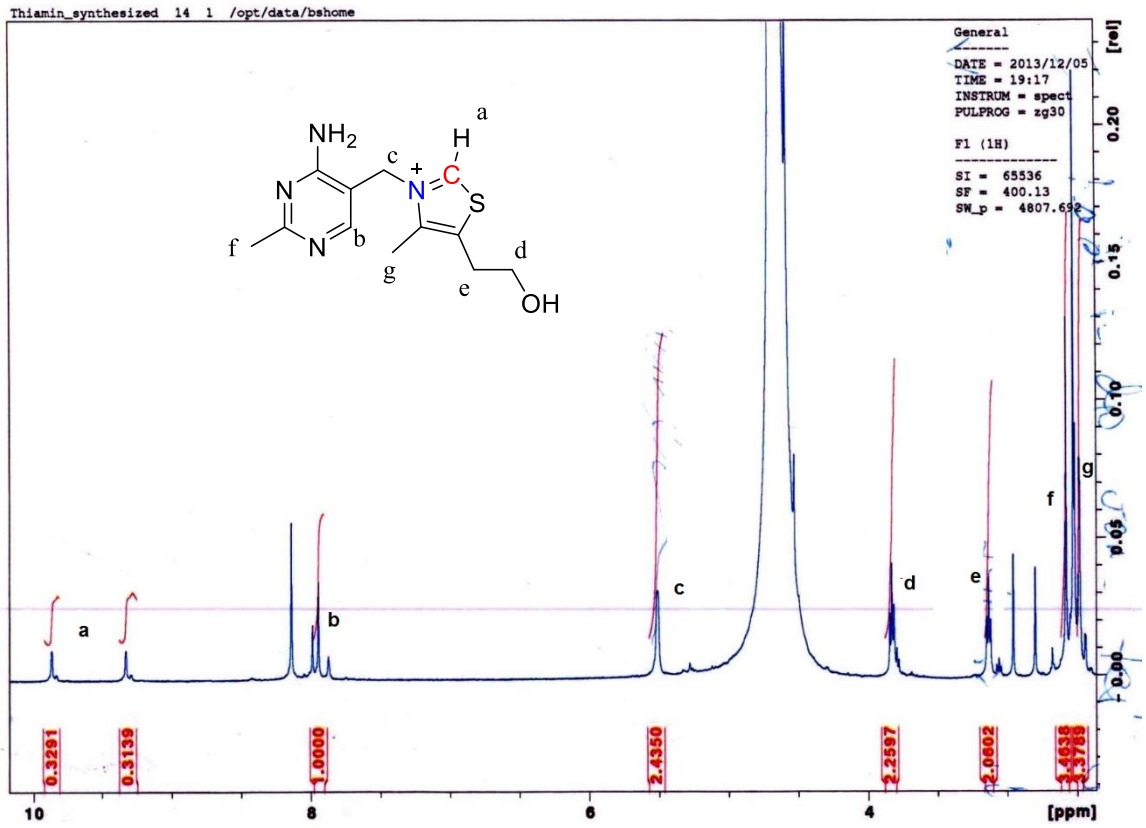

Figure 3.2: Proton NMR spectrum of the labeled thiazole.

3.2.4 Enzymatic pyrophosphorylation of labeled thiamin

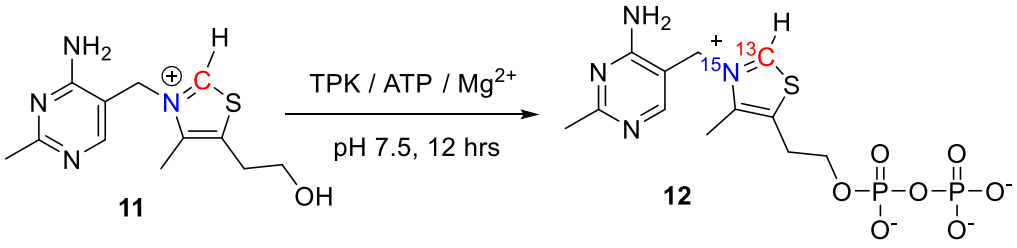

Scheme 3.4: Enzymatic pyrophosphorylation of thiamin using ATP and Mg^{2+} ion

The synthesized thiamin was further pyrophosphorylated by the catalysis of thiamin pyrophosphokinase (TPK) from a mouse with ATP as the phosphate group donor

(Scheme 3.4). His-tagged mouse TPK was cloned into a pET-28b vector and overexpressed in E. coli and purified by standard protocol using a nickel-NTA column. The protein was eluted and desalted and stored in -80 ^{o}C. The synthesized thiamin was dissolved in pH 7.5 phosphate buffer and ATP was added up to 3 times of the thiamin concentration followed by magnesium sulfate. Finally, the TPK enzyme was added, and the mixture was incubated at 37 ^{o}C for 12 hours. The final product **11** was purified by HPLC, dried under reduced pressure and sent out for the biochemical studies with PDC enzyme by Tittmann research group (Figure 3.2).

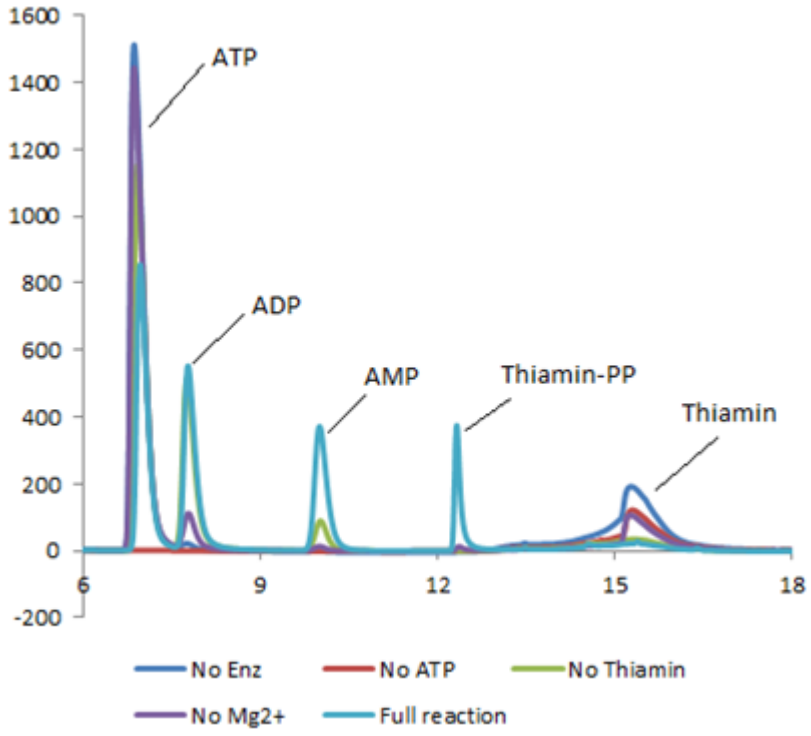

Figure 3.2: HPLC chromatogram of the enzymatic phosphorylation of isotopically labeled thiamin. Formation of TPP was only observed in full reaction.

3.3 Conclusion

A synthetic scheme was designed, tested and optimized by synthesizing thiamin pyrophosphate with the unlabeled precursor. The labeled thiamin molecule has been successfully synthesized following the optimized scheme using labeled precursor (^{13}C, ^{15}N labeled thiourea). The synthesized molecule was characterized by NMR and mass spectrometry. Finally, it was phosphorylated to get the active form of the cofactor. After purification by HPLC, it was sent to the Tittmann research group in Gottingen, Germany for enzymatic studies with fully assembled PDC. The solid-state NMR-based intermediate analysis is in progress.

3.4 Experimental

3.4.1 Synthetic procedure

NMR spectra of the final labeled thiazole and the thiamin were reported. For the other intermediates, NMR spectra of the unlabeled compounds were reported.

*3-acetyl-3-chlorodihydrofuran-2(3H)-one (**2**):* Acetyl-γ-butyrolactone **1** (5g. 0.039mol) was cooled to -18 ^{o}C in a salt-ice bath under a nitrogen atmosphere and sulfuryl chloride (5.4g, 0.04 mol) was added dropwise over a period of 1 hr. The reaction mixture was warmed to room temperature, stirred overnight, poured onto ice, extracted with ethyl acetate and dried over anhydrous Na_2SO_4. Upon concentration the crude product **6** (5g, 80%) was obtained as a colorless liquid, it was subjected to the next step without further purification.

^1H NMR (400 MHz, $CDCl_3$): δ 2.45 (3H, s); 2.61 (1H, m); 3.11 (1H, m); 4.41 (2H, m)

2-amino-4-methyl-5-β-hydroxyethylthaizole : 5-Acetoxy-3-chloro-2-pentanone, (3) (350 mg, 1.96mmole) was added to a solution of ^{13}C, ^{15}N – thiourea (5) (75 mg, 0.96 mmole) in ethanol (10 mL). The mixture was stirred under nitrogen and heated to reflux for 27 h, then cooled and concentrated in vacuum. The crude reaction mixture was dissolved in 2N HCl (5 mL) and stirred at room temperature for 6 hrs. After neutralizing with aqueous ammonia, the solvent was removed under reduced pressure, and the product 6 was purified by column chromatography (silica gel column 10% methanol in chloroform). Yield 90%. Spectral data of the unlabeled compound is reported.

^1H NMR (400 MHz, DMSO-d_6): δ 9.12 (s, 2H), 3.51 (2H, t), 2.65 (2H, t), 2.09 (3H, s)

^{13}C and ^{15}N labeled 4-methyl-5-β-hydroxyethylthaizole: 2-Amino-4-methyl-5-thiazolyl ethyl acetate (7) (100 mg, 0.63 mmole) was dissolved in phosphinic acid (3 mL of 50% aqueous solution). This solution was cooled to -5 ^oC under nitrogen and stirred while adding sodium nitrite (50 mg, 0.73 mmole). Effervescence and a color change from bright yellow to orange were observed. After 45 minutes the solution was neutralized by aqueous ammonia, evaporated to dryness and purified by silica gel column 4% methanol in dichloromethane.

^1H NMR (400 MHz, DMSO-d_6): δ 8.72 (1H, dd), 3.72 (2H, t), 2.98 (2H, t), 2.37(3H, d)

*4-Amino-5-(hydroxymethyl)-2-methylpyrimidine (HMP, **9**).* A solution containing 454 mg (6.58 mmol) of NaNO2 in 5 mL of water was slowly added, using a dropping funnel, to a solution of 1.25 g (5.96 mmol) of Grewe diamineâ dihydrochloride in 12.5 mL of 10%

HCl, at 90 °C. The reaction mixture was stirred at that temperature for 5 hours and then neutralized to pH 8.0 followed by purification by silica gel column with 15% methanol in chloroform. Yield 81%.

^{1}H NMR (400 MHz, D_2O)): δ 7.99 (1H, s), 4.52 (2H, s), 2.39 (3H, s).

*4-Amino-5-(chloromethyl)-2-methylpyrimidine (HMP-Cl, **10**)* This compound was prepared by a modification of the literature procedure.[48] A mixture of 4-amino-5-(hydroxymethyl)- 2-(trifluoromethyl)pyrimidine (550 mg, 3.96 mmol), thionyl chloride (0.85 mL, 1.4 g, 11.9 mmol), and 10 mL of chloroform was refluxed with stirring for 3 h. The product separated as a yellow solid which was filtered and washed several times with anhydrous chloroform and dried under vacuum. This product was used without further purification. Yield – 72%

^{13}C and ^{15}N labeled Thiamin Chloride: Both compound **7** (30 mg, 0.21 mmole) and **10** (66 mg, 0.42 mmole) was mixed with 6 drops of anhydrous DMSO and heated at 100 ^{o}C for 15 - 20 minutes. The reaction mixture was then cooled, and 1N HCL (3 mL) was added and stirred for half hour. The mixture was filtered, and the filtrate was evaporated to dryness under vacuum. The crude mixture was purified by HPLC to get pure labeled thiamin. 36 mg (51%) product was recovered.

1H NMR D_2O: δ 9.59 (1H, d) 8.11 (1H, s), 5.54 (2H, dd), 3.96 (2H, t), 3.26 (2H, t), 2.63 (3H, d), 2.59 (3H, s)

*^{13}C and ^{15}N labeled thiamin pyrophosphate (**12**)* ^{13}C and ^{15}N labeled thiamin **10** (3 mg) and ATP (12 mg) were dissolved in potassium phosphate buffer (5 mL, 100 mM, pH-8.0) containing $MgSO_4$ (20 mM). Purified thiamin pyrophosphokinase enzyme solution (100 μL, 1.0 mM) was added to the mixture and incubated at 37 ^oC for 12 hours. Thiamin pyrophosphate **11** was purified by reverse phase HPLC in quantitative yield.

3.4.2 Overexpression and purification of thiamin pyrophosphokinase

A plasmid encoding mouse thiamin pyrophosphokinase in a pET28a vector was transformed into *E. coli* BL21 (DE3). The gene was overexpressed in LB media at 37 ^oC, and the cell lysate was passed through a GE HisTrap HP (5 mL) column. After washing with 30 mL wash buffer (100 mM potassium phosphate, 150 mM NaCl, 25 mM Imidazole, 2 mM TCEP, pH – 7.5) the protein was eluted with 15 mL elution buffer (100 mM potassium phosphate, 150 mM NaCl, 250 mM Imidazole, 2 mM TCEP, pH – 7.5). After concentration and desalting 3 mL of 1.0 mM purified protein was obtained.

3.4.3 High Performance Liquid Chromatography (HPLC) conditions for the isolation of 11

Agilent 1200 series instrument; Supelcosil SPLC-18-DB column (25 cm x 10 mm, 5 μm). The following gradient was used with (A) water, (B) 10 mM ammonium acetate and (C) methanol; 0 min, 100% B; 5 min, 10% A/90% B; 9 min, 25% A/60% B/15% C; 14 min, 25% A/10% B/65% C; 19 min to 25 min, 100% B.

CHAPTER IV

SYNTHETIC STRATEGY OF ^{18}F-LABELED THIAMIN ANALOGS FOR PET IMAGING TO STUDY DISTRIBUTION OF THIAMIN IN LIVE ANIMALS

4.1 Introduction to PET imaging

Positron Emission Tomography (PET) is a radiological technique that uses a tracer molecule that contains a positron emitting nuclide.[49] These tracer molecules are biologically relevant molecules or their close chemical analogs that can participate in the metabolic processes in the body. Upon administration of the tracer molecule in the living animal body, it is distributed in the entire body by general circulatory systems and accumulates to those parts and organs where it is mostly utilized. The radionuclide emits a positron and that can be detected by an outside detector and a three-dimensional image of the region of distribution can be constructed by computerized tomography.[50] The radionuclides mostly used to prepare tracer molecules are ^{11}C and ^{18}F isotopes. Being very small in size the atoms can be incorporated without making big perturbation to the primary bio-molecule. The most famous example of PET imaging tracer is the 2-deoxy-2-^{18}F-glucose, used in cancer detection.[51] Glucose is primarily utilized in energy metabolism and destined to those places where the rate of metabolism is high. Highly active and energy consuming organs like heart and brain usually demand more glucose than other parts of the body. In the malignant tumors, consumption of glucose is also higher because of the high metabolic rate of uncontrolled growth. Radiolabeled glucose analog easily

accumulates in these cancerous tumors and can be easily detected thus making this tracer a very efficient tool for cancer detection and diagnosis.[52-53] PET imaging is also a very important tool to study the distribution of drug molecules after administration.

Vitamin B1 is a crucial cofactor in all forms of life including humans. It is a long asked question how it is distributed in the body and what are the organs where it primarily accumulates. To study that we planned to synthesize thiamin analogs as tracer molecules that will contain ^{18}F atoms as labeling positron emitting nuclide. ^{18}F has a half-life of 110 min that enables ^{18}F containing tracers to be studied for a longer period of time compared to ^{11}C isotope. Energy generating metabolic process like respiration involves enzymes requiring thiamin for their activity thus in the metabolically active tissues like heart, brain or leg muscle, a greater concentration of thiamin is expected. Injecting radiolabeled thiamin into the body followed by PET scans at different time points will demonstrate accumulation of the cofactor in different body parts and organs. Cancer tissues potentially possess high thiamin requiring cells to maintain an increased rate of respiration and DNA synthesis. Thiamin-dependent enzymes like transketolase, pyruvate dehydrogenase, α-ketoglutarate dehydrogenase are an integral part of these metabolic processes.[54-55] Recombinant thiaminase and thiamin antimetabolite show inhibitory effects on cancer cell growth signifying thiamin dependence for proliferation. These observations give rise to the possibility of accumulation of increased amount of thiamin in the cancer cells and their imaging with ^{18}F-thiamin.

This suggests that ^{18}F-Thiamin may be used to study the distribution of thiamin in the body and as a diagnostic tool for tumor detection. Here we report the development of

synthetic strategies for two fluorine labeled thiamin analogs designed for the PET imaging study. The radiosynthesis of ^{18}F-thiamin will be done at the designated facility with our collaborator at UT Southwestern. The distribution map of thiamin in the body of a living animal will then be obtained by PET scanning.

4.2 Results and discussion

The thiamin analog where the terminal hydroxyl group was replaced by a fluorine atom was chosen as the first target molecule due to its ease of synthesis (Figure 4.1).

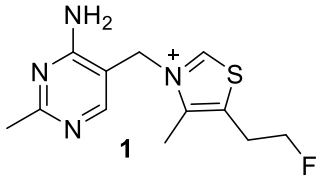

Figure 4.1: Structure of the targeted deoxy-fluorothiamin.

4.2.1 Initial synthetic strategy

The molecule was targeted to be prepared by coupling reaction between the pyrimidine bromide and thiazole fluoride (**3**) (Scheme 4.1).

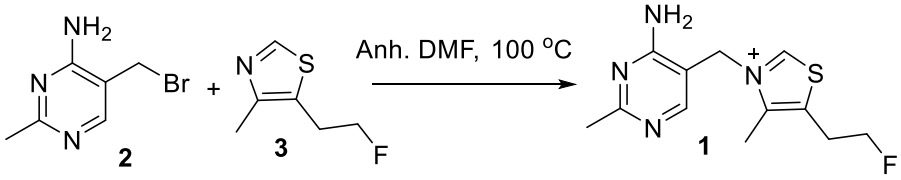

Scheme 4.1: Coupling of pyrimidine bromide and thiazole fluoride to form deoxy fluorothiamin

Deoxyfluorothiazole (**3**) has been synthesized from the commercially available 4-methyl-5-hydroxyethyl thiazole in two simple steps.[56] The terminal hydroxyl group of the starting material was first converted to a good leaving group like triflate or nosylate followed by substitution of that leaving group with fluoride ion (Scheme 4.2). Nosylate has been found to be a better option regarding yield, purification, and stability.

A)

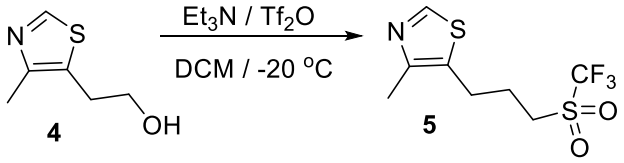

B)

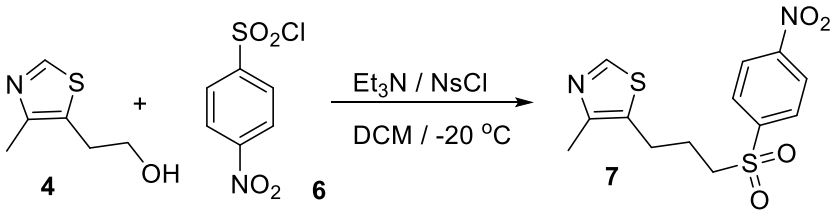

Scheme 4.2: Synthesis of A) triflate and B) nosylate of the thiazole precursor

The fluoride insertion reaction was performed by treating thiazole nosylate with potassium fluoride in the presence of potassium ion chelator 2,2,2-Crypand ligand (Scheme 4.3). Formation of both substitution and elimination product was observed in a ratio of 5:2.[57] Using tetrabutyl ammonium fluoride (TBAF) as a reagent the ratio of the substitution and elimination products (**3** & **8**) was increased to 9:1 for the desired substitution product.

The desired fluorothiazole was purified by column chromatography after which it was subjected to a coupling reaction with 4-amino-5-bromomethyl-2-methyl pyrimidine

in anhydrous DMF at 110 °C (Scheme 4.1). Product 2-fluorothiamin was extracted with water, evaporated to dryness followed by characterization with NMR and mass spec analysis.

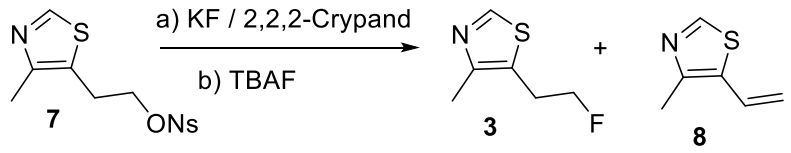

Scheme 4.3: Synthesis of the 4-methyl-5-fluoroethyl thiazole from the corresponding nosylate with available ^{18}F precursor potassium fluoride.

Synthesis of the bromo-HMP (**2**) is conducted by treating HMP (**10**) with a mixture of HBr and acetic acid at 110 °C in a pressure tube (Scheme 4.4).

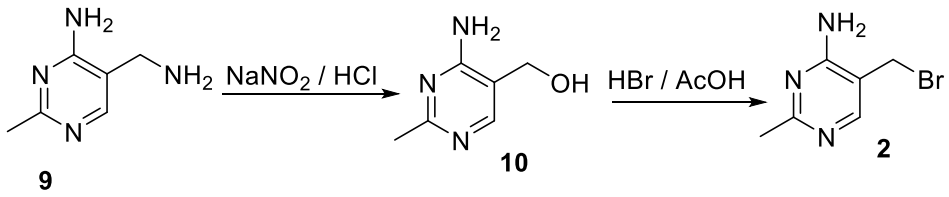

Scheme 4.4: Steps involved in the synthesis of Bromo-pyrimidine (**2**)

Finally, the target molecule (**1**) was prepared via the coupling reaction of **2** and **3** in anhydrous DMF at 100 °C (Scheme 4.1). As the radioactive ^{18}F isotope has a half-life of 110 min, insertion of fluoride at the very end of the synthesis was desirable. However, in this strategy, one round of purification is required before the coupling and another after

it to get 2-fluorothiamin in the pure form. As all the purification steps are time-consuming, another strategy was devised to bypass it.

4.2.2 Second strategy for the synthesis of deoxyfluorothiamin

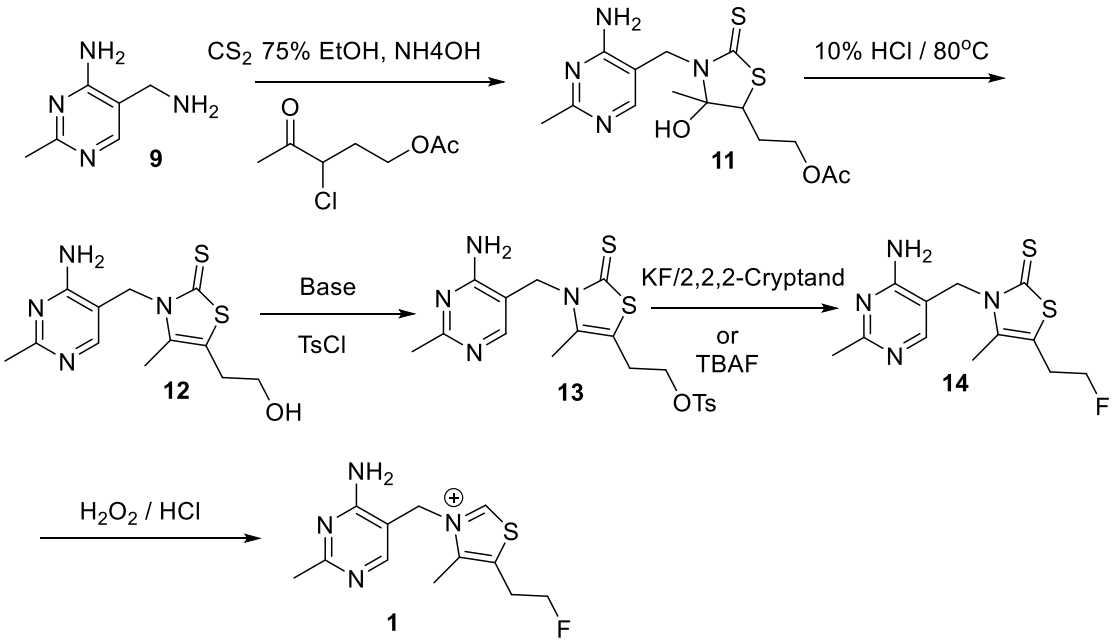

Scheme 4.5: Alternative strategy for the synthesis of F-thiamin.

The major problem of handling thiamin in an organic environment is the polarity of the molecule. It bears a positive charge on it which makes it a cationic highly charged species, insoluble in organic solvents. This prevented us from putting the fluoride label directly on the thiamin molecule. The closest neutral precursor of thiamin is thiamin thiazolone that can be oxidized to thiamin within few minutes. We followed a literature method to prepare thiamin thiazolone starting from grewe diamine (**9**) as one of the starting materials.[39] The terminal hydroxyl group was converted to tosylate and substituted by fluoride using tetrabutyl ammonium fluoride as a reagent. Product formation was also

observed when KF and 2,2,2-Crypand were used as the fluorinating agent (Scheme 4.5***)***. The reaction mixture was subjected to oxidation without further purification and the final compound was purified by HPLC.

4.2.3 Development of synthetic strategy for the second fluoro-thiamin analog

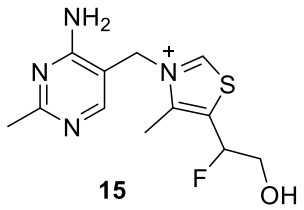

15

Figure 4.2: Structure of the fluorine- thiamin capable of enzymatic phosphorylation

Deoxy-fluorothiamin has a major drawback that it cannot be phosphorylated by thiamin pyrophosphokinase inside the cell. The thiamin pyrophosphokinase converts thiamin to the corresponding pyrophosphate, which is utilized in the cells as the active cofactor. The inability of phosphorylation of the deoxy-fluorothiamin (**1**) can lead to its efflux from the cells giving an erroneous picture of the distribution of the cofactor in the body. Hence, another target molecule (**15**) was chosen for this purpose with least perturbation and having the terminal hydroxyl group intact for phosphorylation (Figure 4.2). According to this strategy, the thiazole part will be synthesized first, and the fluorine will be introduced in the next step. After the fluorothiazole is ready, it will be quickly coupled with the corresponding pyrimidine bromide to form the fluorothiamin. As the coupling was a very crucial reaction and depends on many factors like solubility, temperature and thermal stability of the components, an easy synthetic route was designed

to optimize the coupling reaction condition. Another aim was to test the synthesized fluorothiamin whether it is accepted by *E. coli* as a replacement of thiamin.

Fluorothiazole was synthesized in four steps using **16** as the starting material (Scheme 4.6). Compound **16** was first oxidized by OsO_4 to form the corresponding vicinal diol **17** and N-methyl morpholine N-oxide was used to regenerate the OsO_4 as it was present in a catalytic amount. After selectively protecting the primary hydroxyl group of **17** by silyl ether, **18** was treated with DAST to incorporate the fluoride group in place of the free hydroxyl group to give **19**. Finally, cleavage of the silyl ether linkage of **19** with aqueous fluoride led to the final fluorinated thiazole **20**.

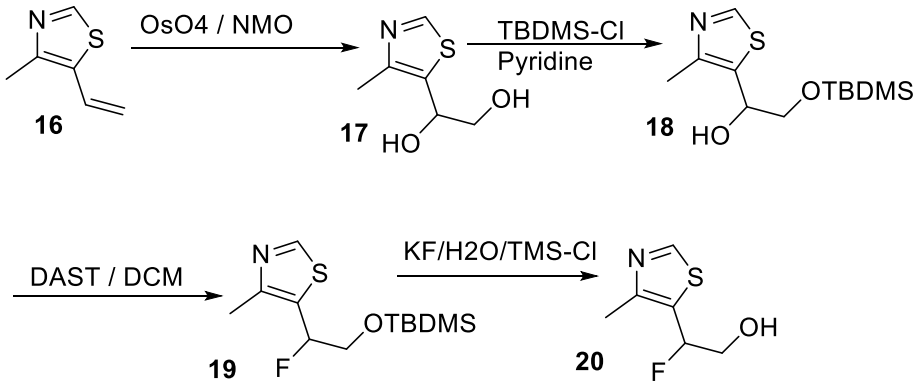

Scheme 4.6: Synthetic route for 2-fluoro-2-(4-methylthiazol-5-yl)ethan-1-ol for biological tests

The coupling reaction was attempted with both chlorinated and brominated versions of the pyrimidine part. The coupling reaction with the HMP-bromide (**2**) remained unsuccessful probably due to an excess of acetic acid present in it, so chloro-HMP (**23**) was considered as a substitute. It was synthesized by treating **10** with thionyl

chloride in chloroform under reflux condition (Scheme 4.7).[10] After several attempts, coupling with chloro-HMP (**23**) at 100 ^{o}C in the presence of anhydrous DMF was successful. The product formation was detected in the mass spec analysis (Figure 4.3). However, the corresponding mass of the hydrolyzed product was also detected indicating that the fluorine atom is labile and can be replaced with hydroxyl group over time when kept as an aqueous solution (Scheme 4.8). The small amount of product was insufficient for NMR analysis.

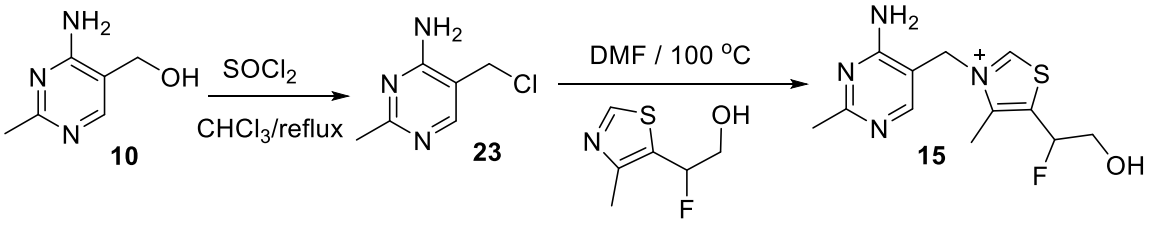

Scheme 4.7: Synthesis of Chloro-pyrimidine and its coupling with **20** to form the final thiamin analog (**15**).

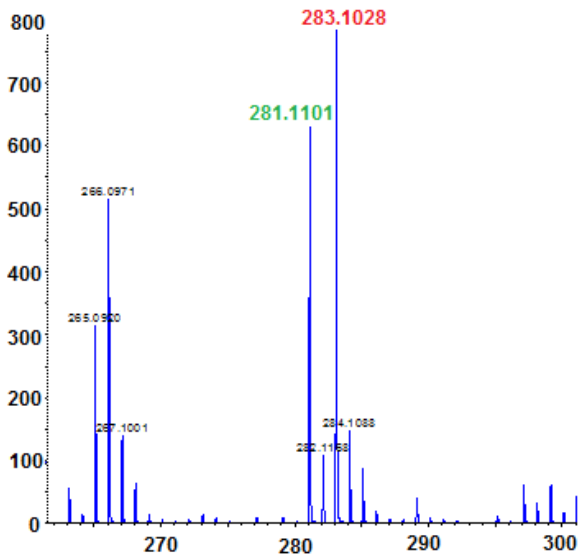

Figure 4.3: Mass spec analysis of the coupling reaction detects the presence of the fluorothiazole as the major product (283.1028). Hydrolysed product hydroxythiamin was also detected at mass of 281.11 (Scheme 4.8)

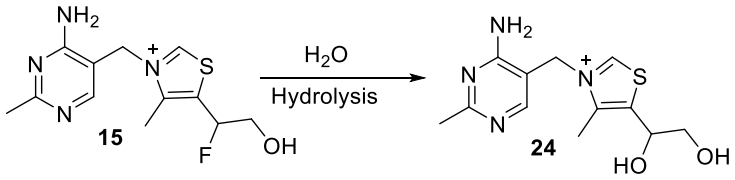

Scheme 4.8: Hydrolysis of fluorothiamin to dihydroxythiamin

4.2.4 Bacterial growth study with fluorothiazole

Fluorothiazole was used as a supplement to ΔThiG knock out mutant of *E. coli*. As ThiG is responsible for biosynthesizing the thiazole part of the thiamin molecule, ΔThiG mutant of the bacteria is unable to make the thiazole and has to acquire it from the media for survival. The cells were grown in minimal media with 50 μM purified fluorothiazole and a growth rate similar to the thiamin supplementation was observed. Later it was discovered that in aqueous media fluorothiazole is hydrolyzed to dihydroxythiazole (**17**) (Scheme 4.9), however, this experiment suggested that thiazole with a substituent at C2' is a biosynthetically competent analog. Instability of fluorothiazole in the aqueous solution closes the option for enzymatic *in vitro* synthesis of fluorothiamin, by thiamin biosynthetic enzymes.

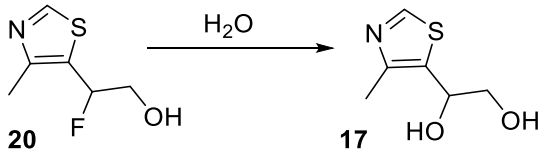

Scheme 4.9: Hydrolysis of the 2-(4-methylthiazol-5-yl)ethan-1-ol to form 2-fluoro-2-(4-methylthiazol-5-yl)ethan-1,2-diol in the aqueous growth media.

4.2.5 Synthesis of fluorothiazole using fluoride ion as the source of fluorine

After successfully testing the tolerance of the substituted thiazole, we attempted to synthesize fluorothizole using fluoride ion as the nucleophile. Since ^{18}F isotope is only available in the form of fluoride and not as DAST, the synthetic method was modified so that KF can be used as the source of fluorine for incorporation (Scheme 4.10). In this strategy after the protection of the primary hydroxyl group, the secondary hydroxyl group was planned to be activated by forming esters like triflate or nosylate. Finally, the good leaving group would be substituted by fluoride from KF. 222-kryptoffix.

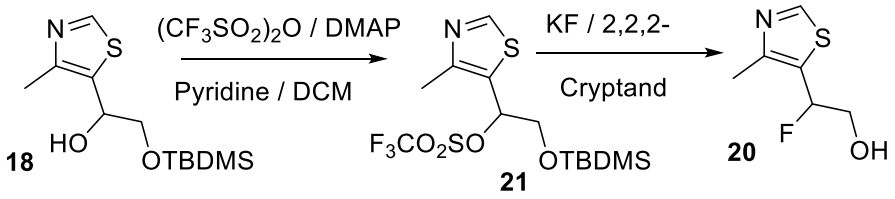

Scheme 4.10: Planned synthesis of 2-fluoro-2-(4-methylthiazol-5-yl)ethan-1-ol

Reaction to synthesize the triflate yielded the corresponding pyridine adduct instead of the desired product which was characterized by NMR and mass spectroscopy (Scheme 4.11). Attempts to incorporate other leaving groups like tosylate or nosylate also remained unsuccessful for this molecule.

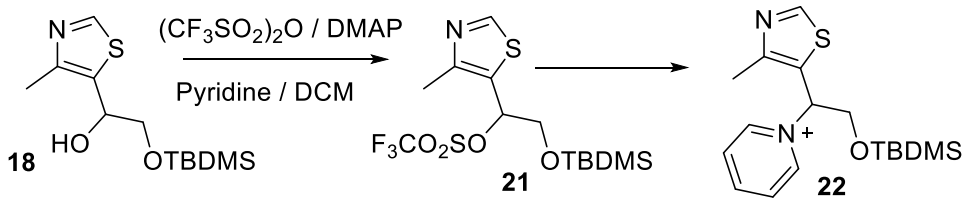

Scheme 4.11: Formation of pyridine-thiazole adduct

4.3 Challenges and future direction

We have successfully demonstrated synthesis of one thiamin analog for PET imaging study and have shown that the second target molecule (**15**) is well accepted as a cofactor in cellular metabolism. Synthesis of a cyclic sulfate followed by fluoride substitution, ring opening and hydrolysis is also a reasonable option for synthesizing the fluoro-thiazole (**20**). A post-doctoral research associate in the lab has proposed another synthetic strategy and for fluorothiazole using hydrofluoric acid (HF) as the fluoride source (Scheme 4.11-A), although it is not an available form of the ^{18}F isotope. A different strategy for the coupling reaction is also proposed (Scheme 4.11-B). Synthesis and purification of the fluoro-thiamin analog using the new strategy is currently underway.

We have collaborated with a research group in UT Southwestern for the PET scanning experiments. The hot synthesis of the molecule will be carried out after the synthetic route to **15** is optimized and the followed by the PET imaging experiments.

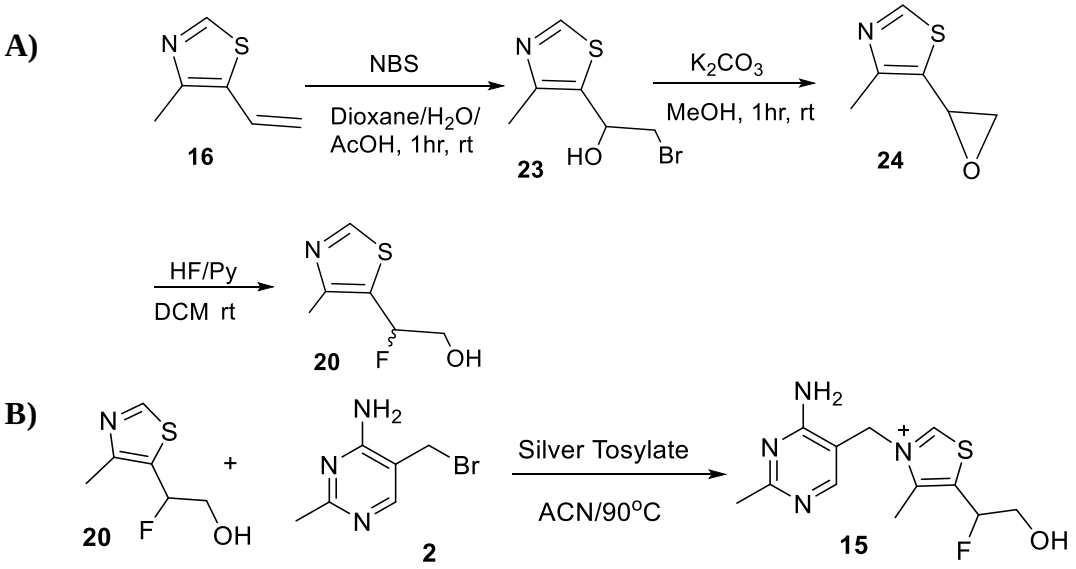

Scheme 4.11: A) Proposed Synthesis of fluorine labeled thiamin using hydrofluoric acid as the fluorinating agent. B) Strategy proposed for the coupling of the pyrimidine and the thiazole part to give the targeted fluorinated thiamin molecule.

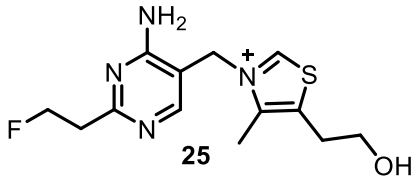

Figure 4.4: Structure of the newly designed thiamin analog

To bypass the problem of hydrolysis of the fluoride at the benzylic like positions, I have designed the another thiamin analog (Figure 4.4). As it has been observed before that methoxythiamin can act as a competent cofactor so we expect effective phosphorylation and good binding of (**25**) in thiamin dependent enzymes. A synthetic route is also designed and the synthesis is currently underway.

4.4 Experimental

4.4.1 Synthetic procedure

*4-Amino-5-(hydroxymethyl)-2-methylpyrimidine (HMP, **9**).* A solution containing 454 mg (6.58 mmol) of $NaNO_2$ in 5 mL of water was slowly added, using a dropping funnel, to a solution of 1.25 g (5.96 mmol) of Grewe diamineâ dihydrochloride in 12.5 mL of 10% HCl at 90 °C. The reaction mixture was stirred at 90 °C for 5 hours and then neutralized to pH 8.0 followed by purification by a silica gel column with 15% methanol in chloroform with 81% yield.

^{1}H NMR (400 MHz, D_2O): δ 7.99 (1H, s), 4.52 (2H, s), 2.39 (3H, s).

*5-(bromomethyl)-2-methylpyrimidin-4-amine (**2**):* A 2:1 mixture of glacial acetic acid and HBr (3 mL) was added to 250 mg (1.78 mmole) of **10** in a pressure tube. The mixture was

heated at 110 ^{o}C for 30 minutes with stirring. The compound first dissolves in the solvent and forms a clear solution and then after few minutes the product separates as a precipitate. It was then filtered and washed with dichloromethane and dried under vacuum. 295 mg (1.49 mmole) product was recovered (Yield 83%). The isolated product was used for coupling reaction without further purification.

1H NMR:

*4-Amino-5-(chloromethyl)-2-methylpyrimidine (HMP-Cl, **23**)* This compound was prepared using some modification of the literature procedure.[48] A mixture of 4-amino-5-(hydroxymethyl)- 2-(trifluoromethyl)pyrimidine (550 mg, 3.96 mmol), thionyl chloride (0.85 mL, 1.4 g, 11.9 mmol), and 10 mL of chloroform was refluxed with stirring for 3 h. The product separated as a yellow solid. This was filtered and washed several times with anhydrous chloroform and dried under vacuum. This product was used without further purification (Yield – 72%).

1H NMR (400 MHz, DMSO-d_6): δ 8.31 (1H,s), 4.63 (2H, s), 2.39 (3H, s)

*2-(4-methylthiazol-5-yl)ethyl trifluoromethanesulfonate (**5**):* To a solution of **4** (500 mg, 3.5 mmole) in 20 mL anhydrous dichloromethane, trimethylamine (1.78 g, 7.0 mmole) was added and stirred at room temperature for 15 min under nitrogen. 4-Nitrobenzenesulfonyl chloride (1.16 g, 5.25 mmole) was then added to it. The mixture was stirred for 4 hours, and the product formation was checked by TLC. After purification by column chromatography 648 mg (67%) of **5** was isolated.

1H NMR DMSO: 9.39 (1H, s), 3.59 (2H, t), 2.92 (2H, t), 2.36 (3H, s)

*2-(4-methylthiazol-5-yl)ethyl 4-nitrobenzenesulfonate (**6**):* To a solution of **4** (500 mg, 3.5 mmole) in 20 mL anhydrous dichloromethane trimethylamine (1.78 g, 7.0 mmole) was added and stirred at room temperature for 15 min under nitrogen. Triflic anhydride (1.28 g, 4.55 mmole) was then added to it in a dropwise manner. The mixture was stirred for 6 hours, and the product formation was checked by TLC. After purification by column chromatography 956 mg (83.5%) of **6** was isolated.

1H NMR (400 MHz, DMSO-d_6): 8.76 (1H, s), 8.39 (2H, d), 8.07 (2H, d), 4.30 (2H, t), 3.13 (2H, t), 2.22 (3H, s)

*5-(2-fluoroethyl)-4-methylthiazole (**3**):* To a solution of **6** (110 mg, 0.34 mmole) in 5 mL anhydrous acetonitrile KF (43.5 mg, 0.75 mmole) and [2,2,2]-kryptofix (282 mg, 0.75 mmole) were added and the mixture was stirred at 80 ^{o}C for 30 minutes under nitrogen. The product **3** (29 mg, 0.2 mmole) was purified by column chromatography (61%).

1H NMR (400 MHz, DMSO-d_6): 8.83 (1H, s), 4.56 (2H, m), 3.15 (2H, m), 2.38 (3H, s)

*3-((4-amino-2-methylpyrimidin-5-yl)methyl)-5-(2-hydroxyethyl)-4-methylthiazole-2(3H)-thione (**12**):* The following components were added in a small round-bottomed flask (25 mL); 3.3 mL absolute ethanol, 0.5 mL 20% ammonium hydroxide and 0.75 mL water. Compound **9** in dihydrochloride form (420 mg, 1.95 mmol) was then added followed by 3-chloro-4-oxopentyl acetate (500 mg, 2.81 mmol) and carbon disulfide (0.15 mL). The reaction mixture was stirred at room temperature for 15 hours, and the product **11** was

extracted with ethyl acetate and used in the next step without further purification. A crude mixture of **11** was dissolved in 5 mL of 10% HCl and stirred at 80 ^{o}C for 20 minutes. Upon neutralization with 25% ammonium hydroxide solution the product separated as a precipitate. After filtration and drying, **12 (**470 mg, 81.5%) was isolated as a pale yellow solid.

^{1}H NMR (400 MHz, DMSO d_6): δ 2.08 (3H, s), 2.28 (3H, s), 2.89 (2H, t,), 3.52 (2H, dd), 5.23 (2H, s), 7.00 (2H, s), 7.41 (1H, s)

*2-(3-((4-amino-2-methylpyrimidin-5-yl)methyl)-4-methyl-2-thioxo-2,3-dihydrothiazol-5-yl)ethyl 4-methylbenzenesulfonate (**13**)*: In a solution of **12** (300 mg, 1.01 mmole) in anhydrous pyridine at 0 ^{o}C Tosyl chloride (300mg, 1.58 mmole) was added and the mixture was stirred for 6 hours. It was allowed to warm to room temperature, and the solvent was removed under reduced pressure. The product **13** (380 mg, 85%) was recovered after purification by column chromatography.

1H NMR (400 MHz, DMSO d_6): δ 2.07 (3H, s), 2.29 (3H, s), 2.93 (2H, t,), 4.13 (2H, dd), 5.18 (2H, s), 7.00 (2H, s), 7.38 (1H, s) 7.43 (2H, d), 7.69 (2H, d).

*3-((4-amino-2-methylpyrimidin-5-yl)methyl)-5-(2-fluoroethyl)-4-methylthiazole-2(3H)-thione (**14**)*: 150 mg (0.33 mmole) of the **13** was dissolved in 3mL of 10% MeOH in acetonitrile. 175 mg (0.67 mmole) of Tetrabutylammonium fluoride hydrate was added, and the reaction mixture was stirred at 75 ^{o}C for 25 minutes. 78.6 mg (80%) of 14 was isolated after purification by column chromatography.

^{1}H NMR (400 MHz, DMSO d_6): δ 2.10 (3H, s), 2.20 (3H, s), 3.00 (2H, m), 4.54 (2H, m), 5.23 (2H, s), 7.00 (2H, s), 7.39 (1H, s).

*3-((4-amino-2-methylpyrimidin-5-yl)methyl)-5-(2-fluoroethyl)-4-methylthiazol-3-ium chloride hydrochloride (**1**)*: To a solution of **14** (50 mg, 0.17 mmole) in 3 mL 10% HCl, 150uL of aqueous H_2O_2 was added. The reaction mixture was stirred at r.t. for 20 minutes, and the mixture was then evaporated to dryness under reduced. The product **1** was formed in almost quantitative yield.

^{1}H NMR (400 MHz, D_2O): δ 2.51 (3H, s), 2.63 (3H, s), 3.51 (2H, m), 4.85 (2H, m), 5.66 (2H, s), 78.10 (1H, s). The proton on C2 of thiazole was not visible due to rapid exchange with deuterium.

*1-(4-methylthiazol-5-yl)ethane-1,2-diol (**17**)*: To a solution of ***(16)*** (625 mg, 5.0 mmole) in a 1:1 mixture of water and THF (20 mL) a 4% aqueous solution of OsO_4 (0.5 mL) was added follower by the addition of N-methyl morpholine N-oxide (880 mg, 7.5 mmole). The mixture was stirred overnight at room temperature, concentrated under reduced pressure and was purified by column chromatography (10% methanol in chloroform) to yield 685 g (~86%) of **17** as a white crystalline solid.

1H NMR (400 MHz, DMSO-d_6): δ 8.74 (1H, s), 4.94 (1H, t), 4.08 (1H, m), 3.70 (2H, m), 2.33 (3H, s)

*2-((tert-butyldimethylsilyl)oxy)-1-(4-methylthiazol-5-yl)ethan-1-ol **(18)***: t-Butyl dimethyl silyl chloride (950 mg, 6.3 mmole) was added to a solution of **17** (500 mg, 3.14 mmole) in 15 mL pyridine. The mixture was stirred under nitrogen for 15 hours, the solvent evaporated under vacuum, and the product was purified by column chromatography (20% ethyl acetate in hexane). The product **18** (1.1 g, 80.5% yield) was obtained as a colorless sticky oil.

1H NMR (DMSO, 400 MHz): δ 8.84 (1H, s), 5.73 (1H,d), 4.87 (1H, m), 3.71 (2H, m), 2.32 (3H, s), 0.80 (9H, s), -0.42 (3H, s), -0.67 (3H, s)

*5-(2-((tert-butyldimethylsilyl)oxy)-1-fluoroethyl)-4-methylthiazole (**19**)*: To a solution of **18** (400 mg, 1.45 mmole) in anhydrous dichloromethane (5 mL) at 78 ^{o}C, Diethylaminosulfur trifluoride (DAST, 0.25 mL) was added drop wise, and the solution was warmed to room temperature and stirred for 3 hours. The solution was then again cooled to -78 ^{o}C and excess unreacted DAST was quenched with methanol (0.3 mL). After warming at room temperature, the organic solution was washed with saturated K_2CO_3 solution twice followed by drying on Na_2SO_4 and purification by column chromatography. 240 mg (60% yield) of **19** was obtained as pale yellow liquid.

1H NMR (DMSO, 400 MHz): δ 9.02 (1H, s), 5.95 (1H, m), 3.92 (2H, m), 2.41 (3H, d), 0.89 (9H, s), 0.47 (3H, s), 0.42 (3H, s)

*2-fluoro-2-(4-methylthiazol-5-yl)ethan-1-ol (**20**)*: To a solution of **19** (100 mg, 0.36 mmole) in 5 mL acetonitrile KF(42 mg, 0.72 mmole), Kryptofix-222 (270 mg, 0.72

mmole) and trimethylsilyl chloride (80 mg, 0.74 mmole) were added and the mixture was stirred at 80°C for 20 minutes. Product **20** (33 mg, 57% yield) was purified by chromatography on silica column.

4.4.2 High Performance Liquid Chromatography (HPLC) conditions for the isolation of 1

Agilent 1200 series instrument; Supelcosil SPLC-18-DB column (25 cm x 10 mm, 5 μm). The following gradient was used with (A) water, (B) 10 mM ammonium acetate and (C) methanol; 0 min, 100% B; 4 min, 8% A/77% B; 8.6 min, 20% A/15% B/65% C; 17 min, 20% A/15% B/65% C; 20 min to 25 min, 100% B. Flow rate 2 mL/min.

CHAPTER V

EXPLOITING THIAMIN AS A DELIVERY VEHICLE FOR CARGO INSIDE LIVING CELL

5.1 Introduction

The ATP-binding cassette (ABC type) family of transporters in bacteria is one of the largest superfamilies of transporters and very well studied for a long time.[58-60] The ABC transporters for different substrates are very similar in their mechanism of action in which a periplasmic substrate-binding protein acts as an initial receptor and the ligand-bound protein then interacts with a membrane-bound carrier protein stimulating the hydrolysis of ATP by the ATPase subunit.[61-62]

Thiamin has a specific and dedicated ABC-type transporter that can transport it through the cell membrane. In the replete condition of thiamin, the biosynthetic pathway in the cell shuts down and it starts to uptake thiamin available in the surroundings, and this process is regulated by a riboswitch.[63] The transportation of thiamin across the cell membrane occurs by active transport by an ABC-type transporter ThiBPQ.[64-66]In this system, ThiB, thiamin binding protein (TBP) is a periplasmic protein and can bind free and phosphorylated thiamin, ThiP is the transmembrane protein, and ThiQ is the nucleotide binding domain (NBD) that binds the ATP.[23, 67] ThiXYZ is another ABC transporter for thiamin uptake consisting of ThiY (Substrate binding domain), ThiX (Transmembrane domain) and the ThiZ (Nucleotide/ATP binding domain).[68-69] This transportation system mostly transports the pyrimidine precursor (HMP) of thiamin rather

than thiamin itself and co-localized with an HMP kinase encoding gene.[70-71] It is involved in the thiamin salvage pathway from degraded forms of thiamin present in the soil.[25]

There are several anti-bacterial organic compounds that do not have the capability of crossing the cell membrane. To deliver these molecules in the cell, a strategy has been designed by linking these molecules with cell penetrating peptides (CPP). The cell membrane prevents proteins, peptides and drug carriers from entering cells unless an active transport mechanism is involved.[72] The exact molecular pathway of cellular uptake of cargo linked to CPP across the cellular membrane is not fully understood. However, a large number of different therapeutic agents have been efficiently delivered by CPPs.[73] Thiamin and its two phosphorylated forms can bind to the thiamin binding protein and transported inside the cell. This suggests that the transporter has high tolerance about the moiety attached to the terminal hydroxyl group. Hence, thiamin can be utilized as a vehicle to deliver cargo inside the cell. The cargo molecules can be linked with thiamin through some cleavable linking functionalities that will enable them to enter the cell with thiamin uptake. The linkage will then be cleaved, and the active molecule will be released inside the cell.

Due to the presence of several non-specific esterases we choose carbamate and ester functional groups for linking the cargo molecule with thiamin. Here we report the development of a synthetic methodology to link cargo molecules with thiamin to be delivered inside the bacterial cell.

5.2 Results

5.2.1 Development of synthetic methodology for ester linkage

As thiamin is a positively charged cationic species, it is completely insoluble in aprotic organic solvents. To link the cargo molecule with thiamin, some thiamin precursor has to be used that can be easily converted to thiamin.

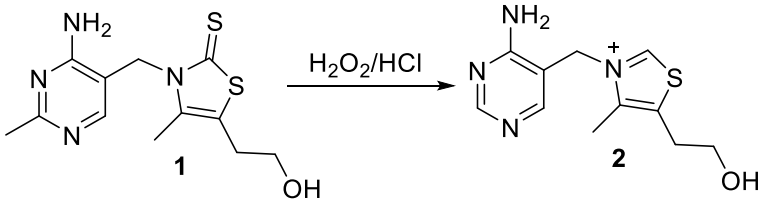

Figure 5.1: Reaction condition for converting thiamin thiazolone to thiamin.

Thiamin thiazolone (**1**) could be an option for this purpose, but it should undergo oxidation under acidic condition to give thiamin (Figure 5.1). As both ester and carbamate linkages are acid labile, this strategy could not be used.

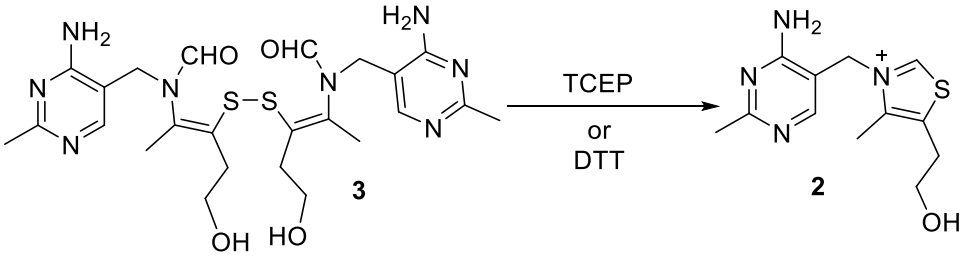

Figure 5.2: Reduction of the disulfide bond of thiamin disulfide to produce thiamin

Thiamin disulfide was chosen as the neutral thiamin precursor to load the cargo. It can be easily converted to thiamin in the presence of a reducing agent like DTT, 2-mercaptoethanol or TCEP (Figure 5.2). These reagents do not harm the ester or carbamate linkage between thiamin and the cargo molecule.

Ester linkage can be used for any molecule that has a carboxylic acid group, where they can be linked with the free hydroxyl group of the thiamin molecule. In this strategy, the carboxylic acid group is activated by N,N′-Dicyclohexylcarbodiimide (DCC) in the presence of a base and then the thiamin precursor is added to the reaction mixture to form the linkage.

Such reaction is quite common in organic chemistry and previously reported.[74] However, we chose DMF as the solvent because of poor solubility of thiamin disulfide in all other solvents. Indole-3-acetic acid was chosen as the example cargo molecule to establish the synthetic viability of this process.

The reaction was carried out at room temperature where a solution of DCC in anhydrous DMF was added to an equimolar mixture of thiamin disulfide (**3**) and indole-3-acetic acid (**4**) in the same solvent (Scheme 5.1). After 19 hours of stirring the compound was purified by column chromatography and reduced by TCEP to yield the final ester linked adduct of thiamin and indole-3-acetic acid (**6**).

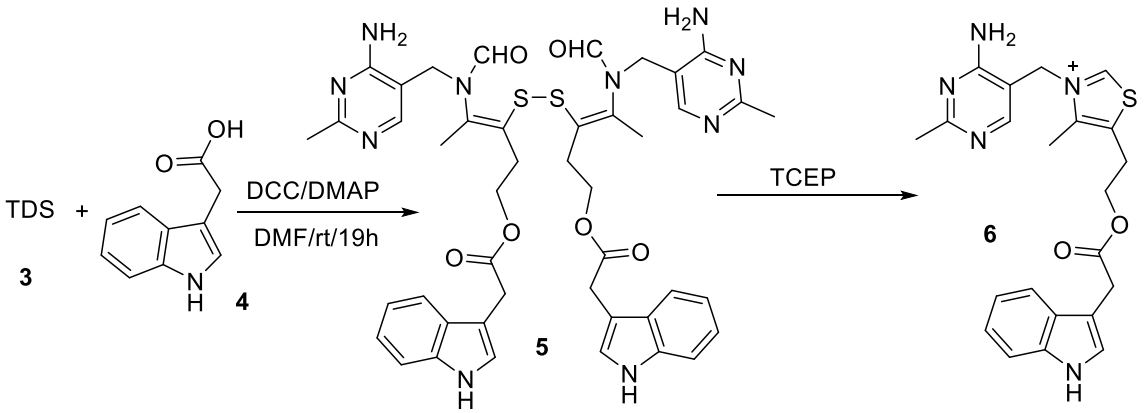

Scheme 5.1: Linking cargo molecule with thiamin by an ester linkage.

5.2.2 Formation of carbamate linkage

Patel *et al*. reported formation of a carbamate linkage between thiamin and amine-functionalized nanoparticle.[75] Unsuccessful attempts to reproduce the same strategy forced us to investigate newer possibilities. First two attempts of activating the thiamin hydroxyl group by carbonyldiimidazole (CDI) (**7**) in short time have failed.[76-77] Finally, successful activation was done by stirring the reaction mixture for 18 hours which was confirmed by formation of carbamate linkage by isopropyl amine (**9**) (Scheme 5.2).[78]

The thiamin disulfide - isopropyl amine adduct (**10**) was purified by column chromatography and the NMR was recorded. Finally the target compound (**11**) was prepared by treating **10** with a solution of TCEP.

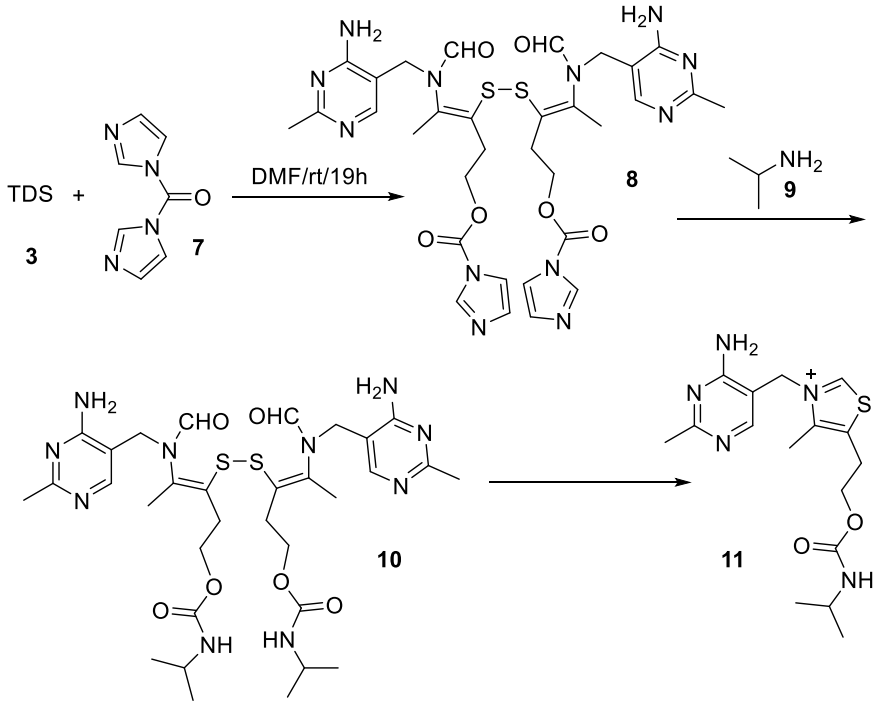

Scheme 5.2: Formation of carbamate linkage with thiamin for amine group containing cargo.

This protocol was explored with the methyl ester of alanine, and a clean mass of the adduct was obtained. Successful demonstration of this methodology was applied to form adduct between thiamin and ampicillin (Figure 5.3).

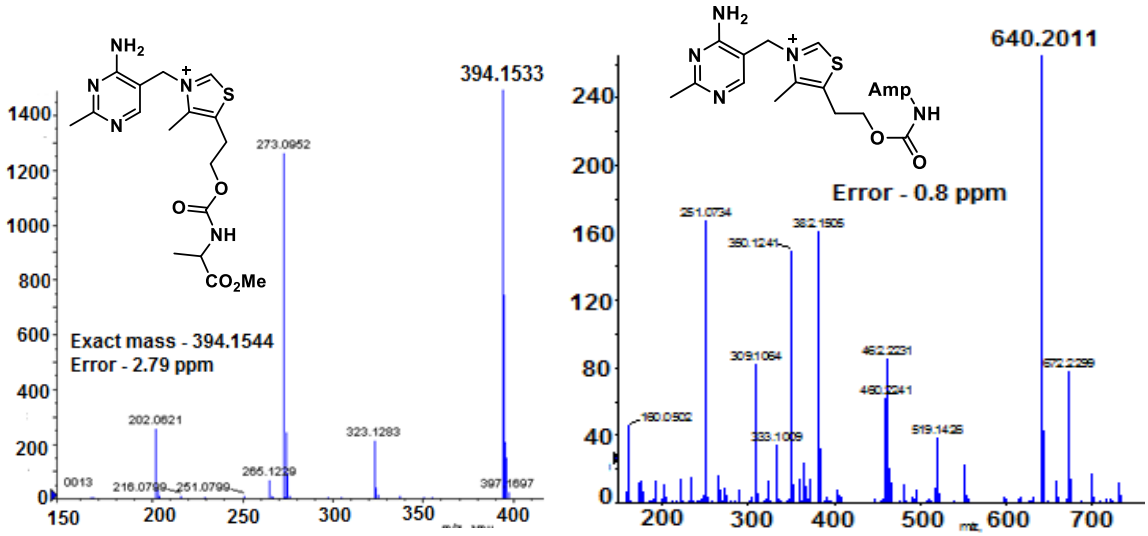

Figure 5.3: Mass spectra (+ve mode) of the thiamin alanine methyl ester adduct and thiamin-ampicillin adduct

We then planned to explore this strategy to deliver alanine phosphonate into the cells, and a synthetic route was optimized to synthesize the Ala-P molecule. Ala-P is an inhibitor for alanine racemase and thus can act as antibiotic. It cannot be transported directly into the bacterial cell and needs a carrier for delivery.

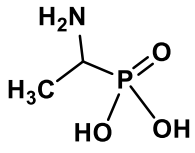

18

Figure 5.4: Structure of the Ala-P molecule.

5.2.3 Synthesis of (1-aminoethyl)phosphonic acid (Ala-P) and thiamin-Ala-P conjugate

The targeted molecule (Ala-P) was attempted to be made from acetyl chloride (**12**), trimethoxy phosphine, and hydroxyl amine. After the condensation reaction, the hydroxyl imine (**14**) was planned to be reduced by catalytic hydrogenation (Scheme 5.3).[79]

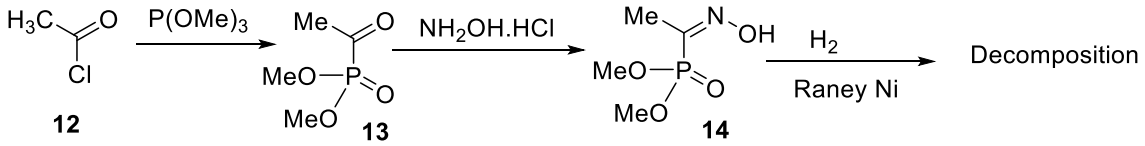

Scheme 5.3: Attempt to synthesize dimethyl ester of Ala-P

The hydroxyl amine (**14**) was successfully prepared, however, the reduction reaction by catalytic hydrogenation with H_2 and Raney nickel gave a complex mixture of compound that could not be purified. To bypass the reduction reaction by hydrogenation the synthetic strategy was revised (Scheme 5.4). Benzyl carbamate was chosen as the source of nitrogen for Ala-P. Oxidation state of the central carbon precursor was also modified from +3 (Acetyl chloride) to +2.

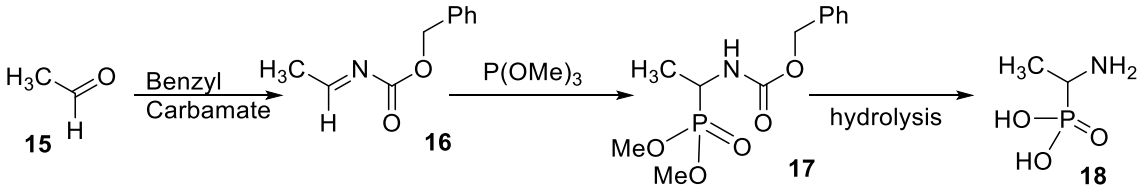

Scheme 5.4: Synthesis of (1-aminoethyl) phosphonic acid avoiding the reduction step

First benzyl carbamate was condensed with acetaldehyde to form **16.** A Michael-type 1,4 addition of trimethyl phosphite across the imine linkage gave **17**. Hydrolysis of

17 with dilute hydrochloric acid yielded the desired Ala-P (**18**).[80] The product obtained was in hydrochloride form.

The product **18** was found to be insoluble in DMF and hence the attempt of the carbamate adduct formation with thiamin was unsuccessful. Neutralization of hydrochloride of Ala-P by methanolic ammonia followed by evaporation of the solvent did not increase the solubility. In the next attempt, the molecule was neutralized by tetrabutyl ammonium hydroxide with the hope that presence of a counter ion with large hydrophobic side chain would increase the solubility. However, the carbamate forming reaction was still unsuccessful.

The strategy was further changed to overcome this problem. As the phosphonate esters can be selectively cleaved by trimethyl silyl bromide we attempted to make Ala-P phosphonate ester, link it to thiamin disulfide followed by deprotection and ring closure (Scheme 5.5).[81] The amine group of Ala-P was first protected by trifluoroacetyl group followed by esterification of the phosphonic acid by ethyl orthoformate to give **19**. The triflate group was removed by treatment of sodium borohydride in ethanol (Scheme 5.5).[82] The resulting compound (**20**) was purified and characterized by NMR.

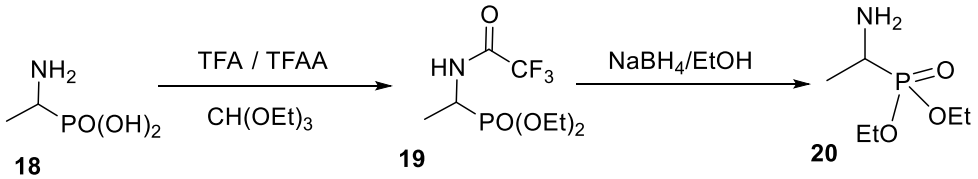

18 **19** **20**

Scheme 5.5: Strategy for the Synthesis of diethyl (1-aminoethyl)phosphonate.

The phenyl ester of Ala-P was prepared to modify the existing protocol (Scheme 5.6).[83] However, attempt to couple any of the esters (**20** and **22**) with thiamin disulfide was unsuccessful.

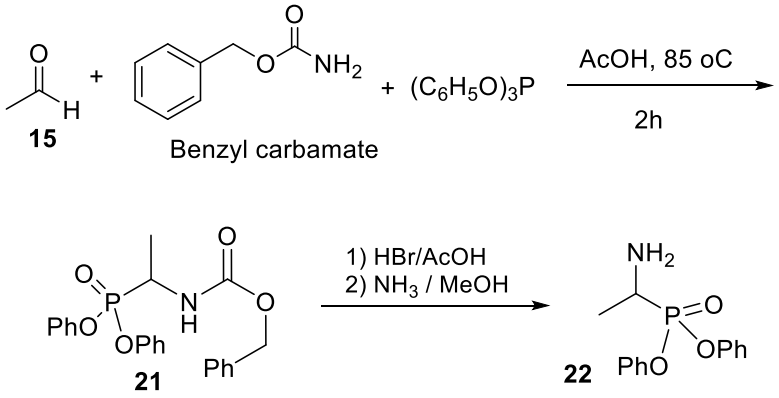

Scheme 5.6: Synthetic scheme for the preparation of diphenyl ester of Alanine phosphonate.

5.3 Conclusion and future directions

A strategy has been successfully designed to deliver cargo molecules inside the cell using thiamin as a delivery vehicle. Ester and carbamate linkages were used as the coupling functionality. Synthetic routes has been optimized to develop a methodology that can be used for a wide variety of cargo molecules. Synthesis of the Thiamin – Ala-P conjugate is currently underway. To avoid the solubility problem, possibility of the synthesis of the carbamate linkage in the water containing media will be explored. After the synthesis, the molecule will be tested for antibacterial activity. To ensure the delivery inside the cell a radiolabeled cargo molecule will be used in future.

5.4 Experimental

5.4.1 Synthetic methods

The chemicals were purchased from Sigma-Aldrich.

*5-(2-(2-(1H-indol-3-yl)acetoxy)ethyl)-3-((4-amino-2-methylpyrimidin-5-yl)methyl)-4-methylthiazol-3-ium (**6**):* Thiamin disulfide (562 mg, 1 mmol), indole-3-acetic acid (175 mg, 1 mmol) and DMAP (146 mg, 1.2 mmol) was dissolved in anhydrous DMF (10 mL) and stirred for 15 min. DCC (310 m, 1.5 mmol) was added and stirred at room temperature for 19 hours. After removing DMF, the intermediate was purified by column chromatography and dissolved in water followed by the addition of TCEP (315mg, 1.1 mmol). The final product (77 %) was characterized by NMR and mass spectroscopy.
1H NMR: 9.32 (1H, s), 7.83 (1H, s), 7.57 (1H, d), 7.49 (1H, d), 7.39 (1H, s), 7.27 (1H, t), 7.13 (1H, t), 5.38 (2H, s), 4.45 (2H, t), 3.92 (2H, s), 3.28 (2H, t), 2.69 (3H,s), 2.37 (3H, s)

*(3Z,3'Z)-disulfanediylbis(4-(N-((4-amino-2-methylpyrimidin-5-yl)methyl)formamido) pent-3-ene-3,1-diyl) bis(isopropylcarbamate) (**10**):* Thiamin disulfide (562 mg, 1 mmol) and 1,1′-Carbonyldiimidazole (243 mg, 1.5 mmol) were taken in anhydrous DMF and stirred at room temperature for 19 hours under inert atmosphere. Isopropyl amine (120 mg, 2 mmol) was added, and the mixture was stirred for another 18 hours. DMF was removed under reduced pressure, and the product was purified by silica column with a linear gradient from 5% - 20% methanol in chloroform. Fractions containing the pure

product were pooled and recovered by evaporating the solvent in a rotary evaporator. 70% product yield was recorded.

1H NMR: 7.83 (1H, s), 7.94 (1H, s), 6.72 (2H, s), 4.35 (2H, s), 3.90 (2H, m) 3.58 (1H, m), 2.47 (2H, t), 2.29 (3H, s), 1.96 (3H, s) 1.04 (6H, d)

*3-((4-amino-2-methylpyrimidin-5-yl)methyl)-5-(2-((isopropylcarbamoyl)oxy)ethyl)-4-methylthiazol-3-ium (**11**):* Compound **10** (220 mg, 0.3 mmol) was dissolved in water (2 mL), and TCEP (95 mg, 0.33 mol) was added and stirred at room temperature for 10 minutes. The product was purified by HPLC and characterized by 1H NMR, UV-Vis, and mass spectrometry.

1H NMR: 8.86, (1H, s); 8.09 (1H, s); 5.64 (2H, s); 4.41 (2H, t); 3.73 (1H, m); 3.41 (2H, t); 2.69 (3H, s); 2.64 (3H, s); 1.17 (6H, d)

*dimethyl (Z)-(1-(hydroxyimino)ethyl)phosphonate (**14**):* Acetyl chloride (155 mg, 2 mmol) was dissolved in 10 ml of toluene and placed in the flask (50 ml). The mixture was cooled to 0 °C, and trimethyl phosphonate (4 mmol, 420 mg) was added very slowly with stirring so that the temperature does not exceed 7–8 °C. The mixture was left for a night, and after the volatile components were removed under reduced pressure. To the remained crude mixture, hydroxylamine hydrochloride (2 mmol, 140 mg), dissolved in 3 ml methanol containing pyridine (160 mg, 2 mmol), was added. The mixture was stirred overnight, and the solvent was removed under reduced pressure and acidified by 2M HCL 20 mL. The product was extracted with ethylacetate (15 mL x 3), dried over anhydrous sodium sulfate

and recovered by remolval of the solvent to yield the desired α-oxymephosphonate. It was characterized by NMR, desired splitting due to the presence of phosphorous was observed.
1H NMR: 3.73 (1H, d), 3.68 (6H, d), 1.43 (3H, d)

*benzyl (1-(dimethoxyphosphoryl)ethyl)carbamate (**17**):* To a well-stirred mixture of benzyl carbamate (151 mg, 1 mmol) and trimethyl phosphite (125 mg, 1 mmol) in 3 mL AcOH : H_2O (1:1), Acetaldehyde (65 mg, 1.5 mmol) was added slowly. The temperature was maintained at 85 ^oC for 2 hrs. The solvent was evaporated under reduced pressure and purified by column chromatography.
1H NMR : 7.32 (5H, m), 4.95 (2H, s), 3.92 (1H, m), 3.65 (6H, d) 1.24 (3H, dd)

*(1-aminoethyl)phosphonic acid (**18**):* Compound **17** was refluxed in HCl in methanol (5 mL) for 15 min. The product was recovered by evaporation of the solvent under reduced pressure. Hydrolysis reaction gave a quantitative product yield.
1H NMR: 3.65 (1H, m), 1.20 (3H, dd)

*Diethyl-1-aminoethyl)phosphonate (**20**):* The 1-aminomethylphosphonic acid hydro-chloride (**18**) (161 mg, 1 mmol) was dissolved in TFA (0.1 mL) – TFAA (0.6 mL) mixture and heated at 50 ^oC for 15 min. Ttiethyl orthoformate (5 mL) was slowly added and the resulting mixture was heated at 110 ^oC for 2 hours followed by evaporation of the solvent giving crude derivative **19**. This compound was then dissolved in ethanol (10 mL), sodium borohydride (228 mg, 6 mmol) was added and the mixture was stirred at r.t. for 1 hr

followed by reflux for 30 min at 80 ^{o}C. The volatile components were removed under reduced pressure and the residue was dissolved in chloroform and washed with 1M aqueous $NaHCO_3$ followed by brine. The chloroform was then evaporated and the crude product was purified via column chromatography (20 % Ethyl acetate in hexane).

1H NMR (CDCl3, 400 MHz), : δ 8.5 (2H, s), 4.45 (1H, m), 4.13 (4H, m), 1.44 (3H, m), 1.32 (6H, m)

*Diphenyl-1-aminoethyl)phosphonate (**22**):* To a mixture of triphenyl phosphite (310 mg, 1 mmol) and benzyl carbamate (151 mg, 1 mmol) in glacial acetic acid 3 mL acetaldehyde (65 mg, 1.5 mmol) was added slowly and the reaction mixture was stirred at room temperature for 2 hours followed by heating at 85 ^{o}C for two hours. The volatile components were removed under reduced pressure to yield the crude product **21 that** was purified via column chromatography (10 % Ethyl acetate in hexane). This was further hydrolyzed by treatment with a solution of 33% HBr in acetic acid at room temperature for one hour followed by solvent evaporation and neutralization of the mixture by a solution of ammonia in etanol. The final compound (60% overall yield) was also purified by column chromatography (15% ethyl acetate in hexane).

1H NMR (DMSO, 400 MHz), : δ 7.30 (6H, m), 7.13 (4H, m), 4.19 (1H, m), 1.35 (3H, m)

CHAPTER VI

ESTIMATION OF THIAMIN QUOTA IN THE HAPTOPHYTES THAT PREFERENTIALLY USE PYRIMIDINE COMPOUNDS TO FULFILL THIAMIN REQUIREMENT

6.1 Introduction

6.1.1 Thiamin biosynthesis and phytoplankton

Thiamin is an important cofactor in all forms of life and it is biosynthesized in most of the bacteria, archaea, fungi and plants. Thiamin biosynthesis requires a certain set of genes encoding all of the biosynthetic enzymes that are required to synthesize thiamin *de novo*. In recent studies, by a complete genome analysis of marine taxa, it has been observed that the complete canonical thiamin biosynthetic pathway is absent in multiple eukaryotic phytoplankton groups.[84-85] This observation suggests that in marine ecology thiamin auxotrophy is common in producers which in turn indicates a regulatory function of thiamin.[86-88] Recently three phytoplankton species and a heterotrophic bacterial group have been identified that fulfill their thiamin requirement through uptake of 4-amino-5-hydroxymethyl-2-methylpyrimidine (HMP), an intermediate precursor compound in thiamin biosynthesis. This observation perfectly agrees with the absence of key thiamin pyrimidine biosynthetic genes in these organisms. Though most of the thiamin auxotrophy studies were carried out by supplementing with thiamin alone, reports exist where 4-amino-5-aminomethyl-2-methylpyrimidine (AmMP), a functional analog of HMP, was taken up by thiamin auxotrophic algae.[89] Moreover, widespread bacterial oligotroph

Pelagibacter ubique (SAR11) can use only AmMP and not exogenous thiamin. This indicates that the strategy for thiamin cycling in marine taxa is complex as recently reported for B_{12} analogs in cyanobacteria and eukaryotic algae.[90]

The complete genome sequence was available for approximately 20 such phytoplankton species, but most of them are thiamin prototrophs. However, In ocean ecosystems the haptophytes are extremely diverse and are the important primary producers, which are thiamin auxotroph too.[91-94] Among these haptophytes, genome sequence was available for *Emiliania huxley* and *Chrysochromulina tobin*.[95-96]

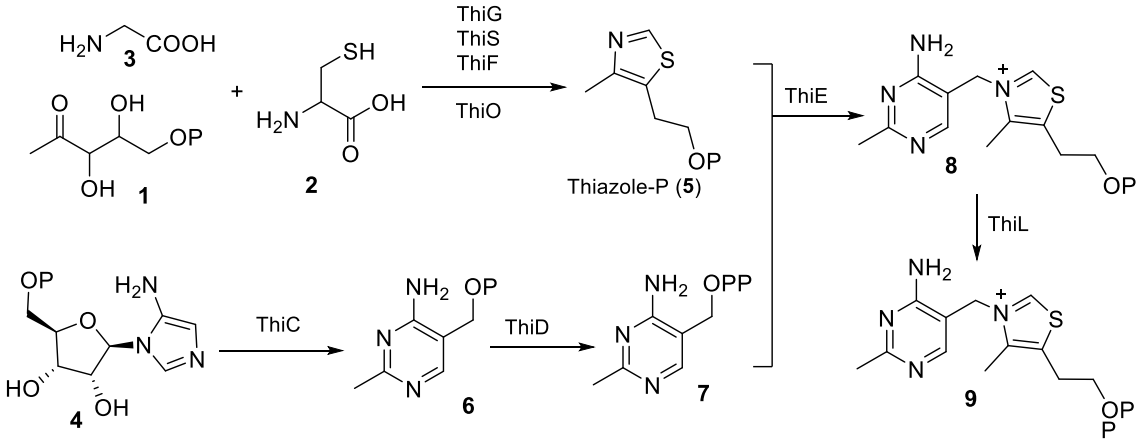

Figure 6.1: Biosynthetic pathway of thiamin pyrophosphate in bacteria

Canonical biosynthesis of thiamin involves two major intermediates that are independently biosynthesized, HMP and 4-ethyl-5-b-hydroxyethylthaizole (HET) as corresponding phosphates (**5** and **7**). **5** was biosynthesized from 1-deoxyxylulose-5-phosphate, tyrosine and cysteine with ThiG, ThiG, ThiO and ThiS proteins, and **7** was biosynthesized from AIR (**4**) by ThiC and ThiD enzymes. Finally, these two precursors are coupled together by ThiE to generate thiamin monophosphate (**8**) by ThiE enzyme

(Figure 6.1).[97] Subsequent phosphorylation gives the biologically active form of the cofactor (**9**). In some organisms, another pathway exists in parallel that involves remodeling of pyrimidine compounds to generate HMP via a salvage pathway.[98] The key enzyme in the salvage pathway is TenA that catalyzes the formation of HMP from thiamin degradation products.[98-99]

6.1.2 Thiamin quota: why it is important

Thiamin cellular quotas are also not known for oceanic phytoplankton. Only data for thiamin quantification is available for prototrophic phytoplankton isolated from brackish water.[100] Hence the estimations of thiamin quotas in marine phytoplankton are based on calculations and not experiments. For a better understanding of thiamin quotas inside the cells, the efficacy of the method has to be evaluated, and these quotas in different growth phase have to be determined. Direct measurement of thiamin quotas in cultures of thiamin auxotrophic haptophyte in different physiological states is essential to set the correct parameters for ecological models in future.

Our collaborator, Warren research group in Monterey Bay Aquarium Research Institute, had identified and compared thiamin biosynthetic pathways from transcriptomes sequenced in all six haptophyte orders as well as the available haptophyte genome sequences.[101-102] Apart from the absence of the HMP synthase in all six orders, the thiamin biosynthetic pathway apparently looks complete. Moreover, thiamin thiazole synthase (ThiG) is observed to be present in all six order as thiazole synthase, which is evolutionarily ancient compared to the eukaryotic analog, Thi4. The first analysis of

salvage pathway of thiamin pyrimidine was performed in this study which revealed the presence of the TenA gene subfamily in all six haptophyte orders. Haptophytes were grown in different concentrations of thiamin and HMP, and the cellular thiamin quotas were measured.

6.2 Results and discussion

6.2.1 Optimization of the thiochrome assay

Thiochrome assay was used to measure the amount of thiamin present in the phytoplankton cells grown in different conditions. Thiamin can be converted to a highly fluorescent compound called thiochrome upon oxidation by ferricyanide in alkaline medium (Scheme 6.1). This compound is detectable in low nanomolar quantities by fluorescence spectroscopy.

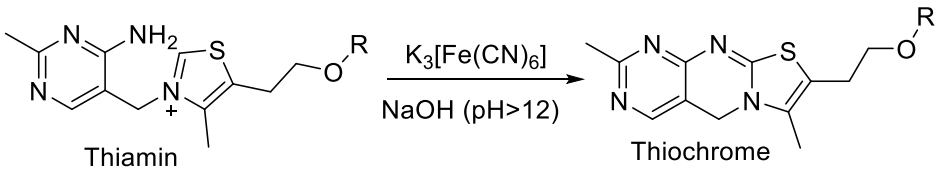

Scheme 6.1: Formation of thiochrome from thiamin by potassium ferricyanide in alkaline medium

One problem encountered with this technique was that some thiamin was being detected even in the absence of any sample or exogenous thiamin. This was due to the presence of thiamin in the water that was being used for making the reagent solutions. This issue was addressed by treating the deionized water with active charcoal under stirring conditions for 15 hours followed by centrifugation and sterile filtration. As active

charcoal can absorb most of the organic compounds, internal thiamin content of water was almost completely removed and was not detected any further by thiochrome assay (Figure 6.2).

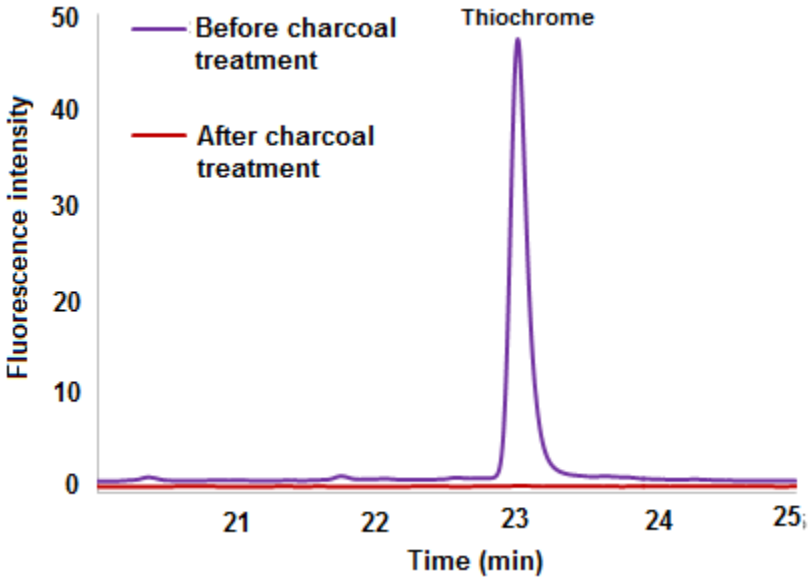

Figure 6.2: Comparison of blank experiments before and after treatment of the water with active charcoal. The thiochrome peak disappears after the treatment.

6.2.2 Growth conditions of the haptophyte cells in the laboratory

E. huxleyi, a member of the haptophyte order, was used to quantify thiamin at the cellular level. Cells were grown in different concentrations of thiamin and HMP, and the growth rate was measured. The total number of cells in the culture was also counted. Thiamin concentration of 300 nM was used as luxury supply. This concentration is about 15000 times of the maximum reported quantity reported in the habitat zone of *E huxleyi* at the Sargasso Sea, it is used as one of the standard concentrations used in the growth media. 10 nM thiamin was chosen as the replete, but the non-luxury concentration in *E.*

huxleyi growth media, five hundred-fold greater than the maximum observed in the Sargasso Sea. The growth rate in these two conditions did not differ significantly (0.74 ± 0.05 day^{-1} in luxury and 0.71 ± 0.04 day^{-1} in replete). HMP (**6**) of the same concentration was also used as a growth supplement for E huxleyi. The limiting condition of thiamin and HMP was chosen as 0.5 nM, which is more comparable to the concentrations reported in the field.[103-104] The growth rate was found to be much slower in this condition (0.21 ± 0.11 day^{-1}).

6.2.3 Estimation of the thiamin content in the haptophyte cells by thiochrome assay

After the growth of *E. huxleyi* in the designated media, the cells were harvested and washed with thiamin-free media for multiple times. The cells were then stored frozen at -80 ^{o}C until subsequent analysis of thiamin content in them. For the analysis, the cells were thawed and resuspended in 7% perchloric acid ($HClO_4$). The suspension was then sonicated to break open the cells and vortexed vigorously to dissolve all the thiamin in the solution. An alkaline solution of potassium ferricyanide ($K_3[Fe(CN)_6]$) was then added to it followed by waiting for 2 minutes and neutralization with hydrochloric acid to pH 7.0. The precipitate was discarded by centrifugation, and the supernatant was analyzed by HPLC, equipped with a fluorescence detector, to detect thiamin in its different states of phosphorylation (monophosphate and pyrophosphate) (Figure 6.3).

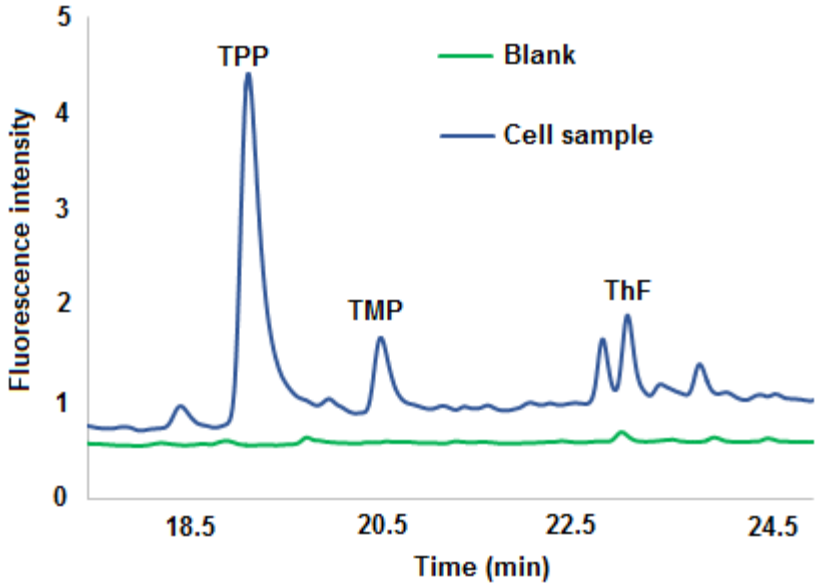

Figure 6.3: Typical chromatogram of the thiochrome assay mixture performed on an *E. huxleyi* cell lysate**.**

It has been observed that thiamin is primarily stored in the cells as thiamin pyrophosphate (**9**). The thiamin monophosphate (TMP) (**8**) and free thiamin (TF) (**10**) is present in lesser quantity compared to TPP. The same pattern was also observed when E. coli was used as a test sample (data not shown). The amount of different forms of thiamin was determined from a standard calibration curve prepared under same experimental conditions.The results of this experiment is represented by the following table.

Table 6.1. Measured cellular quotas for thiamin pyrophosphate (TPP), thiamin monophosphate (TMP), and free thiamin (ThF) in *E. huxleyi* CCMP2090. Error represents the s.d. of three independent measurements and are shown in parentheses.

Treatment	Initial conc. (nmol L^{-1})	Growth rate (day^{-1})	(pmol $cell^{-1}$) TPP	TMP	ThF	T Sum
Replete conditions						
Luxury thiamin	300	0.74 (0.05)	$4.47x10^{-7}$ ($3.66x10^{-7}$)	$4.08x10^{-7}$ ($3.62x10^{-8}$)	$2.6x10^{-7}$ ($1.48x10^{-7}$)	$11.15x10^{-7}$ ($1.83x10^{-7}$)
Replete thiamin	10	0.71 (0.04)	$1.48x10^{-7}$ ($4.00x10^{-8}$)	$5.78x10^{-8}$ ($3.49x10^{-8}$)	$2.11x10^{-8}$ ($1.05x10^{-8}$)	$2.27x10^{-7}$ ($2.48x10^{-8}$)
Replete HMP	10	0.73 (0.06)	$1.43x10^{-7}$ ($8.80x10^{-8}$)	$1.42x10^{-7}$ ($8.00x10^{-8}$)	$1.94x10^{-8}$ ($7.10x10^{-9}$)	$3.04x10^{-7}$ ($7.32x10^{-8}$)
Limiting conditions						
Limiting thiamin	0.5	0.25 (0.13)	$1.60x10^{-7}$ ($6.78x10^{-9}$)	$2.89x10^{-8}$ ($1.48x10^{-8}$)	$3.31x10^{-8}$ ($2.26x10^{-8}$)	$2.22x10^{-7}$ ($7.28x10^{-9}$)
Limiting HMP	0.1	0.21 (0.11)	$1.14x10^{-7}$ ($7.12x10^{-9}$)	$2.08x10^{-8}$ ($1.97x10^{-9}$)	$2.30x10^{-8}$ ($6.00x10^{-9}$)	$1.58x10^{-7}$ ($1.36x10^{-8}$)

The data can also be presented as histogram plot for clear understanding where the thiamin quotas in the cells can be visually compared by the plot.

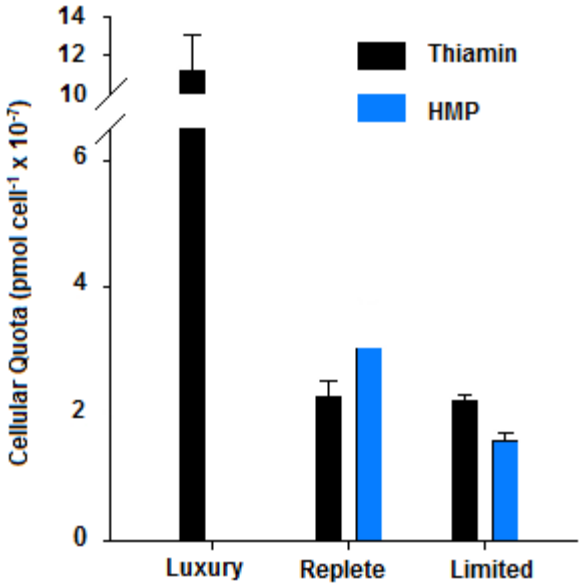

Figure 6.4: Cellular quota of thiamin in *E. huxleyi* cells grown in luxury (300 nM), replete (10 nM) and limited (0.5 nM) concentrations of Thiamin and HMP. Data represents average of three independent measurements.

A very high cellular thiamin quota in the cells grown in luxury thiamin supply indicates that a very high storage of thiamin occurs under the conditions of high availability. In replete conditions, the thiamin storage was six-fold less than the luxury condition. Interestingly, there was not much difference in the thiamin quota for the cells grown under replete or limiting the availability of thiamin or HMP as supplements (Figure 6.4). Previous thiamin measurement data reported in the literature found free thiamin to be the dominant intracellular form which is in complete contrast to the results of this study.[100] The higher thiamin storage in the cells in luxury thiamin availability has little environmental relevance.

The direct measurements of cellular thiamin quotas using thiochrome assay enabled us to evaluate the efficacy of the established procedure for calculating minimum

cellular quota (MCQ). A large discrepancy was observed between the calculated MCQ values and those quantified using the thiochrome assay. The direct measurement results indicate that calculated MCQ overestimates the cellular content of thiamin and do not accurately represent the biochemical status of the cell. The measured MCQ in the HMP amended media was also found to be significantly lower than the calculated value. This observation provides essential information for more accurate parameterization of marine biogeochemical models for examining the role of thiamin-related compounds in primary production.

6.3 Experimental

6.3.1 Growth of E. huxleyi in laboratory

Axenic culture of *E. huxleyi* was obtained from the National Center for Marine Algae and Microbiota (NCMA, Bigelow Laboratory, USA). Axenicity was tested before and after the experiments using DNA stain 4',6-diamidino-2-phenylindole (DAPI) and epifluorescence spectroscopy.[105] All cultures were grown at 21 ^{o}C on a 14:10 hr light:dark cycle (150 μmol photon m^{-2} s^{-1} photosynthetically active radiation) using artificial seawater based medium L1 – Si, with a $1x10^{-8}$ mol L^{-1} H_2SeO_3 amendment.[106-107] Cultures were monitored using an Accuri C6 cytometer (BD Biosciences, USA). Thiamin (as Thiamin hydrochloride, Sigma-Aldrich, USA), 4-methyl-5-β-hydroxyethylthiazole (Sigma-Aldrich, USA), 4-methyl-5-hydroxymethyl-2-methyl pyrimidine (HMP) (synthesized), were used as supplements for growth.[38] Thiamin was not added to controls

or treatments apart from the thiamin-amendment, other medium components remained unaltered from the L1.

The cellular thiamin quotas were determined in mid-exponential phase cells grown for >10 generations in semi-continuous batch cultures. Four conditions of thiamin availability were tested. Thiamin was supplied at 300 nmol L^{-1} in the luxury treatment. In replete conditions both thiamin and HMP were supplied at 10 nmol L^{-1}. In limiting conditions thiamin and HMP were supplied at 500 pmol L^{-1} and 100 pmol L^{-1} respectively. Concentrations in the limiting conditions were different to generate cultures with comparable growth rate. Cultures were transferred after 1 to 2 days so that the cell density cannot exceed 1 x 10^6 cells mL^{-1}.

Thiamin quotas were also quantified in the cells harvested at the onset of the stationary phase to replicate the condition of the cells used for calculation based estimates. In these experiments, triplicate cultures were grown in medium amended with 500 pmol of thiamin or HMP.

6.2.2 Sample preparation for thiamin estimation

For the thiamin estimation, 100 mL of culture was first centrifuged at 4000 x g for 10 min at 4 ^oC. The supernatant was removed, and the pellet was resuspended in 50 mL of thiamin-free media. This process was repeated for total 3 rounds of washing. Following the last washing step, the pellet was resuspended in 1.5 mL of thiamin-free medium, and the cell concentration was quantified using Accuri C6 cytometer (BD Biosciences, USA). A final cell pellet was formed by centrifugation at 10,000 x g for 30 min at 4 ^oC, the

supernatant was removed (and cells quantified), and the cell pellet was flash-frozen in liquid nitrogen before being stored a -80 ^{o}C. The residual number of the cells in the supernatant was subtracted from the number prior to final centrifugation to determine numbers in the pellets.

6.3.3 Thiochrome assay and determination of thiamin content in the cell pellets

Deionized water was treated with active charcoal followed by filtration and confirmed to be thiamin-free by thiochrome assay.[108] All the reagent solutions were prepared using this water. Harvested cell pellets were suspended in 100 μL of 7% perchloric acid ($HClO_4$), sonicated for 2 min. To this sonicated mixture, 4 M potassium acetate (50 μL) and 30 mg/mL potassium ferricyanide ($K_3Fe(CN)_6$) solution in 7M NaOH (50 μL) was added and mixed well by vortexing. After incubating for 2 minutes at room temperature, the reaction mixture was neutralized to pH 7.0 with 6M hydrochloric acid (HCl). The mixture was centrifuged, and the supernatant was analyzed by HPLC (Agilent 1200 series) using reverse phase column. The HPLC was equipped with a fluorescence detector and the thiochrome formed was detected by fluorescence (excitation 365 nm, emission 444 nm).

A calibration curve in the nanomolar concentration range was constructed under the same experimental conditions by plotting the fluorescence signal peak area on the HPLC chromatogram against known concentrations of thiamin pyrophosphate (TPP), thiamine monophosphate (TMP), and free thiamin (ThF). The values of the three forms were summed to determine the pool, T Sum, hereafter referred to as thiamin quota.

6.3.4 HPLC condition

A Supelcosil SPLC-18-DB (25 cm x 10 mm, 5 μm) column was used with a gradient of the following compounds. A) H_20, B) K_2HPO_4 (pH 6.6), C) CH_3OH. The gradient structure was 0 min, 100% B; 5 min, 100% B; 14 min, 7% A/70% B/23% C; 25 min, 25% A/75% C; 28 min to 34 min, 100% B.

CHAPTER VII

SUMMARY OF RESULTS OF PRELEMINARY STUDIES ON MJ0619, A PUTATIVE METHANOPTERIN METHYLTRANSFERASE

7.1 Introduction

7.1.1 Methanopterin and its role in methane biogenesis

Methanopterin (MPT) (**1**) and its derivatives are key cofactors in the methanogenesis process of the methanogenic archaea (Figure 7.1).[109-112] It acts as a one-carbon carrier in the biosynthesis of methane. Methanopterin shares high structural and functional similarity with folic acid (**2**) which is the C_1 carrier in several important biological reactions in all domains of life and the tetrahydro form is the active form for both cofactors (Figure 2).[109, 113] Methanogenic archaea use MPT exclusively for metabolism, however, methylotrophic archaea use MPT for C_1 energy metabolism and folate for biosynthesis of other metabolites (Figure 7.2).[111] The absence of homology between the corresponding biosynthetic enzymes of methanopterin and folate indicates that these cofactors evolved independently.[114] The enzymes that use folate or MPT as cofactors are also not homologous, which reinforces the idea of the independent evolution.[115]

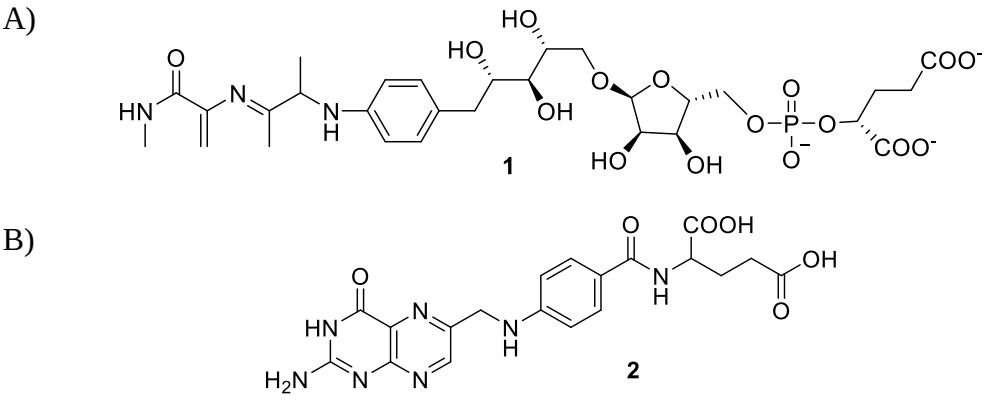

Figure 7.1: Chemical structure of A) Methanopterin and B) Folic Acid

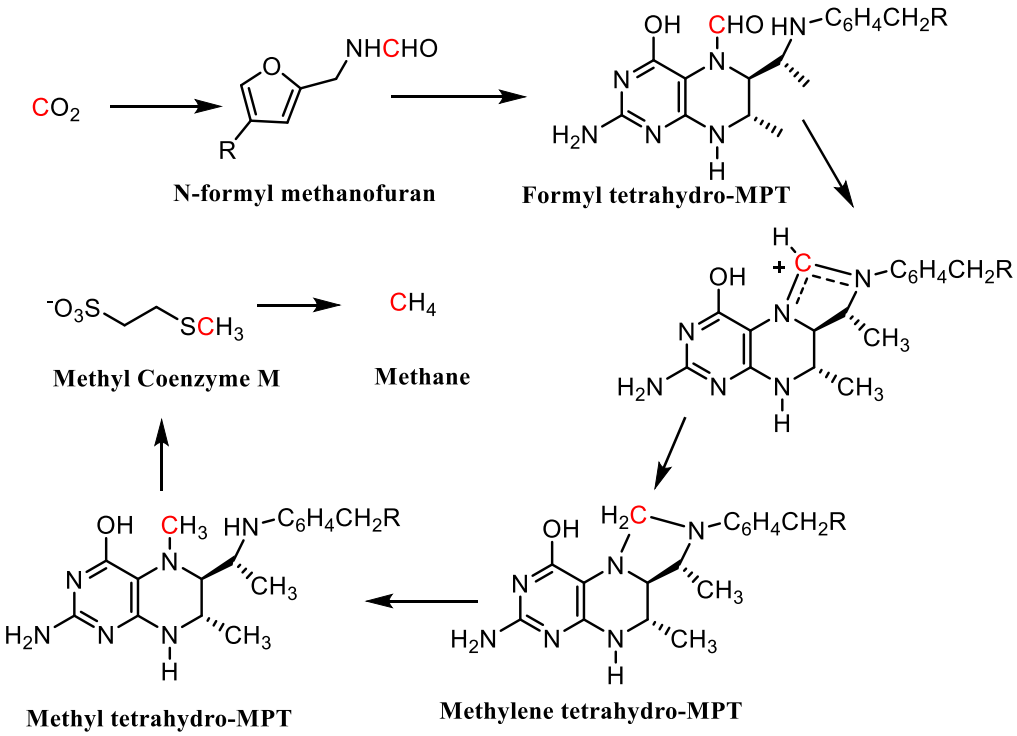

Figure 7.2: Schematic diagram of steps involved in methanogenesis**.**

7.1.2 Biosynthesis of methanopterin: Origin of the methyl groups

The presence of the two methyl groups at C-7 and C-9 of the pterin ring distinguishes methanopterin from the other pterin-based cofactors (Figure 1). Many steps

of the biosynthesis of methanopterin are worked out, however, the source of the two unique methyl groups on the pterin moiety remained an unsolved question (Figure 7.3).[116-120] In earlier reports, studies with CD_3 labeled methionine indicated that it is the source of the two methyl groups in the MPT in methanogens. The insertion of the methyl groups was proposed to be catalyzed via SAM-dependent nucleophilic methylation.[121-123] However, no such methyltransferases in the methanogenic archaeal genome can be identified that are associated with the biosynthesis of MPT and the possibility of radical based methylation was therefore considered.

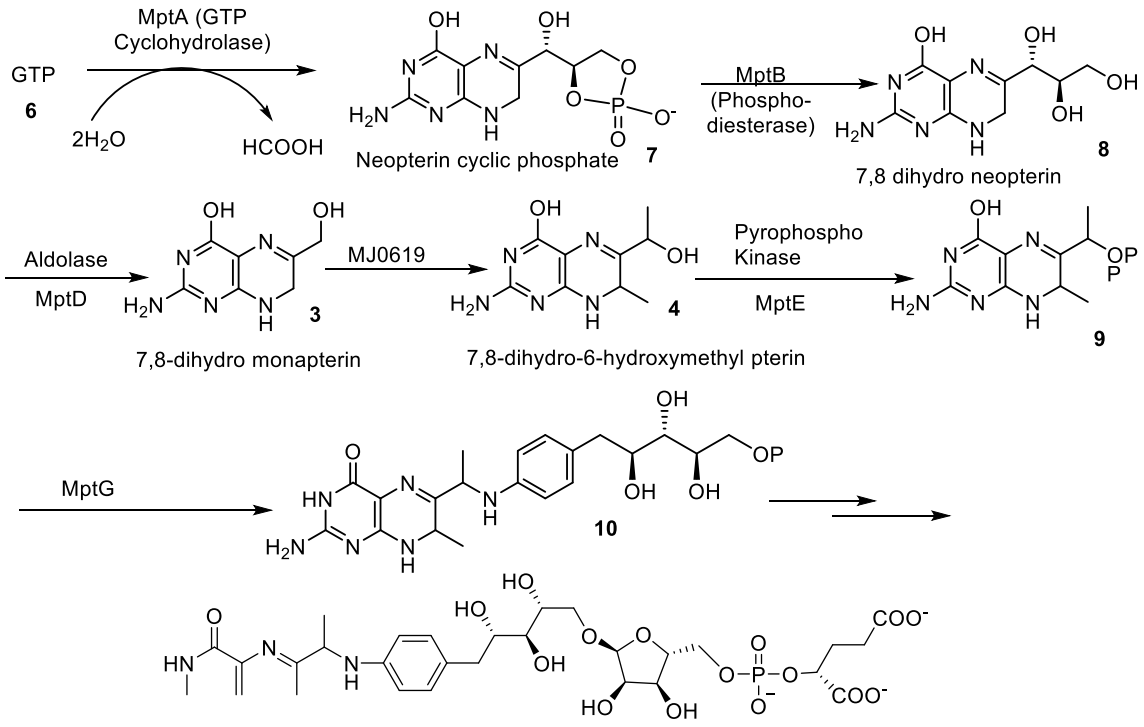

Figure 7.3: Biochemical steps involved in Methanopterin biosynthesis.

7.1.3 Introduction to radical-SAM enzymes

The recently discovered radical SAM superfamily contains thousands of members that catalyze novel biochemical transformations involved in the biosynthesis of cofactors, antibiotics, and other natural products.[124-127] Several examples of radical SAM-based methylation are also reported in the literature.[128] Most radical SAM enzymes contain a canonical CX_3CX_2C sequence motif that harbors a 4Fe-4S cubane cluster.[127, 129] Three cysteine residues ligate to three iron atoms and S-adenosyl methionine (SAM) acts as the ligand of the fourth iron (Figure 7.4).[130]. The chemistry of these enzymes is initiated by one electron transfer from the reduced cluster to SAM followed by homolytic cleavage of SAM to generate 5'-deoxyadenosyl radical (Ado-CH_2 ·). Ado-CH_2 · then abstracts a hydrogen atom from the substrate of the enzyme to generate substrate based radical that undergoes further transformations to yield the product.[126] Modified protein residues in an enzyme can also be a site for radical formation, thus can act as a co-substrate.[131] Reactions after radical formation may lead to various results, such as methylation (RlmN in methylation of nucleotides), methyl-thiolation (MiaB in t-RNA methyl-thiolation), complex rearrangements (ThiC in thiamin biosynthesis, NosL in noshiheptide biosynthesis) and even sulfur insertion (BioB in biotin biosynthesis).[132-136]

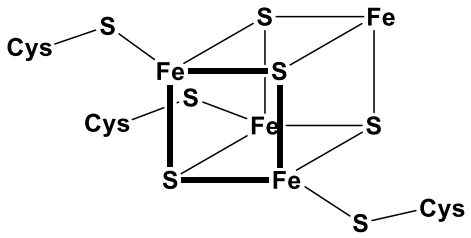

Figure 7.4: Schematic diagram of 4Fe-4S cluster in a radical SAM enzyme. Three iron atoms are ligated by three cysteine residues and the fourth free iron atom binds the SAM molecule during the catalytic cycle.

7.1.4 Discovery of MJ0619, putative methanopterin methyltransferase

Robert White's research group in Virginia Polytechnic identified a gene (MJ0619) that is present very close to another MPT biosynthetic gene, beta-ribofuranosylaminobenzene-5-phosphate synthase, in many methanogens. This enzyme was considered as the putative methyltransferase for the pterin moiety in MPT.[137] Sequence analysis showed that it contains two canonical CX_3CX_2C motifs, characteristic of a radical SAM enzyme. The formation of the methylated pterin moieties was observed upon heterologous expression of that gene in *E. coli*. Previously it was hypothesized that the methylations of the pterin moiety in methanopterin biosynthesis happen in one of the final steps of the biosynthesis, however, in *E. coli* the final biosynthetic intermediates of MPT are unavailable. Hence, 7,8-dihydro-6-hydroxymethylpterin (**3**) was proposed as the possible substrate of MJ0619. No intermediate monomethylated product (**5**) was detected with the wild-type enzyme suggesting consecutive insertion of both the methyl groups (Figure 2). A mutant study by White group observed monomethylation at C-7 with C77A mutant and no methylation with C102 mutant (Figure 7.5). Kylie *et al.* interpreted that the cluster bound at the C102 containing motif (CL-2) does the first methylation at C-7 to form **5** and the cluster bound at C77 containing motif (CL-1) catalyzes the second methylation at C-9 to form **4** as the final product. If the first methylation does not take pace, the second methylation reaction also cannot happen which makes the C102A mutant inactive.

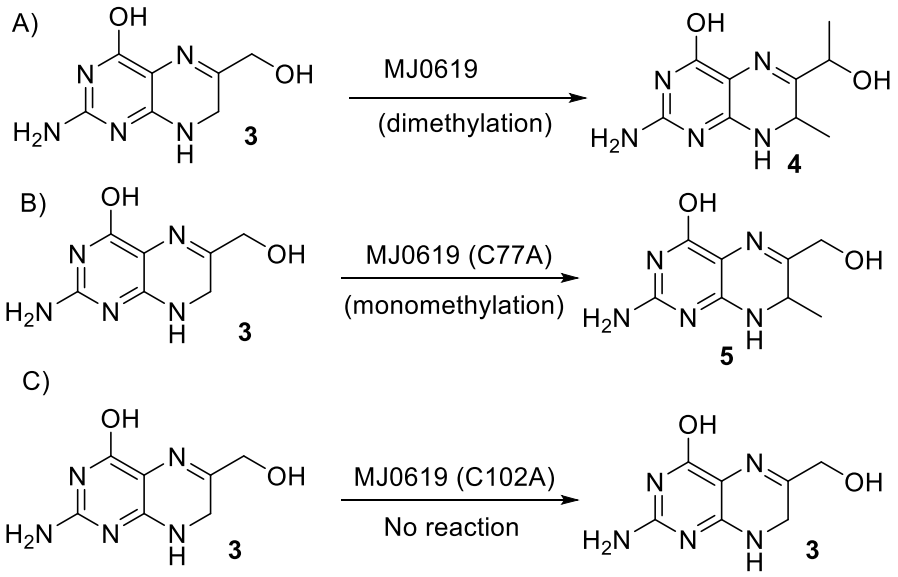

Figure 7.5: Proposed reactions catalyzed by MJ0619 by Allen et al. A) Reaction proposed for wild-type enzyme, B) proposed reaction catalyzed by C77A mutant and C) no methylation observed with C102A mutant of MJ0619**.**

Expression of MJ0619 in *E. coli* grown with CD_3-acetate as the carbon source revealed incorporation of all three deuterium atoms in most of the methylated pterin formed. Methylenetetrahydrofolate was hypothesized as the probable methyl donor in the proposed mechanism to rationalize the isotopic labeling pattern.[137] Participation of methylenetetrahydrofolate as a methyl donor involving radical-based chemistry is unprecedented. Our initial hypothesis of the formation of a substrate-based radical led to the initial mechanistic proposal involving SAM or a modified amino acid residue as the source of the two methyl groups (Figure 7.6).

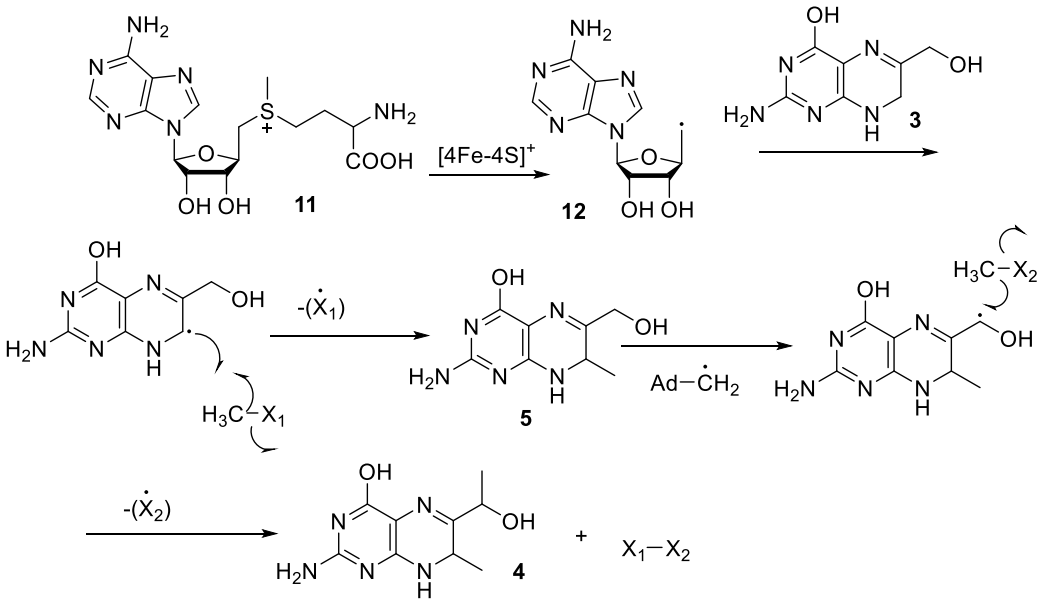

Figure 7.6: Initial proposal for methylation of the pterin moiety. 'X' group denotes the methyl carrier**.**

In this chapter, we report preliminary studies on the *in vitro* analysis of MJ0619 enzyme to characterize its spectroscopic properties, GTP cyclohydrolase activity and radical activity.

7.2 Results

7.2.1 Sequence analysis of MJ0619

The sequence of the MJ0619 protein is given below.

MEKKTLSL**C**PI**C**LKRIPATILEEDGKIIIKKT**C**PEHGEFKDIYWGDAELYKKFDKY

EFIGKIEVTNTKVKNG**C**PYD**C**GL**C**PNHKSTTILANIDVTNR**C**NLN**C**PI**C**FANANK

SGKVYEPSFEDIKRMMENLRKEIPPTPAIQFAGGEPTVRSDLPELIKLARDMGFL

HVQLATNGIKLKNINYLKKLKEAGLSTIYLQFDGISEKPYLVARGKNLLPIKQKV

IEN**C**KKVGFDSVVLVPTLVRGVNDNEVGGIIRYAAENVDVVRGINFQPVSFTGR

VDEKTLLEGRITIPDFIKLVEEQTDGEITEEDFYPVPSVAPISVLVEKLTNDRKPTL

SSHQH**C**GTSTYVFVDEDGKLIPITRFIDVEGFLEIVKEKIEEIGKSKMHDVKVLGE

IALKLPSLIDLDKAPKSVNIKKIIDLILSVLKSDYSALAELHYHMLMIS**C**MHFMDA

YNFDVKRVMR**CC**IHYATPDDRIIPF**C**TYNTLHRQEVEEKFSIPLEEWKRMHKIG

GEDDREDY

MJ0619 has a molecular weight of 57.5 kDa and it has an unusually high cysteine content of 15 residues per monomer. Cysteine residues are coded in bold red. In addition to these two canonical motifs ([C_{73}-C_{77}-C_{80}] and [C_{98}-C_{102}-C_{105}]), two more cluster-binding motifs are predicted at the N- terminal [C_{9}-C_{12}-C_{33}] and the C-terminal [C_{438}-C_{455}-C_{470}] of the protein.

7.2.2 Overexpression and purification of MJ0619

The gene encoding MJ0619 was obtained by custom gene synthesis. It was codon optimized for expression in *E. coli*. The gene was cloned into the pTHT vector, a modified pET-28a vector with an additional site for cleavage of the N-terminal His-tag by the protease from tobacco etch virus (TEV). The plasmid containing the MJ0619 gene was transformed into *E. coli* BL21-(DE3) cells containing a plasmid with the SUF operon for overproduction and delivery of 4Fe-4S clusters to the overexpressing protein. The cells were grown in LB broth at 37 ^{o}C till OD_{600} – 0.6 and the protein production was induced by addition of Isopropyl β-D-1-thiogalactopyranoside (IPTG), with a supplement of Ammonium Iron (II) sulfate hexahydrate [$(NH_4)_2Fe(SO_4)^2 \cdot 6H2O$] and cysteine, at 15 ^{o}C

for 18 hours with gentle shaking. After harvesting by centrifugation, the cells were stored in liquid nitrogen until purification.

The frozen cells were thawed on ice and resuspended in 100 mM Tris buffer (pH – 7.5) in an anaerobic chamber. Lysozyme and benzonase nuclease were added to degrade the cell wall and the RNA in the cell. These cells were then lysed by sonication, centrifuged to remove the cell debris and the supernatant was passed through a freshly charged Ni-NTA His-Trap column. The flow through from the column was discarded and the bound protein was washed with 100 mL of buffer containing 30 mM imidazole to get rid of any non-specifically bound protein. Finally, the protein was eluted with 250 mM imidazole buffer, the colored fractions were pooled and concentrated and buffer exchanged with storage buffer containing 30% glycerol. Purity of the protein was determined by analysis through an SDS-PAGE (Figure 7.7) gel electrophoresis and the protein concentration was determined by Bradford assay.

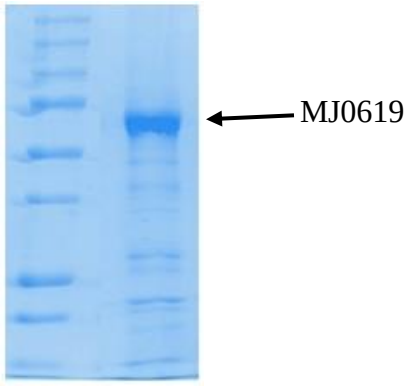

Figure 7.7: SDS-PAGE gel of MJ0619 protein after purification.

7.2.3 Reconstitution of the 4Fe-4S cluster in the purified MJ0619

Initial estimation of the iron and sulfur content of the as isolated protein showed that the number of iron and sulfur atoms per monomer is half of the calculated amount. In vitro reconstitution is thus necessary to maximize the 4Fe-4S cluster content of the protein. For reconstitution of 4Fe-4S cluster in MJ0619, the purified protein was dissolved in PIPES buffer (50 mM, pH – 7.4) and cooled on ice for 30 min in a Coy anaerobic chamber. Solutions of Mohr's salt [$(NH_4)_2Fe(SO_4)^2 \cdot 6H2O$] and sodium sulfide ($Na_2S.9H_2O$) were added in small portions over 45 minutes up to the final concentration of 10 times greater than that of the protein. The mixture was incubated on ice for six hours and then the precipitated iron sulfide was removed by centrifugation. The protein was again desalted to remove excess unbound iron and sulfide and then stored in the same buffer.

7.2.4 Measurement of iron and sulfur content in MJ0619

There are fifteen cysteine residues present in the protein sequence along with two canonical CX_3CX_2C motifs. The protein was likely to contain at least two 4Fe-4S clusters, however, more clusters can be expected harbored by other cysteine residues. Ferrozine assay was used to measure the iron content and protein concentration was measured by Bradford assay. It has been observed that in as isolated protein, there are ~5 iron and sulfur atoms per monomer, however, in the reconstituted protein the number rises to ~15 iron and sulfur per monomer indicating the presence of at least three to the maximum of four 4Fe-4S clusters. This hypothesis is later confirmed by the data from EPR experiments. Possibility of non-specifically bound iron and sulfide ions are also considered.

7.2.5 Construction of the mutants

There are two CX_3CX_2C motifs present in the protein. They are C73-X_3-C77-X_2-C80 (**CL-1**) and C98-X_3-C102-X_2-C105 (**CL-2**). Multiple alignments of MJ0619 with its orthologs have also revealed that these two canonical motifs along with two other non-canonical motifs are conserved. It has been proposed that both of them are catalytically active and each can cleave one SAM molecule to generate 5'-deoxyadenosyl radical. Three mutants were constructed via the standard protocol of single point mutagenesis. In the first two mutants cysteines of the individual motifs were mutated to alanine (M_1 and M_2) and in the third mutant cysteines of both the motifs were converted into alanine (M_3) (Table 7.1).

Table 7.1: Details of the MJ0619 mutants

Mutant Name	Residues modified	Mutated to
M_1	C73, C77, C80	All to alanine
M_2	C98, C102, C105	All to Alanine
M_3	C73, C77, C80, C98, C102, C105	All to Alanine

7.2.6 Spectroscopic analysis of the wild-type protein and the mutants

The wild-type protein MJ0619 and its mutants were analyzed by UV spectroscopy. All of them were observed to have a band at 418 nm and one band at 615 nm (Figure 7.8).

The presence of the 418 nm band suggests the presence of a 4Fe-4S cluster and the 615 nm band might be an indication of a 2Fe-2S cluster or non-specifically bound iron.[138-139]

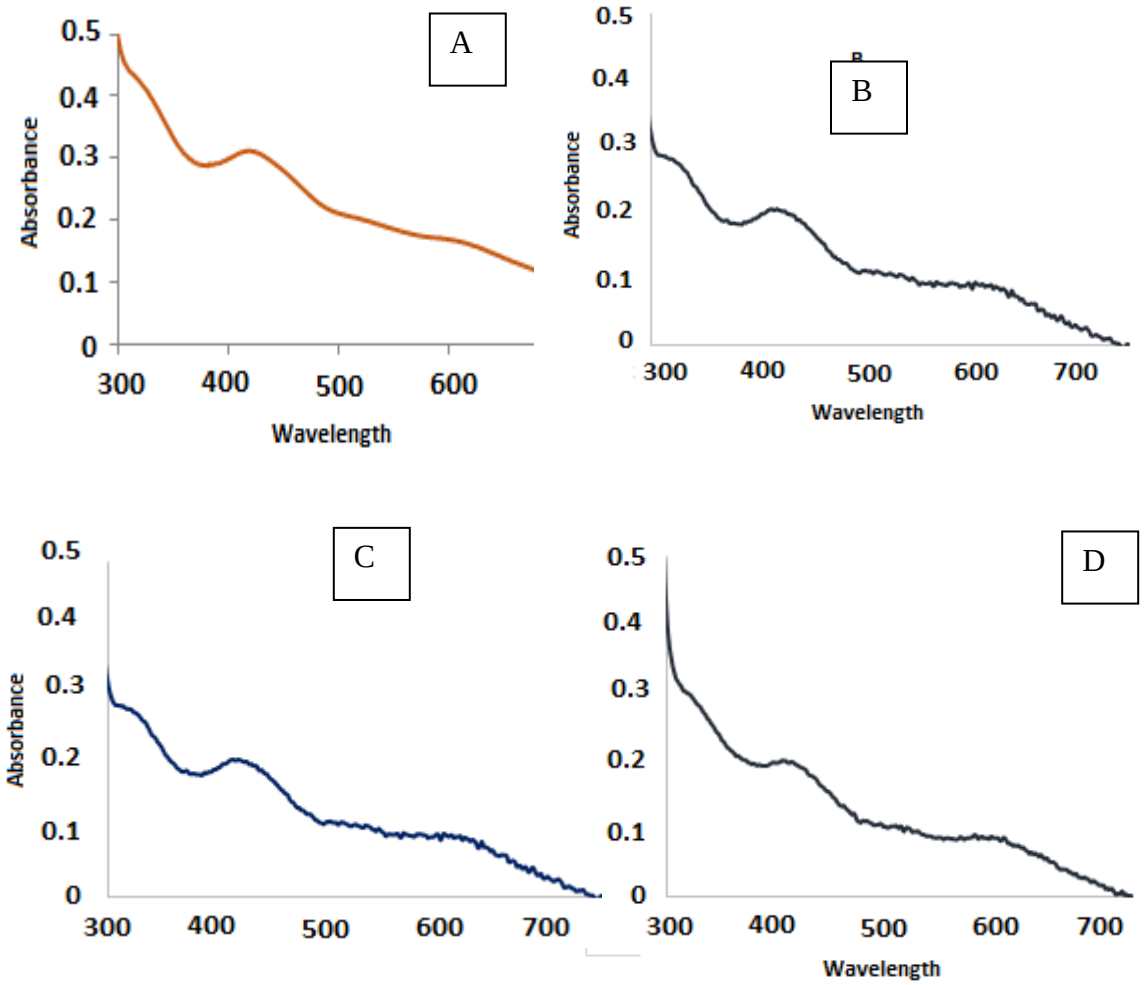

Figure 7.8: UV-Vis spectra of MJ0619 and its mutants. Spectra of A) the wild-type protein, B) M1 mutant, C) M2 mutant and D) M3 mutant. All of them have an absorption band at 418 nm characteristic of 4Fe-4S cluster. The band at ~ 615 nm may be due to a 2Fe-2S cluster or non-specifically bound iron in the protein**.**

The 4Fe-4S cluster band at 418 nm is present in the mutant where both the canonical cluster binding motifs are mutated clearly indicates that there are at least one more 4Fe-4S clusters present in the protein.[140] Putative sites for additional cluster binding are C9-X_2-C12-X_{20}-C33 and C438-X_{16}-C455-X_{14}-C470.

Upon treatment with dithionite, the band at 418 nm is absent suggesting that all the 4Fe-4S clusters present in the enzyme can be reduced by dithionite (Figure 7.9). Some of the clusters were stable even when the protein was exposed to air for few hours. It retains its brown color and the band at 418 nm was still visible.

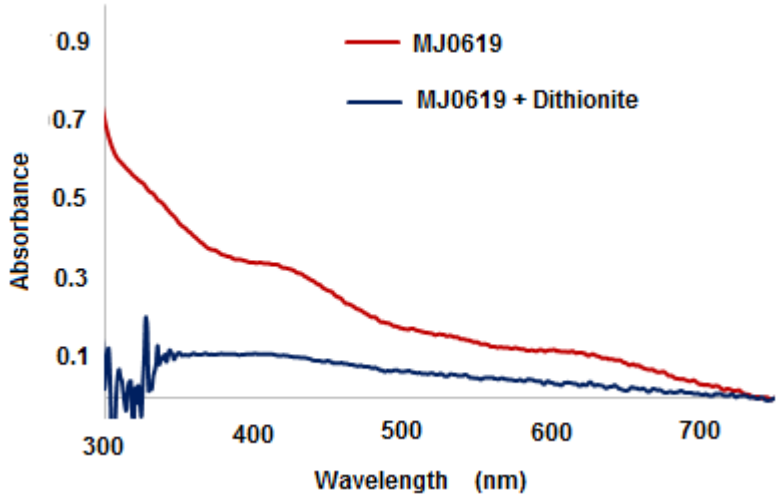

Figure 7.9: UV-Vis spectra of reduced and oxidized cluster. Loss of 418 nm band observed upon reduction**.**

7.2.7 EPR analysis of the wild-type MJ0619 and mutants

The EPR study of the wild type protein and all three mutants revealed that there are signals for two types of clusters with g values ~2.01 and ~2.06 indicating the presence of two types of 4Fe-4S clusters in the protein (Figure 7.10). The EPR band at 2.01 was found to be absent in the M_3 mutant suggesting that it contains a cluster different from the

ones bound at the canonical CX_3CX_2C motifs. No EPR band at g = 1.94, representing a 2Fe-2S cluster, was observed.

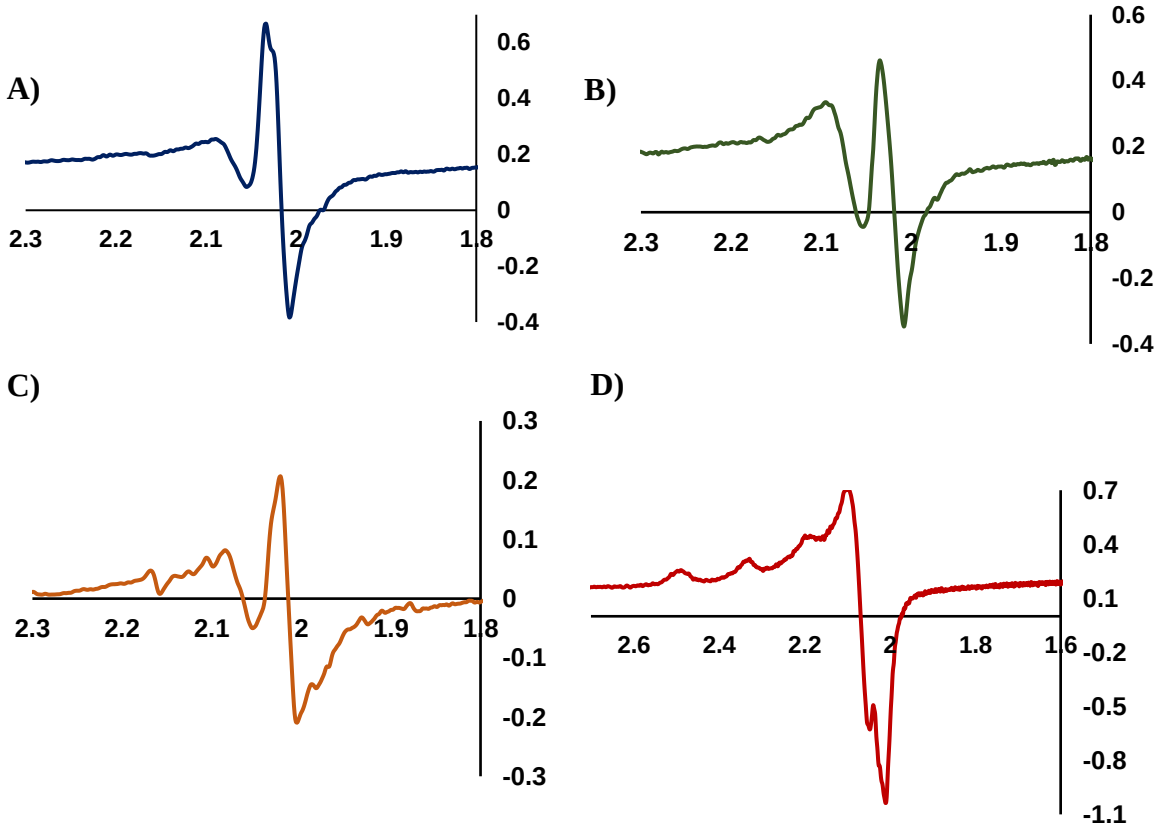

Figure 7.10: EPR spectra of A) Wild-type MJ0619, B) M1 mutant, C) M2 Mutant and D) M3 mutant. Two EPR bands are visible in the wild type, M1 and M2, however, in M3, only one EPR signal was observed.

7.2.8 Homolytic cleavage of SAM by MJ0619: Proof of radical generation

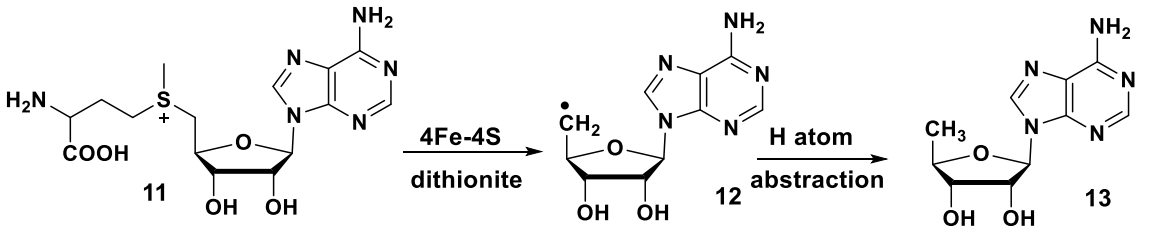

Scheme 7.4: 5'-deoxyadenosyl radical is generated upon transferring one electron from the reduced cluster to SAM molecule. This radical abstracts a hydrogen atom to from 5'-deoxyadenosine.

A radical SAM enzyme can cleave SAM (**11**) reductively in anaerobic conditions in the presence of a reducing agent to produce 5'-deoxyadenosine radical (**12**) (Scheme 7.4). To test the activity of cleaving SAM reductively, MJ0619 was incubated with SAM (1.3 mM) and dithionite (5mM) inside the glovebox. As the enzyme is from *M. jannaschii*, a thermophilic organism, the reaction mixture was heated at 70 ^{o}C for 20 minutes. Although the protein is from a thermophilic organism, it was not stable at that temperature and it is denatured and precipitated out within five minutes of incubation. After removal of the protein, the reaction mixture was analyzed by HPLC (Figure 7.11). Formation of 5'-deoxyadenosine was confirmed by comparing the retention time and UV spectrum with a commercial standard of the compound. LCMS analysis also confirms the compound's identity by obtaining the exact mass (M+1 = 252.1091) in the acceptable error range. Observation through both analytical methods and thereby proves that MJ0619 can cleave SAM reductively by one electron transfer and therefore can be categorized as radical SAM enzyme.

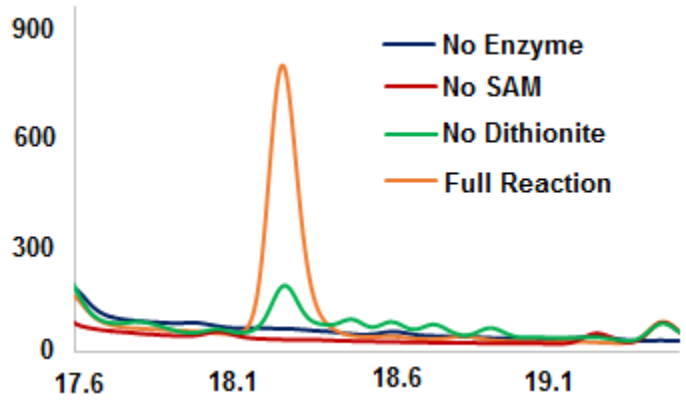

Figure 7.11: HPLC chromatogram of substrate uncoupled 5'-deoxyadenosine formation. No product formation in the absence of SAM or MJ0619 enzyme. Little amount of the product formation is observed in the absence of dithionite due to the presence of some reduced clusters.

7.2.9 Optimization of reaction condition at 37 ºC

SAM is a temperature sensitive molecule and gradually degrades at a higher temperature (70 ºC). The MJ0619 enzyme is also unstable at that temperature and denatures in a very short period of time. This shorter time period might not be sufficient for the radical reaction to happen. Many radical SAM enzymes from thermophilic organisms show activity at room temperature, so MJ0619 was also incubated at room temperature with SAM and dithionite. However, no 5'-deoxyadenosine formation was observed. Next trial was done at 37 ºC that is the optimal growth temperature of E. coli. After incubation of 24 hours uncoupled formation of 5'-deoxyadenosine was observed in the amount comparable with that obtained at 70 ºC. This condition was chosen to carry out the future reactions.

When the same reaction was tried with the mutant enzymes, it was observed that only M1 mutant could produce 5'-deoxyadenosine but either of the M2 and M3 mutant

cannot. Hence it was inferred that the second cluster (CL-2) is responsible for the reductive cleavage of SAM in the presence of dithionite.

7.2.10 Generation of 5'deoxyadenosine with Flavodoxin (FldA) / Flavodoxin reductase (FldR) system

Being successful at 5'-deoxyadenosine formation at 37 ^{o}C, an attempt was made to test the FldA / FldR system as reducing agent instead of dithionite. In the physiological condition in *E. coli* cells, this is the actual system of reduction for 4Fe-4S cluster of the enzyme. Flavodoxin and flavodoxin reductase are cloned individually into pET-28a vector and overexpressed in LB media after transformed into *E. coli* BL21-DE3 cells. The protein overexpression was induced by IPTG (0.5 mM), and it was purified by regular protocol with a Ni-NTA His-Trap column from GE. SDS page gel was run to check the purity of the protein and the concentrations were measured (Figure 7.12).

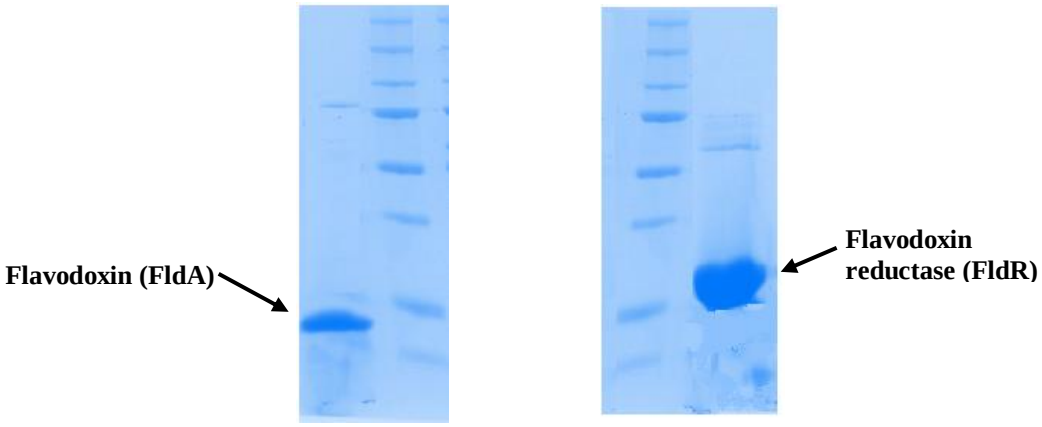

Figure 7.12: SDS-PAGE gel analysis of the purified FldA and FldR. Molecular weights match with the reported values.

The in vitro reaction was carried out in 100 mM Tris buffer, pH – 7.5, SAM 1.5 mM, NADPH 1.5 mM and FldA 50 μM, FldR 50 μM and MJ0619 enzyme ~100 μM. The reaction mixture was incubated at 37^{o}C for 24 hours, enzymes were heat denatured, and the filtrate was analyzed by LCMS after removal of enzymes. Formation of 5'-deoxyadenosine was observed in the full reaction. Formation of a very small amount of 5'-deoxyadenosine in the absence of NADPH is due to the presence of pre-reduced clusters in the MJ0619 enzyme (Figure 7.13). This experiment confirms that the enzyme is active under the physiological conditions in *E. coli* cell. The efficiency of 5'-deoxyadenosine formation is 10 fold less compared to dithionite.

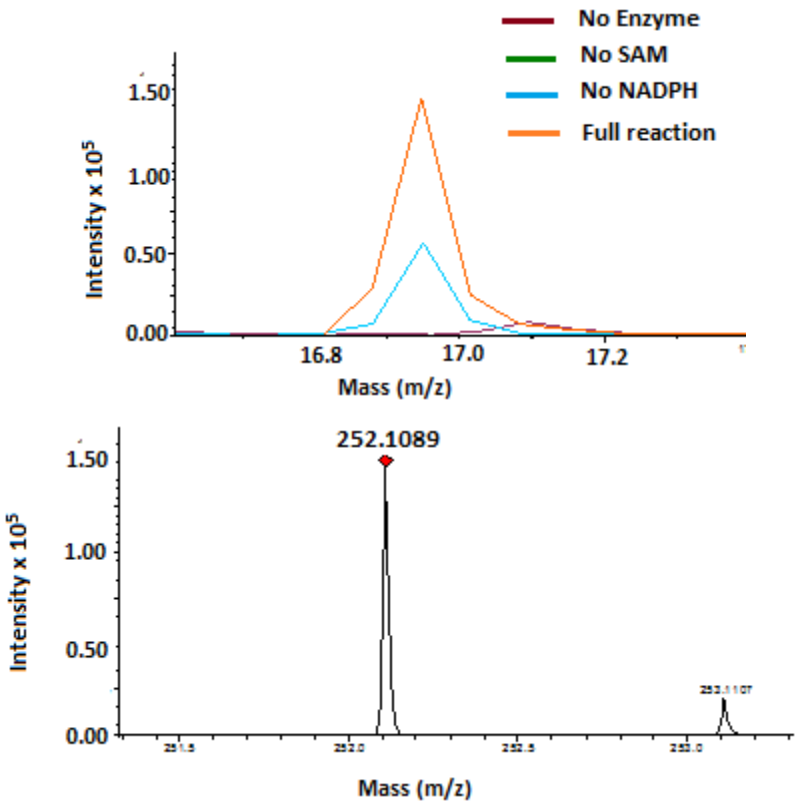

Figure 7.13: A) Formation of 5'-deoxyadenosine in the presence of FldA / FldR as catalysts and NADPH as reducing agent.. B) The exact mass of 5'-deoxyadenosine confirms the identity of the compound.

7.2.11 Assay with GTP, discovery of GTP cyclohydrolase activity

Some orthologs of MJ0619 protein, obtained by BLAST search, were annotated as putative MoaA like proteins. MoaA is involved in the biosynthesis of the molybdopterin cofactor and uses GTP as substrate, hence GTP was tried as a substrate for MJ0619 with SAM and dithionite. Two new peaks in the chromatogram were observed with UV-Vis spectra indicating the presence of 7,8-dihydropterin moiety (Figure 7.14). Upon treatment, with CIP the first peak disappears and gives neopterin which indicates that it is a phosphorylated form of neopterin. The other peak has same UV spectrum as neopterin and

the mass corresponds to the mass of neopterin cyclic phosphate (Scheme 7.5). It also agrees with the literature data that neopterin cyclic phosphate cannot be cleaved by regular phosphatase enzyme.

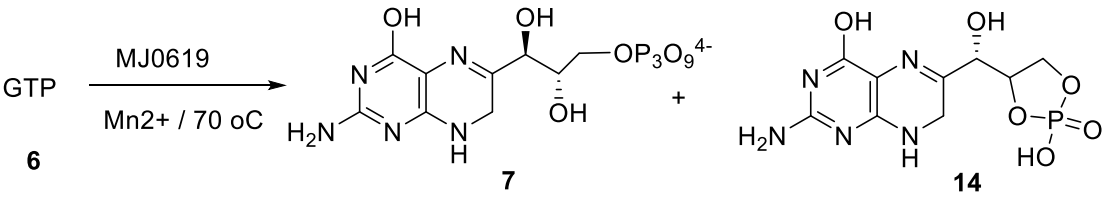

Scheme 7.5: The reaction of GTP cyclohydrolase: conversion of GTP to 7,8-dihydroneropterin-2',3'-cyclic phosphodiester

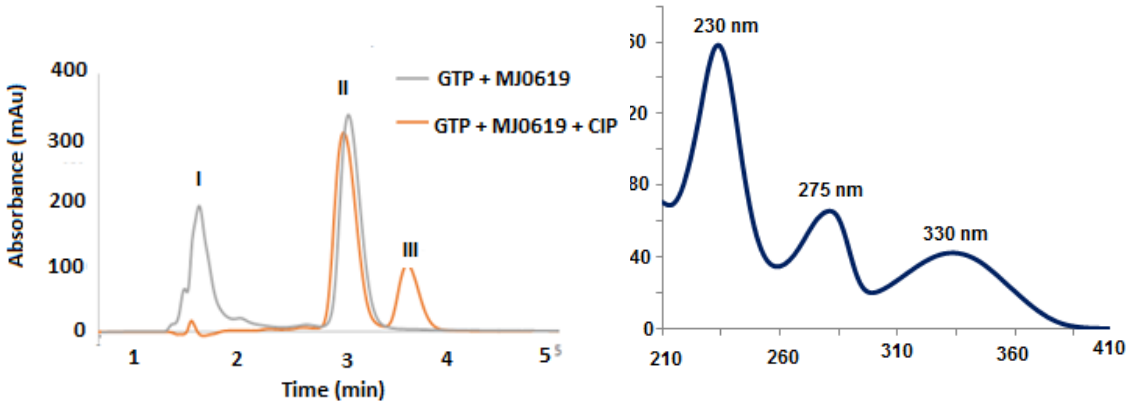

Figure 7.14: A) Reaction product of MJ0619 with GTP before and after CIP treatment. (I) Neopterin triphosphate, (II) Dihydroneopterin phosphodiester and (III) dihydroneopterin. B) UV-Vis spectra of neopterin cyclic phosphate.

We prepared an authentic sample of dihydroneopterin cyclic phosphodiester (**7**) by treating GTP with the dedicated GTP cyclohydrolase enzyme (MptA) involved in the methanopterin biosynthetic pathway. The coelution experiment confirmed the identity of the compound (Figure 7.15). No methylated neopterin was observed. Neither SAM nor dithionite is essential for the cyclohydrolase activity. The addition of Mn^{2+} or Fe^{2+} ion

increases the activity by three fold. Studying different preps of the enzyme it was observed that the enzyme always gives less than one turnover in neopterin cyclic phosphate formation.

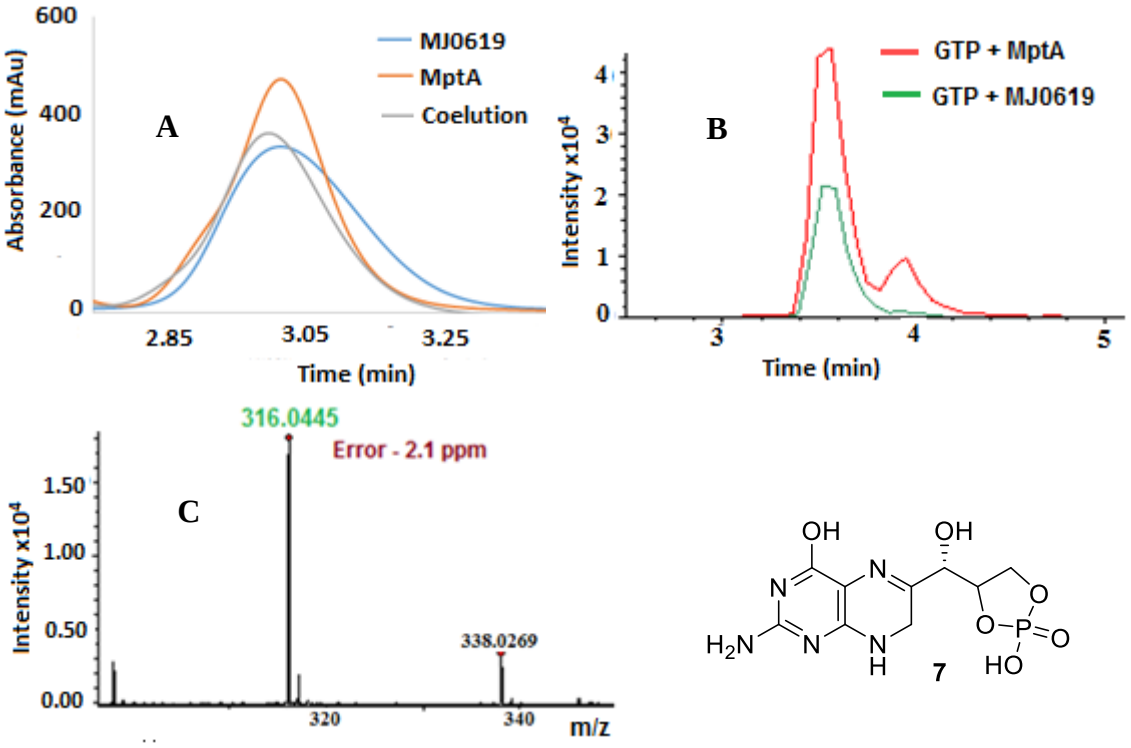

Figure 7.15: A) Coelution experiment (gray trace) of neopterin cyclic phosphate generated by MJ0619 (blue trace) with an authentic sample of the dihydroneopterin cyclic phosphate prepared from GTP and MptA (orange trace). B) Coelution of 7 shown by the extracted ion chromatogram of in LCMS analysis, C) MS-MS spectrum of **7** in negative mode (exact mass 316.0452).

7.2.12 The linear triphosphate is the precursor of the cyclic phosphodiester of dihydro neopterin

A mesophilic ortholog of MJ0619 from *Methanobrevibacter smithii* was obtained by gene synthesis and used to study the time dependence of the cyclohydrolase reaction. It was observed that the amount of the linear phosphate was higher than the cyclic analog

at early time points, however, over time the amount of the linear phosphate decreased, and that of the cyclic phosphate had increased (Figure 7.16). This observation clearly suggests that dihydroneopterin triphosphate was formed first and later it was converted to the corrresponding cyclic phosphodiester.

This reaction mechanism differs a little from the mechanism proposed for the dedicated GTP cyclohydrolase MptA involved in methanopterin biosynthesis where **7** is the only product. Two phosphate groups depart and the cyclic phosphate forms right at the beginning of the reaction mechanism proposed for MptA,[8] however in the case of MJ0619, the linear triphosphate (**15**) is formed first and then it cyclizes to form the cyclic phosphodiester (Scheme 7.6).

The GTP cyclohydrolase activity of MJ0619 is lower at a lower temperature and maximizes at 70 ^{o}C. M-1 and M-2 mutants of MJ0619 also shows the cyclohydrolase activity. Only one turnover is observed and the reason is still unknown. If the reaction time is extended up to 24 hours, complete dephosphorylation of the 7,8-dihydroneopterin cyclic phosphate is observed and 7,8-dihydroneopterin appears as the final product.

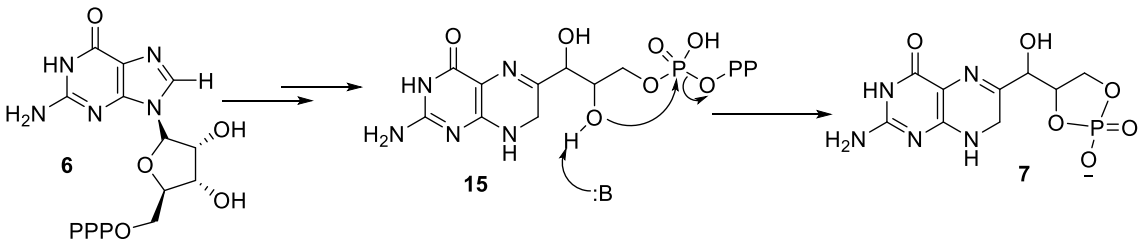

Scheme 7.6: Proposed mechanism of GTP cyclohydrolase activity by MJ0619

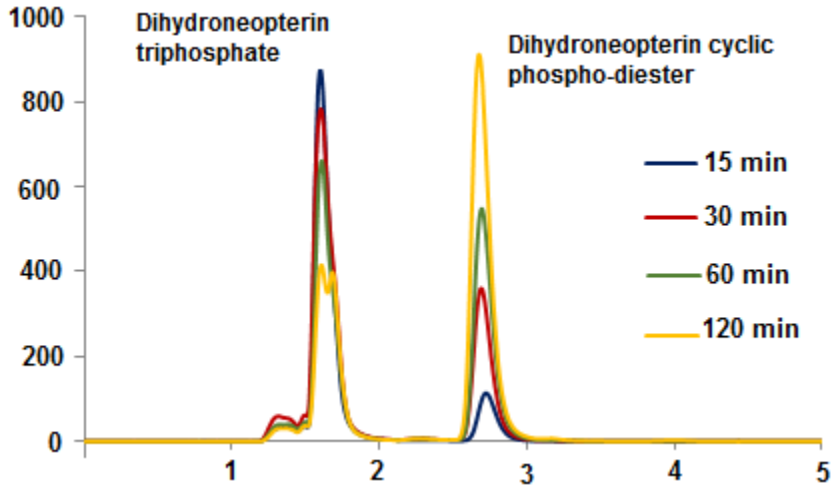

Figure 7.16: Time course of GTP cyclohydrolase activity of MJ0619 ortholog. 7,8-dihydroneopterin triphosphate (**15**) (retention time 1.7 min) was the first product to be formed which later converted to **7** (retention time 2.8 min).

7.2.13 4Fe-4S clusters are necessary for cyclohydrolase activity

The cyclohydrolase activity demonstrated by MJ0619 is a cluster dependent activity. When the iron-sulfur cluster is present, the enzyme shows the activity, however, when the enzyme is expressed without added iron and cysteine and purified aerobically the protein was found to be inactive towards GTP cyclohydrolase activity, as the clusters could not be formed (Figure 7.17).

This observation suggests that presence of the clusters is essential for the cyclohydrolase activity by MJ0619, which, in turn, indicates that the cyclohydrolase activity is not due to any contaminant copurified with the protein.

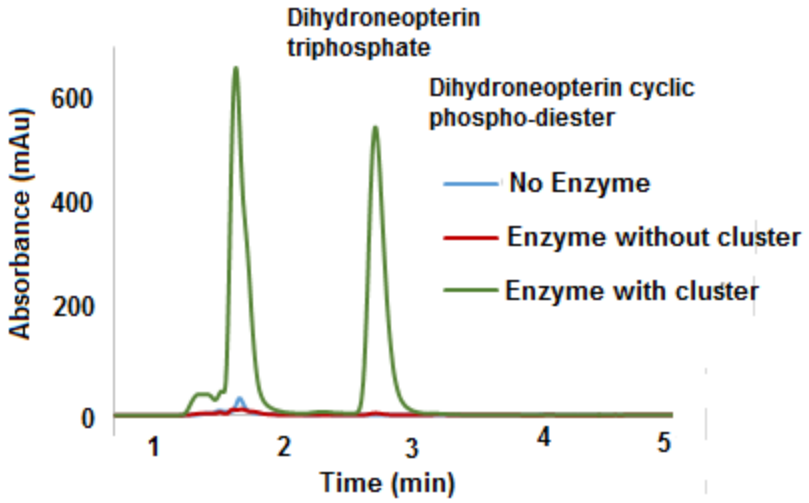

Figure 7.17: Assay for GTP cyclohydrolase activity with the MJ0619 protein in the presence and the absence of bound 4Fe-4S clusters. In the absence of the cluster, the protein was found to be inactive**.**

7.2.14 Phosphatase and nucleosidase activity by MJ0619

While GTP was incubated with the MJ0619 at 37 ^{o}C for 12 hours, two new peaks were observed in the chromatogram that has same UV-Vis spectra with GTP. This similarity in the spectra clearly indicates that those two compounds contain the guanine moiety (Figure 7.18). Later they were identified as guanine and guanosine by comparing with the standards. This observation indicates to the phosphatase and nucleosidase activity of MJ0619 enzyme (Scheme 7.7). When the assay was conducted in a glove box with anaerobically purified enzyme complete substrate consumption along with the formation of 7,8-dihydroneopterin cyclic phosphate, guanosine and guanine were observed. However, the aerobically purified enzyme devoid of any iron-sulfur cluster showed only a little phosphatase activity and all other two activities were absent. The data suggests that

the phosphatase activity is not dependent on the presence of the bound Fe-S clusters in the enzyme, however, the clusters are essential for the nucleoside hydrolase activity.

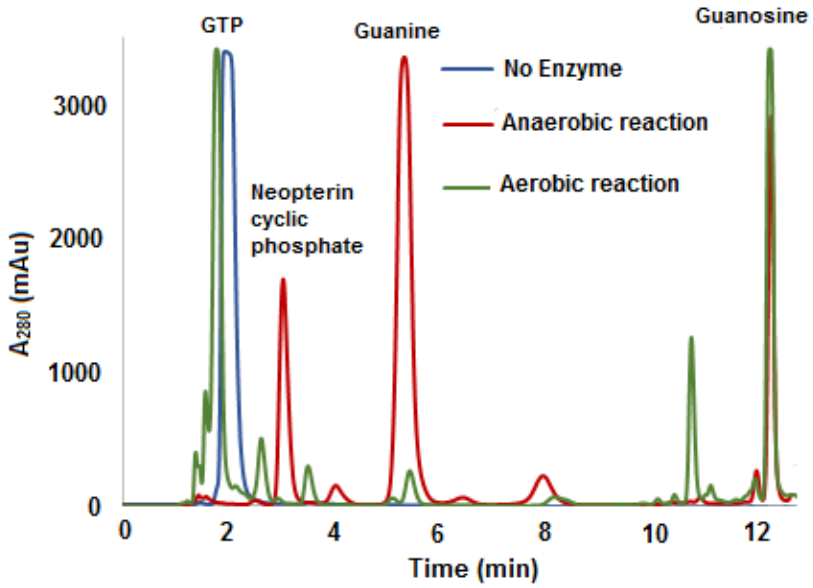

Figure 7.18: Comparison of GTP cyclohydrolase, phosphatase and nucleoside hydrolase activity of MJ0619. In absence of the 4Fe-4S cluster, the enzyme retains its phosphatase activity, however, the nucleosidase activity was lost**.**

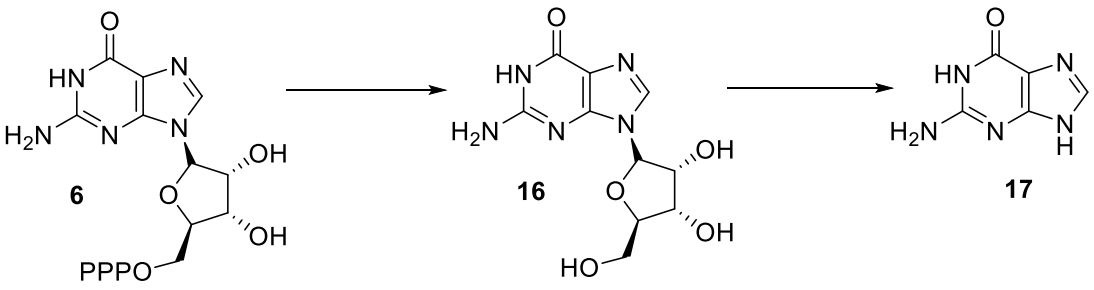

Scheme 7.7: Dephosphorylation and N-glycosidic bond cleavage of GTP by MJ0619.

7.2.15 MJ0619 shows nucleosidase activity on variety of nucleosides

The mesophilic ortholog of MJ0619 from *M. smithii* was tested for nucleosidase activity with a variety of nucleosides to look for whether it can cleave other nucleosides as well to generate the nuclear base and ribose sugar (Figure 7.19). The same experiment with the cluster free aerobic version of the protein was also performed to test the importance of 4Fe-4S clusters in this process. The active anaerobic enzyme was found to be active in cleaving the C-N bond between the nucleobase and the sugar, however, the aerobically purified protein was found to be inactive.

A very slow reaction rate was observed when 5'-deoxyadenosine was tested as a substrate for the nucleosidase activity. Only a little of the substrate was converted into product and most of the starting material remained unreacted in 24 hours. This information indicates that the 5'-hydroxyl group is probably necessary for the tight binding of the substrate in the active site.

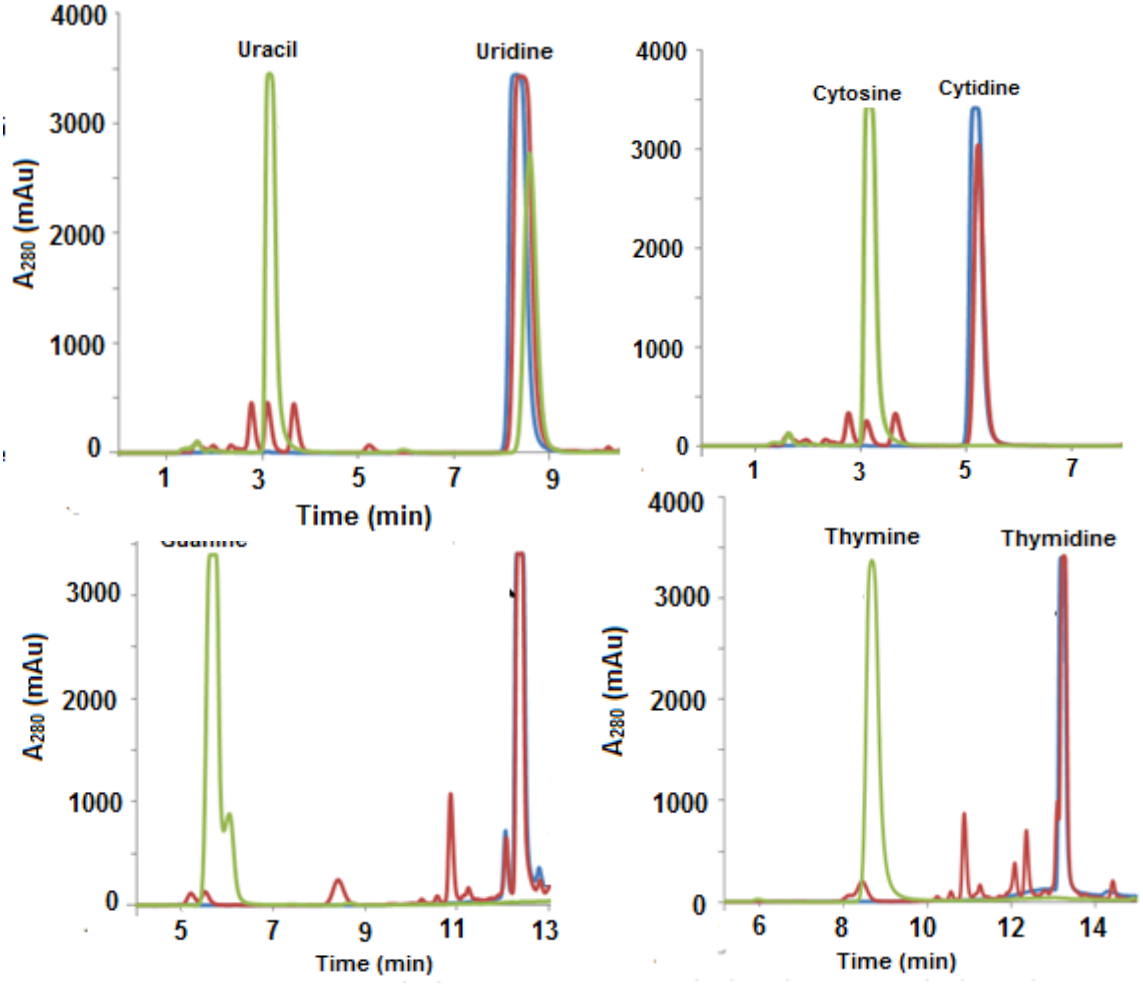

Figure 7.19: HPLC chromatogram of the assay of MJ0619 with a variety of purine and pyrimidine-based nucleosides. HPLC traces: No enzyme control (blue), Reaction with aerobic protein (maroon) and reaction with anaerobic protein (green). The nucleoside hydrolase activity was only observed with the anaerobically purified protein.

7.2.16 Assay with 7,8-dihydro-6-hydroxymethylpterin

Commercially available 7,8-dihydro-6-hydroxymethylpterin was incubated with MJ0619, SAM and dithionite at 37°C for 24 hours. The enzyme was heat denatured, filtered and the filtrate was analyzed by LCMS. In two preps of enzyme, formation of a

peak in the mass-spec was observed that has the same mass and retention time as the 7,8-dihydro-7,9-dimethyl-6-hydroxymethylpterin (Figure 7.20).

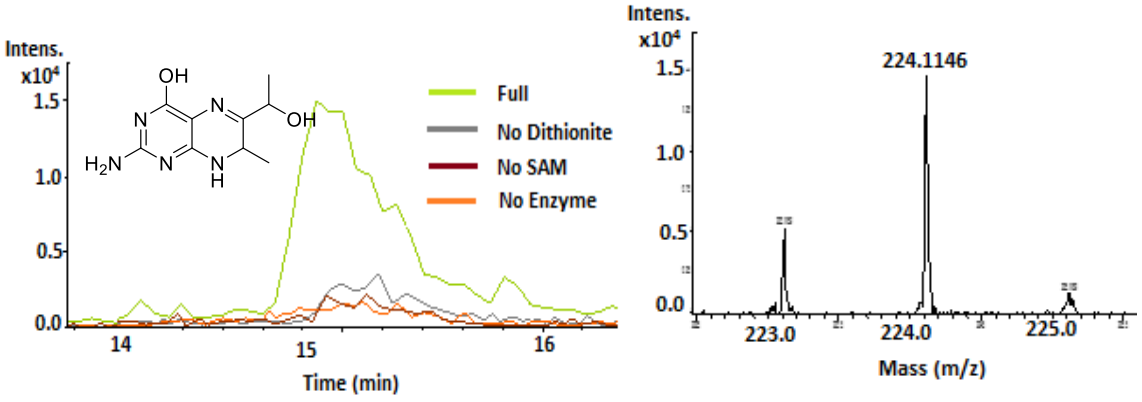

Figure 7.20: LCMS analysis of the reaction of MJ0619 with 7,8-dihydro-6-hydroxymethyl pterin as substrate. Formation of a peak at the same retention time and exact molecular weight of the dimethylated product molecule (**4**) was found. Little formation of the product in no dithionite control is probably due to the presence of pre-reduced clusters in the enzyme **.**

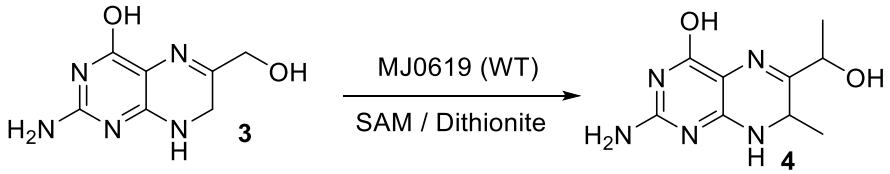

Scheme 7.8: Reaction catalyzed by MJ0619 in presence of SAM and dithionite

No incorporation of deuterium was observed when CD_3 SAM was used (Figure 7.21). All other preps only gave the negligible quantity of the product with very low counts. The addition of methylene tetrahydrofolate, methyl tetrahydrofolate or methylcobalamin did not make any difference in any of the product formation, suggesting that they are not involved in the reaction.

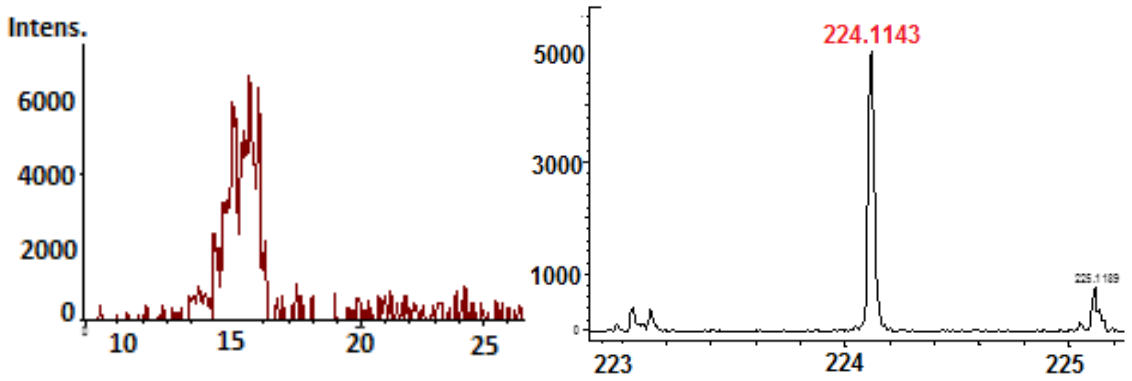

Figure 7.21: Product formation is observed in the reaction conducted with CD_3 – SAM. No deuterium incorporation was observed.

These observations clearly suggest that none of those compounds mentioned above are methyl donors. Thus, it is proposed that the enzyme comes with a very loosely bound methyl donor which can be lost during the purification process. Not all the enzyme preps have an equal amount of the methyl donor bound and hence all of them are not active for methylation.

7.3 Discussion

MJ0619 has been predicted as a radical SAM enzyme, and it has four putative cysteine containing motifs that are conserved in many orthologs. These cysteine containing motifs are used to harbor at least three 4Fe-4S clusters. Among these four motifs two are canonical CX_3CX_2C motifs, characteristics of radical SAM family of proteins. To understand the protein's activity, the protein was overexpressed and anaerobically purified and analyzed by SDS-Page gel and UV-Vis spectroscopy. The data confirmed overexpression of pure protein and the presence of 4Fe-4S clusters in it.

Estimation of iron and sulfur content of the protein suggested the presence of more than two clusters which was confirmed by the presence of the UV band at 418 nm, in M_3 mutant where both the canonical motifs were mutated. Two different signals were observed in the EPR spectra with g values 2.01 and 2.06, of the wild-type enzyme indicating the presence of two different types of clusters. In the presence of either of the canonical motifs, both the signals are present. However, when both are mutated (M_3) the signal at g = 2.01 was absent. This observation indicates that the type of the iron-sulfur clusters bound by the canonical and non-canonical motifs are different and can be differentiated by EPR spectroscopy.

Another characteristic of radical SAM enzymes is the formation of 5'-deoxyadenosine (**13**) when incubated with SAM (**11**) and sodium dithionite even in the absence of the substrate. Wild-type MJ0619 was also incubated under the same condition and formation of **13** was observed. The reaction was slow at 37 ^{o}C, but quite fast at 70 ^{o}C. This observation clearly confirms that MJ0619 is a radical SAM enzyme, can cleave SAM reductively to generate 5'-deoxyadenosyl radical.

Allen *et al.* proposed that both of the two 4Fe-4S clusters are responsible for the generation of one 5'-deoxyadenosyl radical each and thus catalyze two consecutive methylations of the pterin moiety. There was no report in the literature where two 4Fe-4S clusters located so close to each other in one enzyme and can have radical SAM activity independently. To test this hypothesis these cluster binding motifs were mutated and it was found that only M_1 mutant is active but M_2 or M_3 mutants are not. This observation

clearly indicates that only the cluster harbored by the second canonical motif (CL-2) is responsible for SAM cleavage.

As the *in vivo* analysis was performed in *E. coli*, the efficiency of flavodoxin/flavodoxin reductase reducing system was also tested on MJ0619. Formation of 5'-deoxyadenosine indicates that the enzyme would show its native activity inside the cell.

In SEED database, MJ0619 was annotated as a distant ortholog of MoaA, a molybdenum cofactor biosynthetic enzyme, that uses GTP (**6**) as a substrate.[141] This information led us to the testing of GTP as a substrate for MJ0619. Two new peaks were found that has the UV-spectrum similar to 7,8-dhydropterin moiety. Upon treatment with calf intestinal phosphatase (CIP), one of them changed position and the other remained the same. These peaks were later identified as 7,8-dihydroneopterin-3-triphosphate (**15)** and 7,8-dihydroneopterin-2,3-cyclic phosphodiester (**7**). A time course experiment with a mesophilic ortholog of MJ0619 shown that the linear triphosphate is the first intermediate to be formed which was later converted to the final product **7**. The aerobically purified enzyme that was expressed without added iron and sulfur does not show the cyclohydrolase activity which indicates that the presence of the cluster is essential.

Apart from the pterin products two other major peaks were found in the chromatogram which was later identified as guanosine and guanine. The presence of these two peaks indicates the phosphatase and nucleoside hydrolase activity of the MJ0619 enzyme. It was also observed that MJ0619 can accept awide range of nucleosides as substrates for the N-glycosidic bond cleavage. Neither SAM nor dithionite was found

essential for any of these activities. However, the presence of Mg^{2+} ions facilitates the dephosphorylation of GTP.

The proposed substrate (**3**) was reacted with MJ0619. In some of the preps formation of the desired dimethyl product (**4**) was detected by LC-MS. It has the same exact mass with the product standard and comes at the same retention time in the chromatogram (Figure 17). No incorporation of deuterium from CD_3 labeled SAM negates the possibility of SAM or methionine to be the source of the methyl group. No product formation was detected with any mutant enzyme. As the product formation was observed only with few preps we hypothesize that some of the preps co-purify with some unknown methylating agent that is not derived from methionine or serine, however, can be biosynthesized from acetate.

In conclusion, MJ0619 is a radical SAM enzyme that has at least three 4Fe-4S clusters bound in it and can catalyze the reductive cleavage of SAM to generate 5'-deoxyadenosine radical. It also has GTP cyclohydrolase and nucleoside hydrolase type activity in addition to it. It gives dimethyl pterin product **4** formations when 7,8-dihydro-6-hydroxymethyl pterin (3) was used as the substrate. Further investigation is required for a better understanding of the mechanism of this enzyme.

7.4 Experimental

7.4.1 Overexpression and purification of MJ0619

The pTHT vector containing the MJ0619 encoding gene was transformed into *Escherichia coli* Bl-21(DE3) harboring the SUF operon containing plasmid. The starter

culture was prepared by growing the cells aerobically for 12-15 h at 37 °C in 15 mL of LB medium supplemented with 40 μg/mL kanamycin and 25 μg/mL chloramphenicol. A larger culture of 1.5 L of LB medium, supplemented with 40 μg/mL of kanamycin and 100 μg/mL of chloramphenicol was then inoculated with the starter culture. After growing aerobically (180 rpm) at 37 °C for 3-4 hours until the A600 was 0.5-0.6. The cultures were then cooled to 4 °C and ferrous ammonium sulfate (140 mg/L) and L-cysteine (140 mg/L) were added. The protein expression was induced by the addition of 200 μM of isopropyl-1-thio-β-D-galactopyranoside (IPTG, LabScientific). The cultures were grown with slow shaking (110 rpm) at 15 °C for an additional ~ 18 h. and the cells were harvested by centrifugation at 5000 rpm in a Beckman Coulter Avanti J-26 XPI with a JLA-8.1000 rotor (15 min at 4 °C). The cell pellet (~ 3.0 g per liter of larger culture) was stored in liquid nitrogen until use. Cell lysis and protein purification were carried out in a glove bag (CoyLaboratories) under the anaerobic atmosphere of 5% hydrogen and 95% nitrogen. Stored cells were thawed at room temperature and resuspended in 30 mL of Lysis Buffer (100 mM Tris-HCl, pH 7.5 at 25 °C) 20 mg of lysozyme and 5uL of benzonase nuclease (Sigma) was added to it. The entire mixture was incubated on ice for 1.5 hours with continuous stirring and then the cells were lysed by sonication, for 5 × 120 s using a Misonix Sonicator XL-2000 (setting = 9) with 10 minutes interval with stirring. After centrifugation at 15,000 rpm in a Beckman Coulter Avanti J-E with a JA-17 rotor for 30 min at 4 °C, the cell debris was discarded and the cell lysate was passed through a 0.45 μm syringe filter. To purify MJ0619 protein by nickel-NTA affinity chromatography 5 mL HiTrap chelating HP column (GE Healthcare Life Sciences) was charged with 2

column volumes (CV) of 0.1 M NiSO4, washed with 5 CV of filtered water to remove excess nickel, and equilibrated with 3 CV of Lysis buffer. The filtered cell lysate was loaded onto the column at 1 mL / min flow rate and the resin was washed with 10 CV of Wash Buffer (100 mM Tris-HCl, 300 mM NaCl, 30 mM imidazole, pH 7.5 at 25 °C) Finally the protein was eluted with an elution buffer (100 mM Tris-HCl, 300 mM NaCl, 250 mM imidazole, pH 7.5 at 25 °C). The fractions with dark greenish black color contain the desired protein which is pooled and the buffer was exchanged to the storage buffer(100 mM potassium phosphate, pH 7.5 at 25 °C, 2 mM DTT, 30% glycerol) via Econo-Pac 10DG size exclusion chromatography (Bio-Rad) and stored in liquid nitrogen. The protein concentrations were measured by Bradford assay and the SDS page gel analysis showed the His-tagged protein molecular weight ~ 60 kDa.

7.4.2 Estimation of the iron content

Iron content was analyzed via a protocol described in the literature.[142] Following reagent solutions were prepared for this purpose:

Solution A: 8 M guanidine hydrochloride, Solution B: 10 mM aqueous ferrozine (3-(2-Pyridyl)-5,6-diphenyl-1,2,4-triazine-*p,p'*-disulfonic acid monosodium salt hydrate), Solution C: 100 mM L-ascorbic acid in water, Solution D: saturated ammonium acetate solution, Solution E: 2M HCl. To 100 µL of enzyme solution containing 0 to 50 µM MJ0619, 100 µL of solution A and Solution E were added and the solution was diluted to 550 µL. The resulting solution was centrifuged to remove any denatured protein. To 500 µL of the supernatant, 30 µL of the solution C and 30 µL of solution D were added, mixed

thoroughly and incubated at RT for 30 min. The absorbance of the iron ferrozine complex was recorded at 562 nm using a Varian Cary Bio 300 UV-Visible Spectrophotometer (extinction coefficient for iron ferrozine complex is 27.9 mM-1cm-1). A standard curve was also prepared with known iron concentration under identical conditions using Fe(NH4)2(SO4)2 with a concentration range from 0 to 100 μM. The iron content of the protein sample was measured using this standard calibration curve.

7.4.3 Estimation of the sulfur content

Sulfide content was analyzed using the methylene blue assay.[142] Following reagent solutions were prepared for this assay:

Solution A: 1% (w/v) zinc acetate, Solution B: 3 M NaOH, d Solution C: 0.1 % N,N-dimethyl-*p*-phenylenediamine (DMPD) monohydrochloride in 5 M HCl and Solution D: 23 mM $FeCl_3$ in 1.2 M HCl. To a 300 μL solution of the protein (0 – 10 uL) 1 ml of solution A was added followed by 50 μL of solution B: 50 μL of. This mixture was gently vortexed and 250 μL of solution C and 50 μL of Solution D were added. The resulting solution was vortexed in an interval 5 min over a 30 min. After centrifugation of the sample solutions at 15,000 rpm in an Eppendorf 5424 R with an F45-24-11 rotor for 5 min at 25 °C the supernatant was collected and the absorbance at 670 nm was recorded using a Varian Cary Bio 300 UV-Visible Spectrophotometer. A standard curve that was also generated under identical conditions using a fresh solution of sodium sulfide (Na_2S; Sigma-Aldrich) in 0.1 M NaOH with a concentration range from 0 to 150 μM. The sulfide

content of the protein was determined by comparing the unknown readings with the standard curve.

7.4.4 Assay for radical SAM activity

Following are the concentration of different components used to determine the radical SAM activity of the MJ0619 protein. Buffer – 100 mM tris, pH-7.5, SAM – 1.3 mM, Dithionite – 3 mM Enzyme ~ 60 μM. For the high-temperature reaction, the components were mixed together and the mixture was heated at 70 ^{o}C for 20 minutes. For the low temperature, the same reaction mixture was incubated at 37 ^{o}C for 24 hours. After the incubation, the reaction mixture was cooled on ice, centrifuged and the supernatant was passed through a 10 kDa cutoff filter and the filtrate was analyzed by HPLC or LCMS.

7.4.5 Radical SAM activity with FldA / FldR system

Assay was carried out by mixing the following components: Buffer – 100 mM tris, pH-7.5, SAM – 1.3 mM, Dithionite – 3 mM Enzyme ~ 60 μM, FldA – 30 μM, FldR – 30 μM NADPH – 1.5 mM were mixed together by pipetting. The mixture was incubated at 37 ^{o}C for 24 hours. After heat denaturation and filtration the reaction mixtures were analyzed by LCMS.

7.4.6 Assay for GTP cyclohydrolase activity

Following components were mixed to the designated final concentration: Buffer – 50 mM tris, pH-7.5, GTP – 2 mM, $MnCl_2$ 2mM, Enzyme (MJ0619) ~ 90 μM. After mixing

all these components together the reaction mixture was heated at 70 ^{o}C for 20 minutes. After incubation, the reaction mixture was cooled on ice, centrifuged and the supernatant was passed through a 10 kDa cutoff filter and the filtrate was analyzed by HPLC and LCMS.

7.4.7 Assay with 7,8-dihydro-6-hydroxymethyl pterin

Following are the concentration of different components used to for the reaction of MJ0619 protein with 7,8-dihydro-6-hydroxymethyl pterin. Buffer – 100 mM tris, pH-7.5, SAM – 1.3 mM, Dithionite – 3 mM, Substrate – 1 mM and Enzyme ~ 60 μM. The reaction mixture was incubated at 37 ^{o}C for 24 hours. After the incubation, the enzyme was heat denatured at 70 ^{o}C for 20 min, cooled on ice, centrifuged and the supernatant was passed through a 10 kDa cutoff filter and the filtrate was analyzed by HPLC or LCMS.

7.4.8 HPLC method

HPLC analysis using a linear gradient, at a flow rate of 1 mL/min was used with absorbance detection at 254 nm. Solvent A is water, solvent B is 100 mM K2HPO4, pH 6.6 and solvent C is methanol: 0 min, 100% B; 7 min, 10% A, 90 % B; 12 min, 20 % A, 65 % B, 15 % C; 22 min, 25 % A, 10 % B, 65 % C; 25 min, 25 % A, 75% B; 32 min, 100 % B; The analysis was done in an Agilent 1260 series instrument using a Agilent Eclipse XDB HPLC column (15 cm x 4.6 mm, 5 μM particle size).

7.4.9 LCMS method

Samples were analyzed by reverse-phase HPLC on an Agilent 1200 HPLC system equipped with a thermostatted autosampler (10 °C). The stationary phase was Supelcosil LC-18-T (15 cm × 3 mm, 3 μm particles), maintained at 22 °C. The LC eluent consisted of a gradient of 75% methanol in 25% water with 5 mM ammonium acetate buffer, pH 6.6 (0.4 mL/min flow rate). The percentages of ammonium acetate buffer (*B*) and methanol (*M*) at time *t* varied according to the following scheme: (*time Methanol, Buffer)*: (0,0,100), (7,0,100), (10,20,80), (27,100,0), (18,100,0), (29,100,0); (30,0,100); (40,0,100). Compounds were detected using absorbance at 254 nm and also by extracted mass chromatogram. Mass data were collected using an in-line Bruker Daltonics micrOTOF-Q II ESI-Qq-TOF mass spectrometer (HyStar) in positive ion mode as indicated.

REFERENCES

1. Mkrtchyan, G.; Aleshin, V.; Parkhomenko, Y.; Kaehne, T.; Luigi Di Salvo, M.; Parroni, A.; Contestabile, R.; Vovk, A.; Bettendorff, L.; Bunik, V., Molecular mechanisms of the non-coenzyme action of thiamin in brain: biochemical, structural and pathway analysis. *Scientific Reports* **2015,** *5*, 12583.
2. Dwivedi, B. K.; Arnold, R. G., Chemistry of thiamine degradation on food products and model systems. Review. *Journal of Agricultural and Food Chemistry* **1973,** *21* (1), 54-60.
3. Costello, C. A.; Kelleher, N. L.; Abe, M.; McLafferty, F. W.; Begley, T. P., Mechanistic Studies on Thiaminase I: Overexpression and Identification of the Active Site Nucleophile. *Journal of Biological Chemistry* **1996,** *271* (7), 3445-3452.
4. Lienhard, G. E., Kinetic evidence for a (4-amino-2-methyl-5-pyrimidinyl)methyl-enzyme intermediate in the thiaminase I reaction. *Biochemistry* **1970,** *9* (15), 3011-3020.
5. Toms, A. V.; Haas, A. L.; Park, J.-H.; Begley, T. P.; Ealick, S. E., Structural Characterization of the Regulatory Proteins TenA and TenI from Bacillus subtilis and Identification of TenA as a Thiaminase II. *Biochemistry* **2005,** *44* (7), 2319-2329.
6. Campobasso, N.; Costello, C. A.; Kinsland, C.; Begley, T. P.; Ealick, S. E., Crystal Structure of Thiaminase-I from Bacillus thiaminolyticus at 2.0 Å Resolution. *Biochemistry* **1998,** *37* (45), 15981-15989.

7. Blakeslee, C. J.; Sweet, S. A.; Galbraith, H. S.; Honeyfield, D. C., Thiaminase activity in native freshwater mussels. *Journal of Great Lakes Research* **2015,** *41* (2), 516-519.
8. Earl, J. W.; McCleary, B. V., Mystery of the poisoned expedition. *Nature* **1994,** *368* (6473), 683-684.
9. Ringe, H.; Schuelke, M.; Weber, S.; Dorner, B. G.; Kirchner, S.; Dorner, M. B., Infant Botulism: Is There an Association With Thiamine Deficiency? *Pediatrics* **2014**.
10. Honeyfield, D. C.; Brown, S. B.; Fitzsimons, J. D.; Tillitt, D. E., Early Mortality Syndrome in Great Lakes Salmonines. *Journal of Aquatic Animal Health* **2005,** *17* (1), 1-3.
11. Hazell, A. S.; Todd, K. G.; Butterworth, R. F., Mechanisms of Neuronal Cell Death in Wernicke's Encephalopathy. *Metabolic Brain Disease* **1998,** *13* (2), 97-122.
12. Singleton, C.; Martin, P., Molecular Mechanisms of Thiamine Utilization. *Current molecular medicine* **2001,** *1* (2), 197-207.
13. Fujita, A., Thiaminase. *Advances in Enzymology* **1954,** *15*, 389.
14. Ramakrishnan, C.; Ramachandran, G. N., Stereochemical Criteria for Polypeptide and Protein Chain Conformations. *Biophysical Journal* **1965,** *5* (6), 909-933.
15. Douthit, H. A.; Airth, R. L., Thiaminase I of Bacillus thiaminolyticus. *Archives of Biochemistry and Biophysics* **1966,** *113* (2), 331-337.
16. Abe, M.; Ito, S.-i.; Kimoto, M.; Hayashi, R.; Nishimune, T., Molecular studies on thiaminase I. *Biochimica et Biophysica Acta (BBA) - Gene Structure and Expression* **1987,** *909* (3), 213-221.

17. Hutter, J. A.; Slama, J. T., Inhibition of thiaminase I from Bacillus thiaminolyticus. Evidence supporting a covalent 1,6-dihydropyrimidinyl-enzyme intermediate. *Biochemistry* **1987,** *26* (7), 1969-1973.

18. Campobasso, N.; Costello, C. A.; Kinsland, C.; Begley, T. P.; Ealick, S. E., *Biochemistry* **1998,** *37*, 15981-15989.

19. Nicewonger, R.; Costello, C. A.; Begley, T. P., Mechanistic Studies on Thiaminase I. 3. Stereochemistry of the Thiaminase I and the Bisulfite-Catalyzed Degradation of Chiral Monodeuteriothiamin. *The Journal of Organic Chemistry* **1996,** *61* (12), 4172-4174.

20. Wu, M.; Papish, E. T.; Begley, T. P., Mechanistic Studies on Thiaminase I: Identification of the Product of Thiamin Degradation in the Absence of the Nucleophilic Cosubstrate. *Bioorganic Chemistry* **2000,** *28* (1), 45-48.

21. Spurlino, J. C.; Lu, G. Y.; Quiocho, F. A., The 2.3-A resolution structure of the maltose- or maltodextrin-binding protein, a primary receptor of bacterial active transport and chemotaxis. *Journal of Biological Chemistry* **1991,** *266* (8), 5202-5219.

22. Soriano, E. V.; Rajashankar, K. R.; Hanes, J. W.; Bale, S.; Begley, T. P.; Ealick, S. E., Structural Similarities between Thiamin-Binding Protein and Thiaminase-I Suggest a Common Ancestor. *Biochemistry* **2008,** *47* (5), 1346-1357.

23. Bale, S.; Rajashankar, K. R.; Perry, K.; Begley, T. P.; Ealick, S. E., HMP Binding Protein ThiY and HMP-P Synthase THI5 Are Structural Homologues. *Biochemistry* **2010,** *49* (41), 8929-8936.

24. Lai, R.-Y.; Huang, S.; Fenwick, M. K.; Hazra, A.; Zhang, Y.; Rajashankar, K.; Philmus, B.; Kinsland, C.; Sanders, J. M.; Ealick, S. E.; Begley, T. P., Thiamin Pyrimidine Biosynthesis in Candida albicans: A Remarkable Reaction between Histidine and Pyridoxal Phosphate. *Journal of the American Chemical Society* **2012,** *134* (22), 9157-9159.

25. Jenkins, A. H.; Schyns, G.; Potot, S.; Sun, G.; Begley, T. P., A new thiamin salvage pathway. *Nat Chem Biol* **2007,** *3* (8), 492-497.

26. Cooper, L. E.; O'Leary, S. E.; Begley, T. P., Biosynthesis of a Thiamin Antivitamin in Clostridium botulinum. *Biochemistry* **2014,** *53* (14), 2215-2217.

27. Sikowitz, M. D.; Shome, B.; Zhang, Y.; Begley, T. P.; Ealick, S. E., Structure of a Clostridium botulinum C143S Thiaminase I/Thiamin Complex Reveals Active Site Architecture. *Biochemistry* **2013,** *52* (44), 7830-7839.

28. Shin, W.; Oh, D. G.; Chae, C. H.; Yoon, T. S., Conformational analyses of thiamin-related compounds. A stereochemical model for thiamin catalysis. *Journal of the American Chemical Society* **1993,** *115* (26), 12238-12250.

29. Abe, M.; Nishimune, T.; Ito, S.; Kimoto, M.; Hayashi, R., A simple method for the detection of two types of thiaminase-producing colonies. *FEMS Microbiology Letters* **1986,** *34* (2), 129-133.

30. Sambrook, J.; Fritsch, E. F.; Maniatis, T., *Molecular Cloning: A Laboratory Manual*. 1989; Vol. 3.

31. Tanaka, F.; Takeuchi, S.; Tanaka, N.; Yonehara, H.; Umezawa, H.; Sumiki, Y., *Journal of Antibiotics, Series A* **1961,** *14*, 161.

32. Nishimura, T.; Tanaka, N., *Journal of Antibiotics* **1963,** *16*, 179.

33. Drautz, H.; Messerer, W.; ZÄHner, H.; Breiding Mack, S.; Zeeck, A., Metabolic products of microorganisms. 239. Bacimethrin isolated from Streptomyces albus. Identification, derivatives, synthesis and biological properties. *The Journal of Antibiotics* **1987,** *40* (10), 1431-1439.

34. Reddick, J. J.; Saha, S.; Lee, J.-m.; Melnick, J. S.; Perkins, J.; Begley, T. P., The mechanism of action of bacimethrin, a naturally occurring thiamin antimetabolite. *Bioorganic & Medicinal Chemistry Letters* **2001,** *11* (17), 2245-2248.

35. Taylor, E. C.; Knopf, R. J.; Meyer, R. F.; Holmes, A.; Hoefle, M. L., Pyrimido [4,5-d]pyrimidines. Part I. *Journal of the American Chemical Society* **1960,** *82* (21), 5711-5718.

36. Baxter, R. L.; Hartley, A. B.; Chan, H. W. S., Thiamine biosynthesis in yeast-evaluation of 4-hydroxy-5-hydroxymethyl-2-methylpyrimidine as a precursor. *Journal of the Chemical Society, Perkin Transactions 1* **1990,** (11), 2963-2966.

37. Perandones, F.; Soto, J. L., Synthesis of pyrido[2,3-d]pyrimidines from aminopyrimidinecarbaldehydes. *Journal of Heterocyclic Chemistry* **1998,** *35* (2), 413-419.

38. Reddick, J. J.; Nicewonger, R.; Begley, T. P., Mechanistic Studies on Thiamin Phosphate Synthase: Evidence for a Dissociative Mechanism. *Biochemistry* **2001,** *40* (34), 10095-10102.

39. Matsukawa, T.; Hirano, H.; Yurugi, S., [25] Preparation of thiamine derivatives and analogs. In *Methods in Enzymology*, Academic Press: 1970; Vol. Volume 18, Part A, pp 141-162.

40. Huber, W., Hydrogenation of Basic Nitriles with Raney Nickel. *Journal of the American Chemical Society* **1944,** *66* (6), 876-879.

41. Melnick, J. S.; Sprinz, K. I.; Reddick, J. J.; Kinsland, C.; Begley, T. P., *Bioorg. Med. Chem. Lett.* **2003,** *13*, 4139.

42. Milne, J. L. S.; Shi, D.; Rosenthal, P. B.; Sunshine, J. S.; Domingo, G. J.; Wu, X.; Brooks, B. R.; Perham, R. N.; Henderson, R.; Subramaniam, S., Molecular architecture and mechanism of an icosahedral pyruvate dehydrogenase complex: a multifunctional catalytic machine. *The EMBO Journal* **2002,** *21* (21), 5587-5598.

43. Loquet, A.; Habenstein, B.; Lange, A., Structural Investigations of Molecular Machines by Solid-State NMR. *Accounts of Chemical Research* **2013,** *46* (9), 2070-2079.

44. Balakrishnan, A.; Paramasivam, S.; Chakraborty, S.; Polenova, T.; Jordan, F., Solid-State Nuclear Magnetic Resonance Studies Delineate the Role of the Protein in Activation of Both Aromatic Rings of Thiamin. *Journal of the American Chemical Society* **2011,** *134* (1), 665-672.

45. Paramasivam, S.; Balakrishnan, A.; Dmitrenko, O.; Godert, A.; Begley, T. P.; Jordan, F.; Polenova, T., Solid-State NMR and Density Functional Theory Studies of Ionization States of Thiamin. *The Journal of Physical Chemistry B* **2010,** *115* (4), 730-736.

46. Williams, D. L.; Ronzio, A. R., Micro Syntheses with Tracer Elements. VIII. The Synthesis of Thiamin Labeled with C14. *Journal of the American Chemical Society* **1952,** *74* (9), 2409-2410.

47. Dornow, A.; Petsch, G., Über Reduktionen mit Lithiumaluminiumhydrid, V. Mitteil.: Zur Darstellung des Vitamins B1. *Chemische Berichte* **1953,** *86* (11), 1404-1407.

48. Barone, J. A.; Tieckelmann, H.; Guthrie, R.; Holland, J. F., A 2-Trifluoromethyl Analog of Thiamin1. *The Journal of Organic Chemistry* **1960,** *25* (2), 211-213.

49. Gerd, M.; Joel, S. K., Positron emission tomography. *Physics in Medicine and Biology* **2006,** *51* (13), R117.

50. Alauddin, M. M., Positron emission tomography (PET) imaging with (18)F-based radiotracers. *American Journal of Nuclear Medicine and Molecular Imaging* **2012,** *2* (1), 55-76.

51. Verel, I.; Visser, G. W. M.; van Dongen, G. A., The Promise of Immuno-PET in Radioimmunotherapy. *Journal of Nuclear Medicine* **2005,** *46* (1 suppl), 164S-171S.

52. Zhu, A.; Lee, D.; Shim, H., Metabolic PET Imaging in Cancer Detection and Therapy Response. *Seminars in oncology* **2011,** *38* (1), 55-69.

53. Almuhaideb, A.; Papathanasiou, N.; Bomanji, J., (18)F-FDG PET/CT Imaging In Oncology. *Annals of Saudi Medicine* **2011,** *31* (1), 3-13.

54. Cascante, M.; Centelles, J. J.; Veech, R. L.; Lee, W.-N. P.; Boros, L. G., Role of Thiamin (Vitamin B-1) and Transketolase in Tumor Cell Proliferation. *Nutrition and Cancer* **2000,** *36* (2), 150-154.

55. Zastre, J. A.; Sweet, R. L.; Hanberry, B. S.; Ye, S., Linking vitamin B1 with cancer cell metabolism. *Cancer & Metabolism* **2013,** *1* (1), 1-14.

56. Evdokimov, N.; Flores, G.; Clark, P.; Phelps, M.; Witte, O.; Jung, M., 5-(2-[F]Fluoroethyl)-4-Methylthiazole Probe For Positron Emission Tomography Of The Central Nervous System. *Chemistry of Heterocyclic Compounds* **2014,** *50* (2), 303-307.

57. Nielsen, M. K.; Ugaz, C. R.; Li, W.; Doyle, A. G., PyFluor: A Low-Cost, Stable, and Selective Deoxyfluorination Reagent. *Journal of the American Chemical Society* **2015,** *137* (30), 9571-9574.

58. Ames, G. F.-L.; Mimura, C. S.; Holbrook, S. R.; Shyamala, V., Traffic ATPases: A Superfamily of Transport Proteins Operating from Escherichia coli to Humans. In *Advances in Enzymology and Related Areas of Molecular Biology*, John Wiley & Sons, Inc.: 2006; pp 1-47.

59. Linton, K. J.; Higgins, C. F., The Escherichia coli ATP-binding cassette (ABC) proteins. *Molecular Microbiology* **1998,** *28* (1), 5-13.

60. Higgins, C. F., ABC Transporters: From Microorganisms to Man. *Annual Review of Cell Biology* **1992,** *8* (1), 67-113.

61. Liu, C. E.; Liu, P.-Q.; Wolf, A.; Lin, E.; Ames, G. F.-L., Both Lobes of the Soluble Receptor of the Periplasmic Histidine Permease, an ABC Transporter (Traffic ATPase), Interact with the Membrane-bound Complex: Effect of Different Ligand and Consequences for the Mechanism of Action. *Journal of Biological Chemistry* **1999,** *274* (2), 739-747.

62. Liu, C. E.; Liu, P.-Q.; Ames, G. F.-L., Characterization of the Adenosine Triphosphatase Activity of the Periplasmic Histidine Permease, a Traffic ATPase (ABC Transporter). *Journal of Biological Chemistry* **1997,** *272* (35), 21883-21891.

63. Miranda-Ríos, J.; Navarro, M.; Soberón, M., A conserved RNA structure (thi box) is involved in regulation of thiamin biosynthetic gene expression in bacteria. *Proceedings of the National Academy of Sciences* **2001,** *98* (17), 9736-9741.

64. Kawasaki, T.; Esaki, K., Thiamine uptake in Escherichia coli. *Archives of Biochemistry and Biophysics* **1971,** *142* (1), 163-169.

65. Leach, F. R.; Carraway, C. A. C., [16] Thiamine transport in Escherichia coli crookes. In *Methods in Enzymology*, Academic Press: 1979; Vol. Volume 62, pp 76-91.

66. Nishume, T.; Hayashi, R., Thiamine-binding protein and thiamine uptake by Escherichia coli. *Biochimica et Biophysica Acta (BBA) - General Subjects* **1971,** *244* (3), 573-583.

67. Nakayama, H.; Hayashi, R., Biosynthetic pathway of thiamine pyrophosphate: a special reference to the thiamine monophosphate-requiring mutant and the thiamine pyrophosphate-requiring mutant of Escherichia coli. *Journal of Bacteriology* **1972,** *112* (3), 1118-1126.

68. Rodionov, D. A.; Vitreschak, A. G.; Mironov, A. A.; Gelfand, M. S., Comparative Genomics of Thiamin Biosynthesis in Procaryotes: New Genes and Regulatory Mechanism. *Journal of Biological Chemistry* **2002,** *277* (50), 48949-48959.

69. Jeanguenin, L.; Lara-Núñez, A.; Rodionov, D. A.; Osterman, A. L.; Komarova, N. Y.; Rentsch, D.; Gregory, J. F.; Hanson, A. D., Comparative genomics and functional

analysis of the NiaP family uncover nicotinate transporters from bacteria, plants, and mammals. *Functional & Integrative Genomics* **2012,** *12* (1), 25-34.

70. Erkens, G. B.; Berntsson, R. P. A.; Fulyani, F.; Majsnerowska, M.; Vujičić-Žagar, A.; ter Beek, J.; Poolman, B.; Slotboom, D. J., The structural basis of modularity in ECF-type ABC transporters. *Nature Structural and Molecular Biology* **2011,** *18* (7), 755-760.
71. Erkens, G. B.; Slotboom, D. J., Biochemical Characterization of ThiT from Lactococcus lactis: A Thiamin Transporter with Picomolar Substrate Binding Affinity. *Biochemistry* **2010,** *49* (14), 3203-3212.
72. Trabulo, S.; Cardoso, A. L.; Mano, M.; de Lima, M. C. P., Cell-Penetrating Peptides—Mechanisms of Cellular Uptake and Generation of Delivery Systems. *Pharmaceuticals* **2010,** *3* (4), 961-993.
73. Munyendo, W. L. L.; Lv, H.; Benza-Ingoula, H.; Baraza, L. D.; Zhou, J., Cell Penetrating Peptides in the Delivery of Biopharmaceuticals. *Biomolecules* **2012,** *2* (2), 187-202.
74. Fitremann, J.; Bouchu, A.; Queneau, Y., Synthesis and Gelling Properties of N-Palmitoyl-l-phenylalanine Sucrose Esters. *Langmuir* **2003,** *19* (23), 9981-9983.
75. Patel, S. K.; Gajbhiye, V.; Jain, N. K., Synthesis, characterization and brain targeting potential of paclitaxel loaded thiamine-PPI nanoconjugates. *Journal Of Drug Targeting* **2012,** *20* (10), 841-849.
76. Garofalo, A.; Goossens, L.; Lemoine, A.; Ravez, S.; Six, P.; Howsam, M.; Farce, A.; Depreux, P., [4-(6,7-Disubstituted quinazolin-4-ylamino)phenyl] carbamic acid

esters: a novel series of dual EGFR/VEGFR-2 tyrosine kinase inhibitors. *MedChemComm* **2011,** *2* (1), 65-72.

77. Kline, T., Design and Synthesis of bis-carbamate Analogs of Cyclic bis-(3'-5')-Diguanylic Acid (c-di-GMP) and the Acyclic Dimer PGPG. *Nucleosides, nucleotides & nucleic acids* **2008,** *27* (12), 1282.
78. Solyev, P. N.; Shipitsin, A. V.; Karpenko, I. L.; Nosik, D. N.; Kalnina, L. B.; Kochetkov, S. N.; Kukhanova, M. K.; Jasko, M. V., Synthesis and anti-HIV properties of new carbamate prodrugs of AZT. *Chemical Biology & Drug Design* **2012,** *80* (6), 947-952.
79. Drąg, M.; Grembecka, J.; Pawełczak, M.; Kafarski, P., α-Aminoalkylphosphonates as a tool in experimental optimisation of P1 side chain shape of potential inhibitors in S1 pocket of leucine- and neutral aminopeptidases. *European Journal of Medicinal Chemistry* **2005,** *40* (8), 764-771.
80. Soroka, M., The synthesis of 1-aminoalkylphosphonic acids. A revised mechanism of the reaction of phosphorus trichloride, amides and aldehydes or ketones in acetic acid (Oleksyszyn reaction). *Liebigs Annalen der Chemie* **1990,** *1990* (4), 331-334.
81. Salomon, C. J.; Breuer, E., Efficient and selective dealkylation of phosphonate dilsopropyl esters using Me3SiBr. *Tetrahedron Letters* **1995,** *36* (37), 6759-6760.
82. Kudzin, Z. H.; ywa, P.; uczak, J.; Andrijewski, G., 1-Aminoalkanephosphonates. Part II. A Facile Conversion of 1-Aminoalkanephosphonic Acids into 0,0-Diethyl 1-aminoalkanephosphonates. *Synthesis* **1997,** *1997* (01), 44-46.

83. Oleksyszyn, J.; Subotkowska, L.; Mastalerz, P., Diphenyl 1-Aminoalkanephosphonates. *Synthesis* **1979,** *1979* (12), 985-986.

84. Paerl, R. W.; Bertrand, E. M.; Allen, A. E.; Palenik, B.; Azam, F., Vitamin B1 ecophysiology of marine picoeukaryotic algae: Strain-specific differences and a new role for bacteria in vitamin cycling. *Limnology and Oceanography* **2015,** *60* (1), 215-228.

85. McRose, D.; Guo, J.; Monier, A.; Sudek, S.; Wilken, S.; Yan, S.; Mock, T.; Archibald, J. M.; Begley, T. P.; Reyes-Prieto, A.; Worden, A. Z., Alternatives to vitamin B1 uptake revealed with discovery of riboswitches in multiple marine eukaryotic lineages. *ISME J* **2014,** *8* (12), 2517-2529.

86. Bertrand, E.; Allen, A., Influence of vitamin B auxotrophy on nitrogen metabolism in eukaryotic phytoplankton. *Frontiers in Microbiology* **2012,** *3* (375).

87. Gobler, C. J.; Norman, C.; Panzeca, C.; Taylor, G. T.; SaÃƒÂ±udo-Wilhelmy, S. A., Effect of B-vitamins (B1, B12) and inorganic nutrients on algal bloom dynamics in a coastal ecosystem. *Aquatic Microbial Ecology* **2007,** *49* (2), 181-194.

88. Koch, F.; Hattenrath-Lehmann, T. K.; Goleski, J. A.; Sañudo-Wilhelmy, S.; Fisher, N. S.; Gobler, C. J., Vitamin B(1) and B(12) Uptake and Cycling by Plankton Communities in Coastal Ecosystems. *Frontiers in Microbiology* **2012,** *3*, 363.

89. Droop, M. R., Requirement for Thiamine Among Some Marine and Supra-Littoral Protista. *Journal of the Marine Biological Association of the United Kingdom* **2009,** *37* (2), 323-329.

90. Helliwell, Katherine E.; Lawrence, Andrew D.; Holzer, A.; Kudahl, Ulrich J.; Sasso, S.; Kräutler, B.; Scanlan, David J.; Warren, Martin J.; Smith, Alison G., Cyanobacteria and Eukaryotic Algae Use Different Chemical Variants of Vitamin B12. *Current Biology* **2016,** *26* (8), 999-1008.
91. Liu, H.; Probert, I.; Uitz, J.; Claustre, H.; Aris-Brosou, S.; Frada, M.; Not, F.; de Vargas, C., Extreme diversity in noncalcifying haptophytes explains a major pigment paradox in open oceans. *Proceedings of the National Academy of Sciences* **2009,** *106* (31), 12803-12808.
92. Egge, E. S.; Eikrem, W.; Edvardsen, B., Deep-branching Novel Lineages and High Diversity of Haptophytes in the Skagerrak (Norway) Uncovered by 454 Pyrosequencing. *Journal of Eukaryotic Microbiology* **2015,** *62* (1), 121-140.
93. Jardillier, L.; Zubkov, M. V.; Pearman, J.; Scanlan, D. J., Significant CO2 fixation by small prymnesiophytes in the subtropical and tropical northeast Atlantic Ocean. *The ISME Journal* **2010,** *4* (9), 1180-1192.
94. Tang, Y. Z.; Koch, F.; Gobler, C. J., Most harmful algal bloom species are vitamin B1 and B12 auxotrophs. *Proceedings of the National Academy of Sciences* **2010,** *107* (48), 20756-20761.
95. Read, B., Pan genome of the phytoplankton Emiliania underpins its global distribution. *Nature* **2013,** *499* (7457), 209.
96. Hovde, B. T.; Starkenburg, S. R.; Hunsperger, H. M.; Mercer, L. D.; Deodato, C. R.; Jha, R. K.; Chertkov, O.; Monnat Jr, R. J.; Cattolico, R. A., The mitochondrial and

chloroplast genomes of the haptophyte Chrysochromulina tobin contain unique repeat structures and gene profiles. *BMC Genomics* **2014,** *15* (1), 604-626.

97. Jurgenson, C. T.; Begley, T. P.; Ealick, S. E., The Structural and Biochemical Foundations of Thiamin Biosynthesis. *Annual Review of Biochemistry* **2009,** *78* (1), 569-603.
98. Haas Jenkins, A.; Schyns, G.; Potot, S.; Sun, G.; Begley, T. P., *Nat. Chem. Biol.* **2007,** *3*, 492-497.
99. Jenkins, A. L.; Zhang, Y.; Ealick, S. E.; Begley, T. P., Mutagenesis studies on TenA: a thiamin salvage enzyme from Bacillus subtilis. *Bioorganic chemistry* **2008,** *36* (1), 29-32.
100. Sylvander, P.; Häubner, N.; Snoeijs, P., The Thiamine Content of Phytoplankton Cells Is Affected by Abiotic Stress and Growth Rate. *Microbial Ecology* **2013,** *65* (3), 566-577.
101. Keeling, P. J.; Burki, F.; Wilcox, H. M.; Allam, B.; Allen, E. E.; *et al.*, The Marine Microbial Eukaryote Transcriptome Sequencing Project (MMETSP): Illuminating the Functional Diversity of Eukaryotic Life in the Oceans through Transcriptome Sequencing. *PLoS Biology* **2014,** *12* (6), e1001889.
102. Edvardsen, B.; Eikrem, W.; Green, J. C.; Andersen, R. A.; Staay, S. Y. M.-v. d.; Medlin, L. K., Phylogenetic reconstructions of the Haptophyta inferred from 18S ribosomal DNA sequences and available morphological data. *Phycologia* **2000,** *39* (1), 19-35.

103. Sañudo-Wilhelmy, S. A.; Cutter, L. S.; Durazo, R.; Smail, E. A.; Gómez-Consarnau, L.; Webb, E. A.; Prokopenko, M. G.; Berelson, W. M.; Karl, D. M., Multiple B-vitamin depletion in large areas of the coastal ocean. *Proceedings of the National Academy of Sciences* **2012,** *109* (35), 14041-14045.
104. Carini, P.; Campbell, E. O.; Morre, J.; Sanudo-Wilhelmy, S. A.; Cameron Thrash, J.; Bennett, S. E.; Temperton, B.; Begley, T.; Giovannoni, S. J., Discovery of a SAR11 growth requirement for thiamin/'s pyrimidine precursor and its distribution in the Sargasso Sea. *ISME J* **2014,** *8* (8), 1727-1738.
105. Porter, K. G.; Feig, Y. S., The use of DAPI for identifying and counting aquatic microflora1. *Limnology and Oceanography* **1980,** *25* (5), 943-948.
106. Guillard, R. R. L., Culture of Phytoplankton for Feeding Marine Invertebrates. In *Culture of Marine Invertebrate Animals: Proceedings — 1st Conference on Culture of Marine Invertebrate Animals Greenport*, Smith, W. L.; Chanley, M. H., Eds. Springer US: Boston, MA, 1975; pp 29-60.
107. Worden, A. Z.; Nolan, J. K.; Palenik, B., Assessing the dynamics and ecology of marine picophytoplankton: The importance of the eukaryotic component. *Limnology and Oceanography* **2004,** *49* (1), 168-179.
108. Backstrom, A. D.; McMordie, R. A. S.; Begley, T. P., Biosynthesis of Thiamin I: The Function of the thiE Gene Product. *Journal of the American Chemical Society* **1995,** *117* (8), 2351-2352.

109. Escalante-Semerena, J. C.; Rinehart, K. L.; Wolfe, R. S., Tetrahydromethanopterin, a carbon carrier in methanogenesis. *Journal of Biological Chemistry* **1984,** *259* (15), 9447-55.

110. Chistoserdova, L.; Vorholt, J. A.; Thauer, R. K.; Lidstrom, M. E., Transfer Enzymes and Coenzymes Linking Methylotrophic Bacteria and Methanogenic Archaea. *Science* **1998,** *281* (5373), 99-102.

111. Vorholt, J. A.; Chistoserdova, L.; Stolyar, S. M.; Thauer, R. K.; Lidstrom, M. E., Distribution of Tetrahydromethanopterin-Dependent Enzymes in Methylotrophic Bacteria and Phylogeny of Methenyl Tetrahydromethanopterin Cyclohydrolases. *Journal of Bacteriology* **1999,** *181* (18), 5750-5757.

112. Fischer, R.; Thauer, R. K., Methyltetrahydromethanopterin as an intermediate in methanogenesis from acetate in Methanosarcina barkeri. *Archives of Microbiology* **1989,** *151* (5), 459-465.

113. Escalante-Semerena, J. C.; Leigh, J. A.; Rinehart, K. L.; Wolfe, R. S., Formaldehyde activation factor, tetrahydromethanopterin, a coenzyme of methanogenesis. *Proceedings of the National Academy of Sciences* **1984,** *81* (7), 1976-1980.

114. Grochowski, L. L.; White, R. H., 7.20 - Biosynthesis of the Methanogenic Coenzymes. In *Comprehensive Natural Products II*, Elsevier: Oxford, 2010; pp 711-748.

115. MADEN, B. E. H., Tetrahydrofolate and tetrahydromethanopterin compared: functionally distinct carriers in C1 metabolism. *Biochemical Journal* **2000,** *350* (3), 609-629.

116. Grochowski, L. L.; Xu, H.; Leung, K.; White, R. H., Characterization of an Fe2+-Dependent Archaeal-Specific GTP Cyclohydrolase, MptA, from Methanocaldococcus jannaschii. *Biochemistry* **2007,** *46* (22), 6658-6667.

117. White, R. H., The Conversion of a Phenol to an Aniline Occurs in the Biochemical Formation of the 1-(4-Aminophenyl)-1-deoxy-d-ribitol Moiety in Methanopterin. *Biochemistry* **2011,** *50* (27), 6041-6052.

118. Mashhadi, Z.; Xu, H.; White, R. H., An Fe2+-Dependent Cyclic Phosphodiesterase Catalyzes the Hydrolysis of 7,8-Dihydro-d-neopterin 2′,3′-Cyclic Phosphate in Methanopterin Biosynthesis. *Biochemistry* **2009,** *48* (40), 9384-9392.

119. Crécy-Lagard, V. d.; Phillips, G.; Grochowski, L. L.; Yacoubi, B. E.; Jenney, F.; Adams, M. W. W.; Murzin, A. G.; White, R. H., Comparative Genomics Guided Discovery of Two Missing Archaeal Enzyme Families Involved in the Biosynthesis of the Pterin Moiety of Tetrahydromethanopterin and Tetrahydrofolate. *ACS Chemical Biology* **2012,** *7* (11), 1807-1816.

120. Wang, Y.; Xu, H.; Grochowski, L. L.; White, R. H., Biochemical Characterization of a Dihydroneopterin Aldolase Used for Methanopterin Biosynthesis in Methanogens. *Journal of Bacteriology* **2014,** *196* (17), 3191-3198.

121. White, R. H., Biosynthesis of the 7-methylated pterin of methanopterin. *Journal of Bacteriology* **1986,** *165* (1), 215-218.

122. White, R. H., Biosynthesis of methanopterin. *Biochemistry* **1990,** *29* (22), 5397-5404.

123. White, R. H., Methanopterin biosynthesis: methylation of the biosynthetic intermediates. *Biochimica et Biophysica Acta (BBA) - General Subjects* **1998,** *1380* (2), 257-267.

124. Frey, P. A.; Hegeman, A. D.; Ruzicka, F. J., The Radical SAM Superfamily. *Critical Reviews in Biochemistry and Molecular Biology* **2008,** *43* (1), 63-88.

125. Haldar, S.; Paul, S.; Joshi, N.; Dasgupta, A.; Chattopadhyay, K., The Presence of the Iron-Sulfur Motif Is Important for the Conformational Stability of the Antiviral Protein, Viperin. *PLoS ONE* **2012,** *7* (2), e31797.

126. Broderick, J. B.; Duffus, B. R.; Duschene, K. S.; Shepard, E. M., Radical S-Adenosylmethionine Enzymes. *Chemical Reviews* **2014,** *114* (8), 4229-4317.

127. Sofia, H. J.; Chen, G.; Hetzler, B. G.; Reyes-Spindola, J. F.; Miller, N. E., Radical SAM, a novel protein superfamily linking unresolved steps in familiar biosynthetic pathways with radical mechanisms: functional characterization using new analysis and information visualization methods. *Nucleic Acids Research* **2001,** *29* (5), 1097-1106.

128. Zhang, Q.; van der Donk, W. A.; Liu, W., Radical-Mediated Enzymatic Methylation: A Tale of Two SAMS. *Accounts of Chemical Research* **2012,** *45* (4), 555-564.

129. Marsh, E. N. G.; Patwardhan, A.; Huhta, M. S., S-Adenosylmethionine radical enzymes. *Bioorganic Chemistry* **2004,** *32* (5), 326-340.

130. Krebs, C.; Broderick, W. E.; Henshaw, T. F.; Broderick, J. B.; Huynh, B. H., Coordination of Adenosylmethionine to a Unique Iron Site of the [4Fe-4S] of

Pyruvate Formate-Lyase Activating Enzyme: A Mössbauer Spectroscopic Study. *Journal of the American Chemical Society* **2002,** *124* (6), 912-913.

131. Grove, T. L.; Livada, J.; Schwalm, E. L.; Green, M. T.; Booker, S. J.; Silakov, A., A substrate radical intermediate in catalysis by the antibiotic resistance protein Cfr. *Nat Chem Biol* **2013,** *9* (7), 422-427.
132. Yan, F.; LaMarre, J. M.; Röhrich, R.; Wiesner, J.; Jomaa, H.; Mankin, A. S.; Fujimori, D. G., RlmN and Cfr are Radical SAM Enzymes Involved in Methylation of Ribosomal RNA. *Journal of the American Chemical Society* **2010,** *132* (11), 3953-3964.
133. Hernández, H. L.; Pierrel, F.; Elleingand, E.; García-Serres, R.; Huynh, B. H.; Johnson, M. K.; Fontecave, M.; Atta, M., MiaB, a Bifunctional Radical-S-Adenosylmethionine Enzyme Involved in the Thiolation and Methylation of tRNA, Contains Two Essential [4Fe-4S] Clusters. *Biochemistry* **2007,** *46* (17), 5140-5147.
134. Zhang, Q.; Li, Y.; Chen, D.; Yu, Y.; Duan, L.; Shen, B.; Liu, W., Radical-mediated enzymatic carbon chain fragmentation-recombination. *Nat Chem Biol* **2011,** *7* (3), 154-160.
135. Fenwick, M. K.; Mehta, A. P.; Zhang, Y.; Abdelwahed, S. H.; Begley, T. P.; Ealick, S. E., Non-canonical active site architecture of the radical SAM thiamin pyrimidine synthase. *Nature Communications* **2015,** *6,* 6480.
136. Berkovitch, F.; Nicolet, Y.; Wan, J. T.; Jarrett, J. T.; Drennan, C. L., Crystal Structure of Biotin Synthase, an S-Adenosylmethionine-Dependent Radical Enzyme. *Science (New York, N.Y.)* **2004,** *303* (5654), 76-79.

137. Allen, K. D.; Xu, H.; White, R. H., Identification of a Unique Radical S-Adenosylmethionine Methylase Likely Involved in Methanopterin Biosynthesis in Methanocaldococcus jannaschii. *Journal of Bacteriology* **2014,** *196* (18), 3315-3323.
138. Ugulava, N. B.; Gibney, B. R.; Jarrett, J. T., Biotin Synthase Contains Two Distinct Iron−Sulfur Cluster Binding Sites: Chemical and Spectroelectrochemical Analysis of Iron−Sulfur Cluster Interconversions. *Biochemistry* **2001,** *40* (28), 8343-8351.
139. Flühe, L.; Knappe, T. A.; Gattner, M. J.; Schäfer, A.; Burghaus, O.; Linne, U.; Marahiel, M. A., The radical SAM enzyme AlbA catalyzes thioether bond formation in subtilosin A. *Nat Chem Biol* **2012,** *8* (4), 350-357.
140. Benjdia, A.; Subramanian, S.; Leprince, J.; Vaudry, H.; Johnson, M. K.; Berteau, O., Anaerobic sulfatase-maturating enzyme – A mechanistic link with glycyl radical-activating enzymes? *FEBS Journal* **2010,** *277* (8), 1906-1920.
141. Mehta, A. P.; Hanes, J. W.; Abdelwahed, S. H.; Hilmey, D. G.; Hänzelmann, P.; Begley, T. P., Catalysis of a New Ribose Carbon-Insertion Reaction by the Molybdenum Cofactor Biosynthetic Enzyme MoaA. *Biochemistry* **2013,** *52* (7), 1134-1136.
142. Mahanta, N.; Fedoseyenko, D.; Dairi, T.; Begley, T. P., Menaquinone Biosynthesis: Formation of Aminofutalosine Requires a Unique Radical SAM Enzyme. *Journal of the American Chemical Society* **2013,** *135* (41), 15318-15321.